Trans-Golgi Network as independent organelle

from Golgi apparatus in plant cells

Dissertation

zur

Erlangung des Doktorgrades (Dr. rer. nat.)

der

Mathematisch-Naturwissenschaftlichen Fakultät

der

Rheinischen Friedrich-Wilhelms-Universität Bonn

vorgelegt von

Giovanni Stefano

aus

San Pietro Vernotico, ITALY

Bonn, 2009

SUMMARY

In eukaryotic cells, GTPase-Activating Proteins (GAPs) are a family of proteins, which acts on small GTP-binding proteins of the Ras superfamily. GAP proteins have a conserved structure and use similar mechanisms, promoting hydrolysis of GTP to GDP. GAPs include several groups based on their substrate proteins, such as ARF (ADP Ribosylation Factor) GAPs, RAB (RAS-like protein in Brain) GAPs, and RHO (RAS Homologue) GAPs.

ARFGAPs act specifically inducing hydrolysis of GTP on ARFs. In *Arabidopsis thaliana* genome, there are 15 proteins with ARFGAP domains (named AGD1-15) which are classified as ARFGAP Domain (AGD) proteins. These proteins have been highly conserved during the evolution of eukaryotes.

In this thesis, the cellular role of an ARFGAP (AGD5) has been investigated. This group of proteins includes five ARFGAP members (AGD5-AGD10) which contain only the AGD domain at the amino terminus. These proteins are structurally related to the yeast ARFGAPs (Age2p, Gcs1p and Glo3p) which perform their function at the TGN (Trans-Golgi Network). Mutagenesis experiments in yeast cells that have a suppressed GAP activity for Glo3p and Gsc1p showed an impaired retrograde protein transport from ER to Golgi apparatus.

In animal cells, overexpression of ARF1GAP determines re-absorbance of Golgi membrane proteins into the ER disrupting retrograde trafficking, as shown using brefeldin-A (BFA), which is a protein trafficking inhibitor.

This suggests that ARF1GAP play a regulator role towards ARF during Golgi apparatus to ER transport.

ARFGAPs are generally considered a group of proteins, which stimulate the intrinsic GTPase activity of ARF proteins. However, an additional role has been suggested in the regulation of membrane traffic.

Thus, GAP proteins may play a crucial role in regulating the disassembly and dissociation of vesicle coats. In plant cells, as in animal and yeast cells, ARFs may also have different effectors and regulator proteins that can control the trafficking pathway. Analysis of the *Arabidopsis thaliana* genome has highlighted the conservation of numerous proteins including the GAP proteins. Among all these proteins, only a few have been characterized in detail. Recent studies have shown that three ARFGAPs, called VAN3, OsAGAP, SCARFACE, may play an important role in vesicle transport from the plasma membrane to the endosomes, and vice versa, having a role also in auxin signalling. In plant cells, the precise function of ARFGAPs at the TGN and its regulators are unknown.

In this thesis, the biological function of an ARFGAP, classified as AGD5, from *A. thaliana* has been investigated by using confocal microscopy techniques, site-directed mutagenesis and biochemical experiments. Using these methodologies, the sub-cellular localization and biological role of AGD5 in protein trafficking in plant cells were investigated.

YFP-AGD5 localizes to TGN

To determine the subcellular localization of AGD5, a protein fusion construct with YFP (yellow fluorescent protein) was produced, YFP-AGD5, and expressed in tobacco leaf epidermal cells. Laser confocal microscopy analyses indicated that

YFP-AGD5 labelled mobile punctate structures that were motile in the cell. To identify the nature of the structures, *Nicotiana tabacum* leaf epidermal cells were cotransformed with YFP-AGD5 fusion and various Golgi apparatus, TGN and endosome markers. It was found that the distribution of YFP-AGD5 was different compared to ERD2, which is a Golgi apparatus marker. Instead it was partly similar to that of ARF1, which mainly localize to the Golgi apparatus but also to additional non-Golgi structures. This shows that YFP-AGD5 and ARF1 co-localize to extra Golgi structures. Furthermore, YFP-AGD5 was coexpressed with various endocytic and TGN markers and it was found that AGD5 labels compartments stained with SYP61, which is also a TGN marker.

YFP- AGD5[R59Q] localize to TGN, and functions on ARF1 in vivo

It has been shown that YFP-AGD5 colocalizes with ARF1 on the TGN. Judging from its subcellular localization, AGD5 probably acts as an ARFGAP on ARF1. It was examined whether AGD5 acts on ARF1 *in vivo* by coexpressing tobacco cells with YFP tagged *AGD5[R59Q]* a GAP-negative mutant.

The cells expressing ARF1 alone showed a punctate subcellular distribution, which represents Golgi apparatus and non-Golgi structures.

In contrast, in cells coexpressing ARF1 and *AGD5[R59Q]*, ARF1 was distributed at punctate structures and in the cytosol. This suggests that ARF1 in such cells may remain as a GTP-bound form on membranes where AGD5 is normally the primary ARFGAP. In any case, the above observations indicate that AGD5 is likely to function in an ARF1 dependent process.

AGD5 interacts with ARF1 *in vivo* and *in vitro*

The results of the previous section indirectly suggest that AGD5 is involved in the activation of ARF1 on the TGN in plants.

To confirm the role of AGD5 in the activation of ARF1 to the TGN, and to obtain direct evidence that AGD5 would alter ARF1 distribution a glutathione agarose affinity assay based on the interaction of a recombinant GST-AGD5 with mutant GTP bound form ARF1-YFP protein expressed in tobacco leaves was developed. Results indicate that there is an interaction between AGD5 and *ARF1GTP*. However, the data do not allow us to establish whether the binding of ARF1 to AGD5 is direct. Therefore, to determine if the interaction between ARF1 and AGD5 required the presence of other cytosolic or TGN associated proteins, ARF1 and AGD5 were produced in *E. coli* and tested for the interaction with ARF1 and purified AGD5 *in vitro*. This experiment demonstrates that the interaction of ARF1 with AGD5 is not dependent on other cytosolic proteins and it could be due to a direct association of the two molecules.

Overexpression of YFP-AGD5 in Arabidopsis stable plants

To determine the cellular expression pattern of AGD5 in plants, the P35S:-YFP-AGD5 construct was introduced into *A. thaliana* via Agrobacterium-mediated transformation. Confocal microscopy on transgenic lines showed that the fluorescence is mainly distributed in the root. The subcellular distribution of YFP-AGD5 was detected as punctate structures along the root but mainly in the apical part.

Analysis of root hairs in transgenic lines overexpressing AGD5 displays the bulged root hair phenotype. Furthermore, the overexpression causes defects in root tip growth.

Additionally, AGD5 in pollen of transgenic Arabidopsis plants was found to cause various pollen tube phenotypes, including expanded tubes with swollen tips, twisted tubes, and bifurcate tips.

AGD5 affects protein secretion in *N. tabacum* transformed protoplasts

To demonstrate further that *AGD5[R59Q]* (GAP-negative mutant) has a negative effect compared to AGD5 wild type form on protein export from the TGN, tobacco leaf protoplasts were cotransfected with the secretory marker SecRGUS. AGD5 did not affect SecRGUS secretion, but the *AGD5[R59Q]* mutant exhibited a negative effect on the secretion of SecRGUS. These data mirror our confocal microscopy results showing that AGD5 affected the distribution of ARF1 at the TGN, suggesting that the mutant form may block anterograde (from ER to Golgi apparatus) export.

This work established that AGD5 localizes to the TGN. Furthermore, this study has highlighted a new interactor, an ARFGAP, for the small GTPase ARF1 protein at the TGN organelle suggesting an additional role in vesicle transport along the endocytic pathway. Therefore, this work represents a starting point to analyze the AGD5 influence on ARF1 functionality during auxin receptor recycling.

TABLE OF CONTENTS

LIST OF FIGURES

LIST OF TABLES

LIST OF ABBREVIATIONS

ARF   ADP Ribosilation Factor

ARL   ARF-Like protein

bp   base pair

cDNA   complementary DNA

CFP   Cyan Fluorescent Protein

DNA   DeoxyriboNucleic Acid

dNTPs   deoxyriboNucleotide TriPhosphates

ECL   Enhanced ChemiLuminescence

EDTA   EthyleneDiamineTetraAcetic acid

EE   Early Endosome

ER   Endoplasmic Reticulum

ERD2   Endoplasmic Reticulum retention Defective 2

GAP   GTPase Activating Protein

GDP   Guanosine DiPhosphate

GEF   Guanine nucleotide Exchange Factor

GFP   Green Fluorescent Protein

GST   Glutathione S-Transferase

GTP   Guanosine TriPhosphate

His   Histidine

IPTG   IsoPropyl-beta-D-ThioGalactopyranoside

Kb   Kilobase

LB   Luria Bertani (medium)

LV	Lytic Vacuole
MES	2-(N-Morpholino) EthaneSulfonic acid
MVB	MultiVesicular Body
PBS	Phosphate Buffered Saline
PCR	Polymerase Chain Reaction
PVC	PreVacuolar Compartment
RAB	RAS-like protein in Brain
RAS	Receptor Activated Small GTPases
RHO	RAS HOMOLOGUE
SAR	Secretion Associated and RAS related
SDS	Sodium Dodecyl Sulfate
SNAREs	Soluble N-ethyl maleimide sensitive factor Attachment protein RECEPTORs
TAE	Tris-Acetate-EDTA
TEMED	TEtraMethylEthyleneDiamine
TFBI	TransFormation Buffer I
TFBII	TransFormation Buffer II
TGN	Trans-Golgi Network
YFP	Yellow Fluorescent Protein
YT	Yeast extract Tryptone

1. INTRODUCTION

1.1 Vesicular traffic in the secretory and endocytic pathways

Eukaryotic cells have a complex internal membrane system, which allows them to release macromolecules through the secretory pathway or to take up nutrients and signal molecules by a process called endocytosis.

The secretory pathway is a highly conserved complex of endomembranes: the endoplasmic reticulum (ER), the Golgi apparatus, Trans-Golgi Network (TGN), the vacuole, plasma membrane and vesicles in which there are cargo molecules transported between all these compartments (Figure 1.1). The endocytic pathway involves vesicles, which bud from the plasma membrane taking up membrane and soluble extracellular molecules moving via the endosome. Besides, recent results indicate that TGN can be considered as an integral part of the endocytic pathway.

Endocytosis and exocytosis are two essential processes governing cell growth, cell fate, development, as well as cell-cell interactions and cell interactions with the external milieu. In addition, viruses, toxins and symbiotic microorganisms utilize the endocytic pathways to get inside the cell.
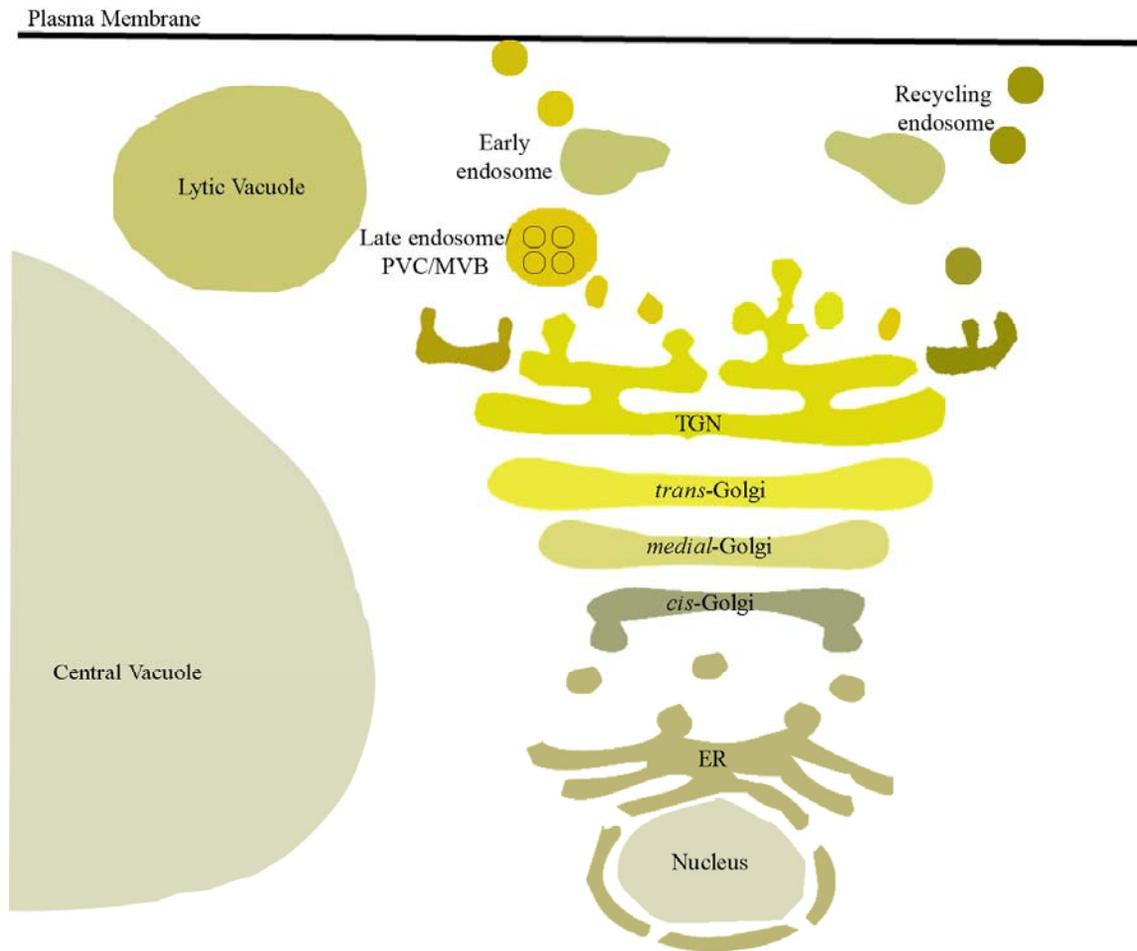
Figure 1.1: Secretory and endocytic pathways.

1.2 Secretory pathway

1.2.1 Endoplasmic reticulum

The ER of plant cells is closely associated with the nucleus, which is enclosed, in a double membrane called nuclear envelope. In eukaryotic cells, the ER is an irregular network of highly dynamic interconnected tubules: this adaptable organelle can re-organize, enlarge and contract its membrane system spatially

and temporally (Staehelin, 1997; Boevink et al., 1998; Boevink et al., 1999). Electron microscopy analyses have revealed the general organization of the ER that is characterized by different regions and sub-regions morphologically distinct with specific functions. This network of membrane systems is physically linked (Staehelin, 1997; Koizumi et al., 2001). Additionally it has been shown, that a rearrangement of the ER membrane system occurs during mitosis (Staehelin, 1997; Hepler, 1982) and during cell differentiation (Harris and Chrispeels, 1980). Confocal microscopy has highlighted new morphological insights into the reo-organization of the ER under stress effects and external stimuli (Cole and Lippincott-Schwartz, 1995; Staehelin, 1997).

The ER membrane network has been found to be involved in the biosynthesis, processing and export of proteins, glycoproteins and lipids (Vitale and Denecke, 1999; Vitale and Galili, 2001). Before reaching their final destination, proteins destined to be secreted or proteins resident in specific organelles are first translocated into ER. The translocation and release of newly synthesized proteins into the ER lumen involves ribosomes docked onto a protein pore, for which the major component of translocation apparatus is Sec61 protein, highly conserved in prokaryotes and eukaryotes (Zhou and Schekman, 1999). Once into the ER, the joint action of resident enzymes and molecular chaperones processes the nascent polypeptides, which undergo a series of post-translational modifications like folding, assembly and oligomerization (Hammond and Helenius, 1995; Bonifacino and Weissman, 1998). Proteins properly modified can run off the ER and be transported to the Golgi apparatus by vesicles. Abnormal

proteins are retained in the ER, accumulated in the dilated region or degraded (Bonifacino and Weissman, 1998). In general, physiological quality control mechanisms represent an important step to avoid the export of malformed ER proteins that can interfere with normal cellular functions (Bonifacino and Weissman, 1998).

1.2.2 Golgi apparatus

Golgi apparatus of eukaryotic cells represents the central station along the secretory pathway, which has an important role in protein glycosylation and sorting processes. In animal cells, many Golgi apparatus resident proteins are involved in forming a proteinaceous skeleton responsible to preserve the structure of this organelle (Franke et al., 1972; Cluett and Brown, 1992). In plant cells, it is unknown how the Golgi apparatus maintains its structure. In a recent study, Renna et al., (2005) have identified an integral membrane Golgi matrix protein in tobacco plant cells, which could be important for the maintenance of the Golgi apparatus architecture.

In mammalian cells, the single Golgi complex is localized to the center of the cell in the perinuclear region around the centrosome, anchored by a microtubule-dependent mechanism (Polishchuk and Mironov, 2004). By contrast, in plant cells, the Golgi apparatus is organized as numerous individual stacks of cisternae that are dispersed through the cell in the cytoplasm, and closely associated to the cortical ER network in leaf cells (Boevink et al., 1998; Brandizzi et al., 2002b; Saint-Jore et al., 2002). The number of stacks and their distribution

within the plant cell has been shown to be cell type-dependent. Generally, plant

cells have an average of several hundreds of Golgi stacks (Mollenhauer and

Morré, 1994; Staehelin and Moore, 1995; Dupree and Sherrier, 1998). Each

Golgi stack is functionally and structurally a polarized structure that includes a

series of flattened cisternae, morphologically distinct in *cis-, medial-* and *trans-*

compartments followed by the TGN (Staehelin and Moore, 1995; Dupree and

Sherrier, 1998). In mammalian cells, ER intimately associated with *cis-*

compartment continuously exchanges cargo molecules with this cisterna,

receiving proteins and lipids. The traffic between the ER and the Golgi apparatus

is regulated through COPII vesicles involved in the anterograde cargo transport,

and COPI vesicles implicated in anterograde and retrograde transport (Jackson

et al., 1993; Pepperkok et al., 1993). Several lines of evidence support the idea

that protein export from the ER takes place in specialized regions of the ER,

defined as ER export sites (ERES) (Aridor and Balch, 1999; Hammond and

Glick, 2000; Aridor et al., 2001). In plant cells, three models that describe ER-to-

Golgi protein export have been proposed (Figure 1.2). The first model, called

'vacuum cleaner model' suggests that Golgi stacks move along the ER surface

sweeping up export vesicles that bud from the ER continuously (Boevink et al.,

1998). To now, no experimental data have been produced to support this model.

The second model is known as 'stop and go' or 'kiss and go' (Nebenfür et al.,

1999). This model suggests that spatially-fixed ERES are present on the ER

surface, the Golgi stops on ERES and collects cargo.

The third model was established on the analysis of the dynamics of a fluorescent

fusion of SAR1, the GTPase that initiates COPII assembly at ERES (daSilva et

al., 2004). In fact, it has been shown in *N. tabacum* leaf epidermal cells that

ERES and Golgi complex form secretory units that move together (daSilva et al.,

2004). The ERES-Golgi apparatus movement does not influence the ER-to-Golgi

transport of cargo molecules (Brandizzi et al., 2002a). Subsequently,

glycosyltransferase localized to *cis, medial* and *trans* compartments transfers

monosaccharides to the nascent polypeptide chains (Polishchuk and Mironov,

2004). Once the modified polypeptide molecules reach the *trans*-compartment

they are packaged into shuttle vesicles and they are distributed to various

destinations within and out the cell. The plant Golgi apparatus has also an

important role in the biosynthesis of cell wall polysaccharides that are transported

by vesicles out of the plasma membrane (Staehelin, 1997; Dupree and Sherrier,

1998).
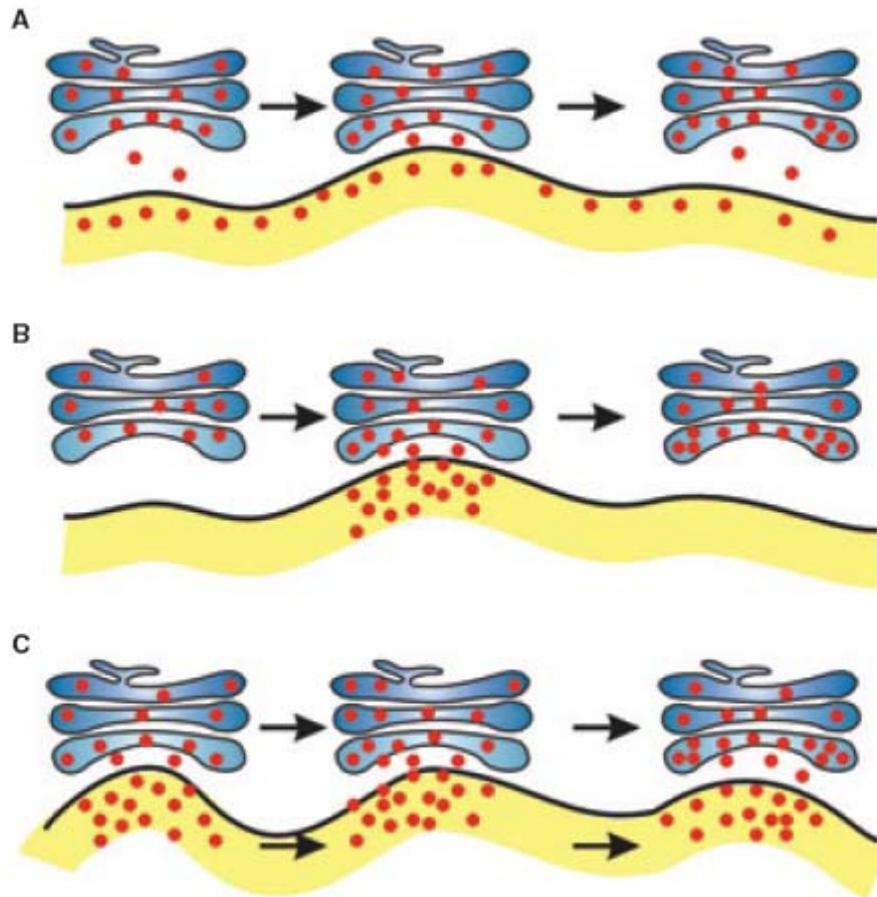
Figure 1.2: Schematic representation of the three models for proteins transfer from the ER to the Golgi apparatus. A) The vacuum cleaner model. B) The stop-and-go model. C) The mobile ERES model. (Hanton et al., 2005).

1.2.3 Trans-Golgi Network

In yeast and mammalian cells, TGN has a central role in the secretory and endocytic pathways. Once in the TGN, newly synthesized proteins, as well as lipids, reach their final cellular destination.

In yeast cells, four different trafficking ways, can occur from the TGN: the first route considered the constitutive or default pathway could deliver cargo molecules to the plasma membrane, the second pathway transport molecules to

the endosomal membrane system, the third pathway has as final destination the

vacuole. Additionally recent evidences have suggested a fourth pathway, which

delivers cargo to the EE (Early Endosome) from the TGN.

Cargo transport at the TGN occurs in vesicles which are different from the COPI

vesicles involved in intra-Golgi transport. It has been demonstrated that transport

from TGN to endosomal/vacuolar system takes place by a mechanism of clathrin

coated vesicles (Ladinsky et al., 1999).

The adaptor complex AP-3 mediates the transport from the TGN to the vacuole.

This route has been discovered following the alkaline phosphatase (ALP)

pathway, in fact in absence of one of the subunits of the adaptor complex AP-3,

ALP is not addressed to the vacuole (Cowles et al., 1997). On the other side

proteins using alternative pathways to reach the vacuole, are not influenced by

AP-3 mutants (Stepp et al., 1997).

An alternative route that allows transit from the TGN to the PVC (prevacuolar

compartment) is the carboxypeptidase Y (CPY) pathway (Rothman and Stevens,

1986). Recent studies have identified the adaptor proteins involved in this

trafficking (Mullins and Bonifacino, 2001).

In mammalian cells, at the TGN two separate routes occur, one to the sorting

endosome /early endosome and MVB (multivesicular body)/late endosome.

In mammalian cells, the TGN represents the exit compartment within the

secretory pathway involved in the sorting of cargo molecules (Teuchert et al.,

1999).

Proteins destined for regulated secretion are packaged into vesicles that await a signal to discharge their contents. TGN is also a site for sorting proteins to the appropriate plasma membrane domain in polarized cells. Clathrin/AP-1 vesicles have been implicated in mediating anterograde trafficking to the EE and retrograde trafficking from the EE to the TGN (Meyer et al., 2000; Waguri et al., 2003; Murphy et al., 2005).

In plant cells, retrograde trafficking is only hypothesized and anterograde trafficking from the TGN to the partially coated reticulum (PCR) or MVB has not yet been demonstrated.

Since its discovery, TGN has been considered to be the last station of the Golgi apparatus. However, several lines of evidence indicate that the TGN should be considered as an independent organelle in plant cells (Saint-Jore-Dupas et al., 2004; Uemura et al., 2004).

The SNAREs SYP41/SYP61 are the first identified proteins labelling a compartment defined as TGN. These can often be seen by confocal microscopy to be physically separated from the Golgi apparatus (Uemura et al., 2004). This result suggests that the TGN can be considered as an independent organelle separated from the Golgi bodies. Several other marker proteins localizing at the TGN are now available, but they have undefined roles in the secretory or endocytic pathway. Among these a vacuolar H (+)-ATPase (V-ATPase) is specifically localized to the TGN and styryl dye FM4-64 coexpression allows to determine the speed with which cargo molecules reaches the TGN (Dettmer et al., 2006). Support to the idea that the TGN has a specific function in secretory

pathways, cames from analysis of the secretory carrier membrane protein1

(SCAMP1), which also marks the TGN (Lam et al., 2007).

1.2.4 Vacuole

In animal cells, lysosomal enzymes destined to late endosome (lysosome) leave

the TGN through clathrin-coated vesicles (Kornfeld, 1990). In plants, cargo

transport from the TGN within the cell appears to proceed by three different

pathways. There are two secretory routes described that proceed from the TGN

to the two kinds of vacuoles in the cell: a storage vacuole (SV) and a lytic

vacuole (LV). Soluble proteins leave the TGN through a third pathway that reach

directly the plasma membrane (Paris et al., 1996). The proteins can leave the

TGN to reach the storage vacuole through dense vesicles. In some conditions, it

is possible to see dense vesicles starting in the *cis*-Golgi area, and this means

that the storage pathway may bypass the TGN (Hinz et al., 1999; Hillmer et al.,

2001; Saint-Jore-Dupas et al., 2004). On the other side clathrin-coated vesicles

shuttle cargo molecules to the lytic vacuole (Saint-Jore-Dupas et al., 2004). A

family of vacuolar sorting receptors (VSR), which are resident in the TGN, is

responsible for the proteins transport to the lytic vacuole through clathrin-coated

vesicles (Kirsch et al., 1994; Paris and Neuhaus, 2002). Studies in *A. thaliana*

identified a dynamin-like 6 protein (ADL6) which appears to be responsible for

the scission of the clathrin-coated vesicles from the trans-Golgi apparatus. In

fact, in a dominant negative mutant (*ADL6[K51E]*) for this protein the transport

between the trans-Golgi and lytic vacuole is blocked, while the transport to the

plasma membrane is still active (Jin et al., 2001). In conclusion, the transport of

cargo molecules to the storage and lytic vacuoles or plasma membrane takes

place on the basis of the budding of different vesicles from trans-Golgi or TGN

working as a sorting compartment.

1.2.5 Plasma membrane

In plant cells, the transport carriers mediating delivery of polysaccharides and

secretory proteins, between trans-Golgi or TGN and plasma membrane still

needs a detailed analysis. In tobacco cells, the transport of polysaccharides to

the plasma membrane has been shown by the use of specific cytochemical

staining or by immunolocalization and appears to occur by uncoated secretory

vesicles of different sizes (Staehelin, 1991). Recently, in tobacco protoplasts, it

has been demonstrated that cell wall polysaccharides and secretory proteins

reach the plasma membrane by different secretory pathways (Leucci et al.,

2007). A first report indicate that the transport of soluble cargo from trans-Golgi

to plasma membrane also occurs, as seen for secGFP, a secreted form of GFP

(Boevink et al., 1999; Batoko et al., 2000). However, owing to the lack of

ultrastructural data on transport vesicles and membrane carriers it is unknown

how proteins can reach the plasma membrane; indeed, the targeting signals

important for transport vesicles destined to the plasma membrane are unknown

(Hadlington and Denecke, 2000). Studies, in tobacco cells, on single-span

proteins have shown that the length of the transmembrane domain for type I

proteins play a role in defining the final localization (Brandizzi et al., 2002b). In

the most recent experimental evidence, it appears that deletion of a large loop in

the cytosolic domain of a multitransmembrane-spanning protein, a plasma

membrane H^+-ATPase from *Nicotiana plumbaginifolia* hampers the plasma

membrane targeting. These findings suggest that one or more signals may be

necessary for the correct targeting to the plasma membrane of multispanning

proteins (Lefebvre et al., 2004). In eukaryotic cells, SNARE proteins (soluble N-

ethyl-maleimide sensitive factor attachment protein receptors) associated with a

membrane are responsible in regulating the vesicles fusion specificity during the

trafficking of proteins from one compartment to another (Uemura et al., 2004). In

A. thaliana genome seventeen SNAREs localized on the plasma membrane have

been identified, and this may confer some level of specificity for vesicle fusion

(Uemura et al., 2004); indeed, recent studies have been suggested a role for

SYP121 and SYP122 in driving independent secretory events (Rehman et al.,

2008). The traffic to the plasma membrane appears also to be regulated by the

interaction between the cytoskeleton and the vesicles (Picton and Steer, 1983;

Hawes and Satiat-Jeunemaitre, 2005). However, very little it is known about

mechanisms of cargo transport to the plasma membrane.

1.3 Endocytic pathway

In Eukaryotic cells, the endocytic pathway comprises a certain number of

intracellular organelles, which can be considered as compartments functionally

and physically distinct connected with each other by vesicular traffic.

The organelles involved in this pathway are called endosomes (Figure 1.3).

In mammalian cells, endosomes are distinguished into four subgroups: early endosomes, late endosomes, recycling endosomes, and lysosomes (Mellman, 1996).

In mammals, the first step in the endocytic pathway is the formation of vesicles from the plasma membrane (Brandhorst and Jahn, 2006).

The vesicles deliver internalized molecules to early or sorting endosomes, which when acidified by ATP-dependent proton pumps, promote ligand-receptor dissociation. Consequently the receptor should be recycled back to the cell surface to start another round of delivery (Mukherjee et al., 1997).

Early endosome can be considered as the central station involved in the continuous generation of vesicles with different destinations.

A first step is the receptors recycling back to the plasma membrane.

A second pathway involves the formation of a compartment which is called recycling endosome. Proteins leave this compartment to recycle back to plasma membrane or to reach the TGN.

Trans Golgi network can receive vesicles from early endosome and consequently ship TGN-derived vesicles back to early compartment (Itin et al., 1997).

Finally, early endosome should gradually mature by reciprocal fusion events to develop into late endosomes/lysosomes (Steinman et al., 1983; Mellman, 1996; Brandhorst and Jahn, 2006). This model is called maturation model and is supported by time lapse video microscopy (Gruenberg et al., 1989; Dunn and Maxfield, 1992; Aniento et al., 1993; Maxfield and McGraw, 2004).

On the other side this scientific evidence does not assist the shuttle model which

considers the endosome as stable organelles whose contents can be transported

between them by vesicles (Damke et al., 1994; Mellman, 1996).

In yeast cells, the endocytic pathway comprises endocytic vesicles, early

endosome, late endosome called prevacuolar compartment, and the vacuole

which is considered equivalent to mammalian lysosome (Mellman, 1996; Munn,

2000). In general, trafficking routes are similar to that of mammalian cells.

In plant cells, several proteins involved in endocytic machinery are well

conserved compared to yeast and mammalian cells (Jurgens and Geldner,

2002). The proteins identified can operate in different types of endocytic

processes: clathrin independent which should include phagocytotic, fluid-phase

and lipid raft-mediated endocytosis, and on the other hand a clathrin dependent

pathway (Murphy et al., 2005). Direct experimental evidence of a clathrin-

independent process come from root cells which internalize Rhizobia by a

phagocytotic process which involves a small GTPase of the Rab family (Son et

al., 2003). Fluid-phase endocytosis, a clathrin-independent process, has been

demonstrated in recent times in plant cells using a membrane-impermeable

fluorescent dye, Lucifer Yellow (LY) (Baluska et al., 2004). A recent discovery

had found that plant cells can take up sucrose using fluid-phase endocytosis and

at the same time sucrose is a signal for the activation of the endocytic pathway

(Etxeberria et al., 2005). In *N. tabacum* cells, the occurrence of lipid raft-

mediated endocytosis was recently demonstrated (Mongrand et al., 2004). In

support of these findings, there are new studies that have identified lipid rafts

associated with GPI-anchored proteins (Borner et al., 2003; Lalanne et al., 2004).
These proteins have found to be associated with PINFORMED (PIN) auxin efflux
proteins; this suggest a role for lipid raft and GPI-anchored proteins in protein
recycling (Grebe et al., 2003; Willemsen et al., 2003).
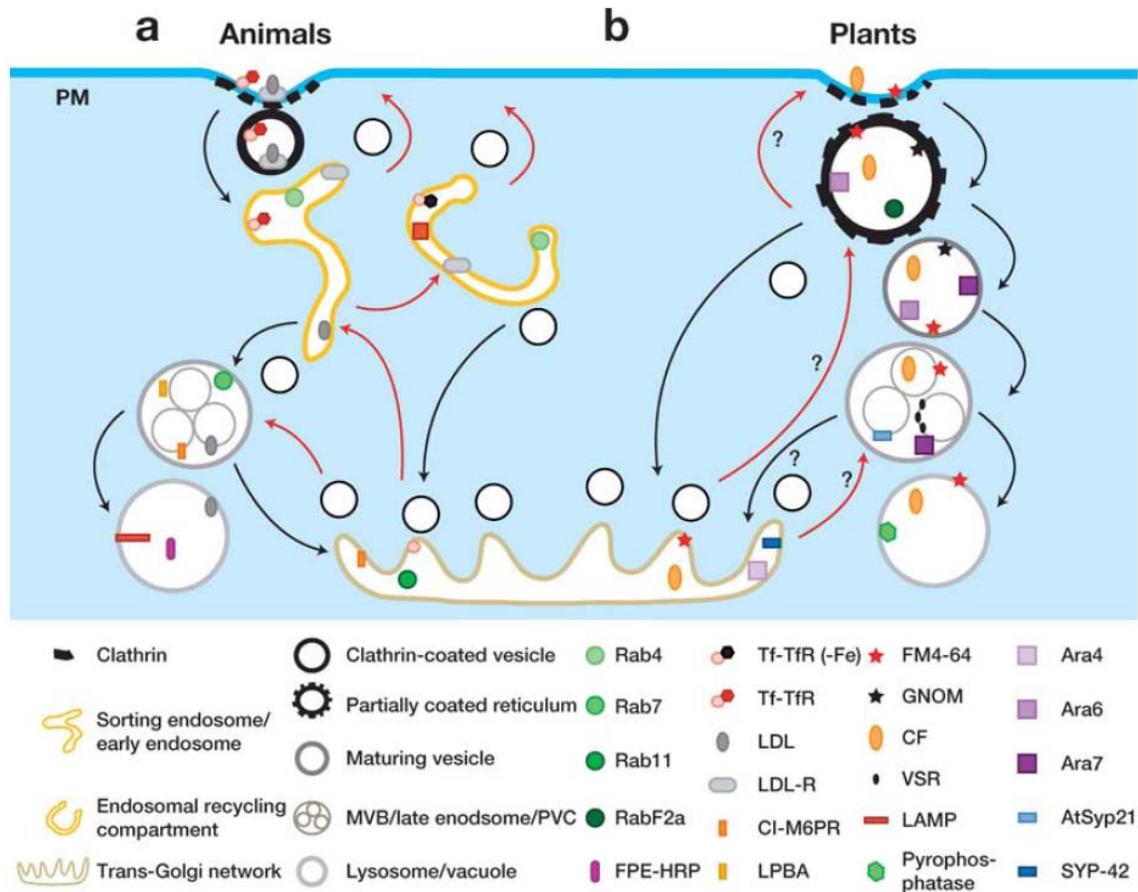
Figure 1.3: Endocytotic pathways in animals and plants. (*A*) In animals, clathrin-coated and
receptor-mediated endocytosis from the plasma membrane (PM) is directed to the sorting
endosome/early endosome [Rab4, LDL-receptor (LDL-R) and transferrin receptor (TfR) markers].
From there, cargo is transported to the PM, endosomal recycling compartment [Rab4, Rab11,
LDL-R, transferrin bound to transferrin receptor (Tf-TfR)], or multivesicular body (MVB)/late
endosome [Rab7, M6PR, lysobisphosphatidic acid (LPBA). From the endosomal recycling

compartment, cargo can go back to the PM or the Trans-Golgi Network (TGN) (Rab11). From the MVB/late endosome, cargo can move to the TGN [cationic-independent mannose-6-phosphate receptor (CI-M6PR)] or the lysosome [fluid-phase endocytosed HRP (FPE-HRP),lysosome-associated membrane protein (LAMP). Cargo can also travel from the TGN to the sorting endosome/early endosome and MVB/late endosome. (*B*) In plants, cargo and PM proteins/markers move into the partially coated reticulum (PCR) [catonized ferritin (CF), GNOM, Ara6, FM4-64,RabF2a]. From there, cargo traffic to MVBs [CF, FM4-64, Ara7, AtSyp21, VSR proteins] through vesicle maturation with overlapping compartment markers [Ara6 and Ara7] or the TGN [CF, FM4-64, SYP-42, Ara4]. From the MVB/late endosome/prevacuolar compartment (PVC), cargo is trafficked to the vacuole [CF, FM4-64, pyrophosphatase]; trafficking to the TGN is hypothesized. Trafficking from the TGN to the PCR or MVB has not been demonstrated (Picture taken from Murphy et al., 2005).

1.4 Small GTPase Superfamily of *A. thaliana*

In eukaryotic cells, the TGN could be considered a major station that directs newly synthesized cargo to different subcellular destinations and receives extracellular and recycled molecules from endocytic compartment. In this way, it represents the heart of the secretory and endocytic membrane trafficking pathways. These two different pathways are under the control of several members of the small GTPase superfamily (Schwaninger et al., 1992; Carter et al., 1993; Wu et al., 2004). In eukaryotic cells, signal transduction, cytoskeleton organization, cell cycle control and membrane traffic are some of the cellular processes in which these small GTPase proteins participate, as key regulators of vesicle biogenesis in intracellular traffic (Zerial and McBride, 2001; Memon, 2004). The small GTPase gene superfamily of Arabidopsis includes ARF (ADP

ribosylation factors), Rab (Ras-like proteins in brain), Rop (Rho (Ras homologue) of plants), RAN (Ras-like nuclear) (Vernoud et al., 2003; Memon, 2004). They work as a molecular switch by cycling between the active GTP-bound and inactive GDP-bound forms (Figure 1.4). The exchange of GDP with GTP on these GTPases occurs through a guanine nucleotide exchange factors (GEF); on the other hand, the GTPase-activating proteins (GAPs) accelerate GTP hydrolysis then the GTPase switches in the inactive form, predominantly cytosolic (Vernoud et al., 2003).
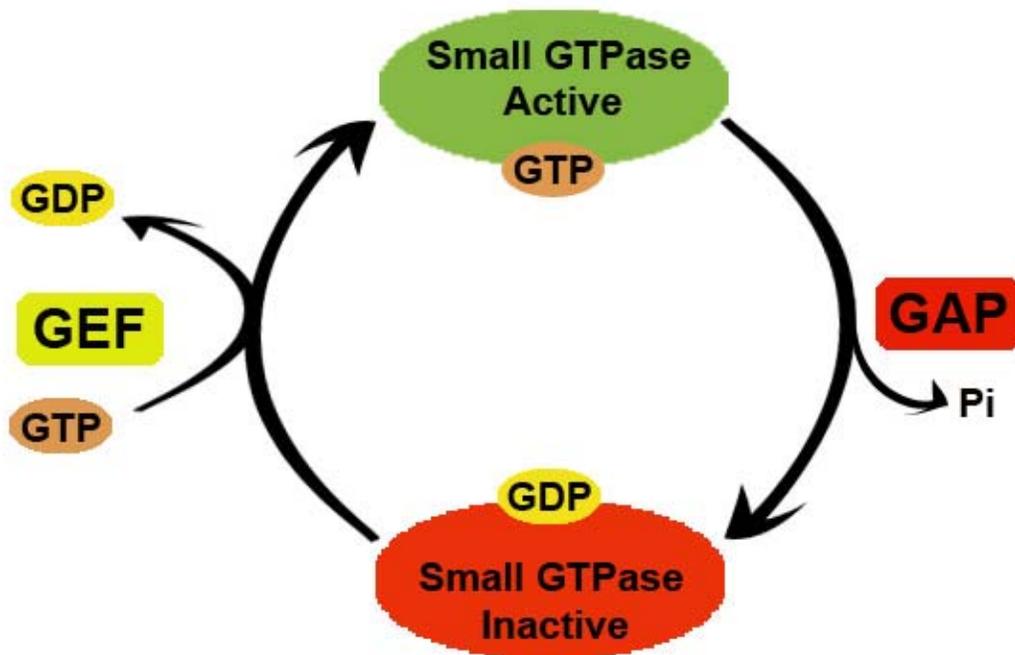
Figure 1.4: small GTPase cycle

1.4.1 ARF family

The *A. thaliana* genome encodes 21 putative ARF GTPases, which share many

important regions with other mammalian and yeast ARFs (Gebbie et al., 2005).

ARF GTPases are highly conserved and ubiquitously expressed proteins,

involved in the secretory and endocytic pathways (Burd et al., 2004; Memon,

2004). They can act recruiting cytosolic coat proteins (COP-I, COP-II, and

clathrin coats) to sites of vesicle budding (Kirchhausen, 2000). This family can be

divided into three groups: ARF, SAR and ARL proteins (Vernoud et al., 2003).

1.4.1.1 ARFs (ADP Ribosylation Factors)

In Arabidopsis, twelve ARF isoforms were identified (Vernoud et al., 2003;

Memon, 2004). They share amino acid sequences, protein size, and gene

structure with mammalian and yeast ARFs (Gebbie et al., 2005). In mammalian

and yeast cells, Class-I ARFs are the best characterized. ARF1 has been shown

to act at multiple steps in contrast to RAB GTPases which works at single steps

in membrane trafficking. Indeed, ARF1 plays a pivotal role in regulating the

assembly of different vesicle coat complexes. In the retrograde traffic between

the Golgi apparatus and ER, ARF1 is responsible for correct formation of COPI-

coated vesicles on Golgi complex. Additionally, ARF1 regulates the budding

vesicle at the TGN and endosome surface interacting with the clathrin-AP1,

clathrin-AP3 and AP-4 machinery (Roth, 1999; Jackson and Casanova, 2000;

Boehm et al., 2001; Memon, 2004). Besides, ARF1 has been implicated in the

binding of GGAs (Golgi associated, γ-adaptin homologous, ARF-interacting

proteins) to TGN regulating membrane traffic (Boman et al., 2000; Boman, 2001). The orchestration of mitotic Golgi apparatus breakdown, chromosome segregation, and cytokinesis appears to be regulated by ARF1 (Altan-Bonnet et al., 2003).

In plants, ARF1 is specifically investigated for its role in the assembly of COPI-coated vesicles (Pimpl et al., 2000) and in maintaining the integrity of Golgi apparatus (Ritzenthaler et al., 2002; Stefano et al., 2006). Recently, it has ascribed a new role to ARF1 in membrane trafficking. Indeed, ARF1 has been established to recruit the plant golgin protein, GDAP1(GRIP-related ARF-binding domain-containing Arabidopsis protein 1) (Matheson et al., 2007).

In plant cells, despite these scientific advances the role of ARF1 still is to be analyzed in detail.

1.5 ARFGAP proteins

Studies, in eukaryotic cells, have shown that many intracellular vesicle transport pathways are under the influence of small GTPase proteins which requires GTP hydrolysis through the action of ARFGAP proteins. In this way GAPs can regulate the ARF activity in the cell.

In mammalian and yeast cells, ARFGAPs are divided in two types: small BFA sensitive and large GAPs (Cukierman et al., 1995; Poon et al., 1996; Brown et al., 1998; Premont et al., 1998; Randazzo and Hirsch, 2004). All members share a small catalytic zinc finger domain which promotes the GTP hydrolysis on ARF proteins.

The zinc finger motif, responsible for a correct GTP hydrolysis activity, is composed of about 80 amino acids with a conserved sequence including four cysteines necessary for zinc coordination ($NX_2CX_2CX_4PXWX_5GX_3CX_2CXHR$ where X indicate a non conserved amino acid)(Cukierman et al., 1995; Memon, 2004). Another important feature of GAP proteins is a conserved arginine residue within the ARFGAP catalytic domain (Cukierman et al., 1995; Randazzo et al., 2000; Memon, 2004).

This conserved amino acid appears to promote the catalytic activity allowing the ARF proteins transition from GTP to GDP form. Mutagenesis experiment for ASAP1, an GAP protein, have shown that alteration of this aminoacidic residues reduce the ARFGAP activity to 0.001% of the wild-type value (Randazzo et al., 2000).

In plant cells, the cellular role of ARFGAP proteins needs to be investigate in detail.

Recently, in plant systems, several ARFGAP proteins for ARFs have been identified and they all show a characteristic zinc finger domain (Bischoff et al., 1999; Donaldson and Jackson, 2000; Vernoud et al., 2003).

In *A. thaliana* genome there are 15 proteins with ARFGAP domains, which are classified as ARFGAP Domain (AGD) proteins (Vernoud et al., 2003) . These proteins have been highly conserved during evolutionary process of eukaryotes. AGD proteins were identified with BLASTP using as template the AGD of ASAP1(Vernoud et al., 2003). A classification based on phylogenetic analysis and domain organization groups AGD proteins into four distinct classes.

The AGD1-AGD4 represents the first of these groups which contains in addition

to the AGD domain two or three ankyrin repeat domains, and a pleckstrin

homology (PH) domain involved in phospholipid signalling events (Vernoud et al.,

2003). Besides these domains, AGD1, AGD2, and AGD3 possess an extra

amino-terminal domain called BAR (Bin1-amphiphysin-Rvs167p/Rvs161p). This

specific domain appears to be present only in the plant ARFGAP proteins. In

mammalian cells, studies on adaptor proteins with BAR domain have established

a role for these molecules into actin regulation and synaptic vesicle endocytosis

(Wigge and McMahon, 1998; Balguerie et al., 1999; Vernoud et al., 2003).

In class 2 are grouped five ARFGAP members (AGD5-AGD10) which contain

only the AGD domain at the amino terminus. These proteins are structurally

related to the yeast ARFGAPs (Age2p, Gcs1p and Glo3p) which perform their

functions at the TGN (Cukierman et al., 1995; Jurgens and Geldner, 2002).

Class 3 is represented by AGD11, AGD12, and AGD13. All the members of this

group contains, immediately after the N-terminal GAP domain, a Ca^{2+} -binding

C2 domain which is involved in the binding of different ligands like phospholipid,

inositol polyphosphate, or other proteins (Shao et al., 1997; Jensen et al., 2000;

Vernoud et al., 2003).

Additionally there are two more AGD proteins (AGD14-AGD15), grouped in the

class 4. One of them, AGD14 shows a single transmembrane domain which is a

unique feature of this ARFGAP member.

Some of the AGD proteins described above contain additional domains, which

should regulate temporally and spatially the ARFGAP activity within the cell or

can act as negative regulators of ARF proteins. In fact, recently studies have

shown that ARFs are involved in the regulation of membrane trafficking and coat

protein complexes machineries recruitment (Jensen et al., 2000; Stefano et al.,

2006).

Understanding the mechanisms by which ARFGAPs are regulated will determine

the role of this class in regulating and sorting of cargo proteins and recruitment of

vesicle coat proteins.

1.6 Effectors of ARFGAP proteins

In plants, the cellular role of ARFGAP proteins is not very well understood.

ARFGAPs may interact with different proteins regulating membrane traffic and

actin cytoskeleton. In mammalian cells, ARFGAP1 had been shown to bind to

ERD2 that is a receptor for proteins with ER retention sequence KDEL involved

in retrograde transport from the Golgi apparatus to the ER (Aoe et al., 1997;

Inoue and Randazzo, 2007). Besides, ARFGAP1 interacts with p24 cargo

proteins.

Transferrin receptor (TfR), cellubrevin and integrin β1 has been demonstrated to

interact with ACAP1, which could function as binding cargo to carry it into vesicle

trafficking (Yang et al., 2002). AGAP1, AGAP2, SMAP2 has been reported to be

associated with clathrin adaptor proteins, like AP-3, AP-1 and CALM (Inoue and

Randazzo, 2007). Some ARFGAPs had been shown to regulate enzymes

involved in controlling lipids signalling. As well as ARF, also other small GTPase

proteins act with ARFGAPs in regulating the structure of actin cytoskeleton.

Structural studies aimed at clarifying the functional relationships between

domains within single ARFGAPs will be necesary for understanding the

molecular features on which the distinct activities associate with specific

ARFGAPs, are based and integrated.

1.7 Objectives

This thesis is focused on the subcellular localization of ARFGAP (AGD5) and on

the interaction between the ARFGAP (AGD5) and the small GTPase, ARF1.

The aims of this thesis are:

1. To examine the localization of AGD5 in plant cells, *N. tabacum*. and *A. thaliana*,

2. To understand the cellular role of this ARFGAP and its molecular partner in plant cells,

3. To test the interaction between AGD5 and ARF1,

4. To identify specific sequence regions, important for the interaction between AGD5 and ARF1.

The molecular characterization of the AGD5 will contribute to the understanding

of mechanisms underlying the cycling of coat protein in the Trans-Golgi Network.

2. MATERIALS AND METHODS

2.1 Materials

2.1.1 Biological materials

Four week old greenhouse plants of *N. tabacum* (cv Petit Havana) were grown in a greenhouse using commercial peat moss-based mix soil, with 16 hours in the light at 27 ºC and 8 hours in the dark at 24 ºC, at a light irradiance of 200 µE.m^{-2}.sec^{-1}. *A. thaliana* plants were cultivated in a growth chamber using a mix of soil that have substantial peat moss with inert media watered with nutrient solutions, with 16 hours in the light at 23 ºC and 8 hours in the dark at 21 ºC, at a light irradiance of 150 µE m^{-2} sec^{-1}. The plasmids, and bacteria (*A. tumefaciens* and *E. coli* strains) used in this work, are listed in Table A1. The multiple cloning sites of different plasmids are shown in Figure A1-4. The cDNA for AGD5 (At5g54310) and ARF1 (At2g47170) were purchased from RIKEN bioresource center (http://www.brc.riken.jp/lab/epd/Eng/).

2.1.2 Solutions, enzymes and primers

All the solutions used in this work are listed in Table A2.

The different enzymes used: *Pfu* DNA Polymerase, Ribonuclease A (RNase A), and restriction endonucleases were purchased from Fermentas Life Sciences (www.fermentas.com). T4 DNA ligase was purchased from Invitrogen (www.invitrogen.com).

The primers used for PCR reactions were purchased from Invitrogen and they are listed in Table A3.

2.1.3 Chemicals

The GFX PCR DNA and gel band purification kit, used for DNA purification, was purchased from Amersham Biosciences (www6.amershambiosciences.com). Glutathione S-Transferase (GST) purification kit for protein purification was purchased from BD biosciences (www.bdbiosciences.com). All other chemical reagents were purchased from VWR (www.vwr.com) and Sigma (www.sigma-aldrich.com).

2.1.4 Media

All the media used in this work are listed in Table A4. LB (Luria Bertani) medium was used to grow *E. coli* and *A. tumefaciens* by adding the appropriate antibiotic to select resistance. YT (Yeast extract Tryptone) medium was used to prepare chemically competent *E. coli* MC1061.

2.1.5 Antibodies

The anti-GFP and anti-GST were purchased from Abcam (www.abcam.com). The anti-His6 and the secondary antibody (goat anti-rabbit linked to horseradish peroxidase) were purchased from Santa Cruz biotechnology (www.scbt.com). The antibodies were used at suitable dilution as specified by the supplier: anti-GFP at 1:2000; anti-GST at 1:1000; anti-His6 at 1:500 and secondary antibody at 1:5000.

2.2 Methods

2.2.1 PCR (Polymerase Chain Reaction)

The PCR reaction mixtures were performed as listed in Table A5. All the PCRs

are carried out in a MyCycler thermal cycler (www.biorad.com). The amplification

parameters used in this thesis are generalized as follows:

The first step allows an initial DNA template denaturation: the reaction was

incubated at 94 ºC for 4 min; the next step was carried out for 20 cycles consists

of 3 stages: the first stage is a denaturation stage carried at 94 ºC for 30

seconds. The following stage, which is dependent on the primer sequences, is

the annealing phase usually between 48-55 ºC for 30-45 seconds. Finally the last

stage of the second step is the elongation phase generally at 72 ºC for 1 minute

for the synthesis of PCR fragments of 500 bp using *Pfu* Polymerase or 1000 bp

using *Taq* Polymerase. Then, the extending phase represents the last step

performed at 72 ºC for 5 min, to fill-in the protruding ends of newly synthesized

PCR products. The reactions were hold at 4 ºC until analyzed by gel

electrophoresis (refer to section 2.2.4).

2.2.2 Overlapping PCR

Site-directed mutagenesis were generated by a method of overlapping PCR

which creates amino acid substitutions by combining two DNA fragments,

produced in separate PCR reactions (Higuchi et al., 1988; Ho et al., 1989). The

two fragments were amplified by using one non-mutagenic in 5' or 3' and one

mutagenic primer. Then the fragments were purified by DNA extraction from

agarose gel, as described in section 2.2.5. The two products having a complementary region were used as new DNA template and overlapped in a second PCR reaction mixture, by using the two non-mutagenic primers for 5' and 3' end.

2.2.3 Mutations created in AGD5 and ARF1 proteins

Overlapping PCR was used to create point mutations as described in Table A6. The insertion of the mutations was confirmed by analysis with an automated DNA sequencer and the data were processed by using Chromas lite software.

2.2.4 DNA gel agarose

Agarose gel electrophoresis was used to separate and analyze DNA. It is possible to look at the DNA, to quantify it or to isolate a particular band of interest. Gels were stained with addition of ethidium bromide (final concentration 0.5 µg/ml) which allows to visualize it by UV light. To prepare samples for electrophoresis, 1/10 of 5 x loading buffer was added. Electrophoresis was run at 100 V, for about 30 min until the bromophenol blue dye moved 80% of the gel length.

2.2.5 DNA extraction from agarose gel

The gel after the electrophoresis was placed on a transilluminator, and then the DNA bands were visualized by UV light (302 nm). The band of interest was cut out using a scalpel blade; next gel slice containing the band was carefully removed from the gel and placed on a 1.5 ml eppendorf tube. The DNA

fragments were extracted from agarose gels using a GFX PCR DNA and gel band purification kit from Amersham Biosciences. The protocol was provided by the kit.

2.2.6 Vector preparation

The vector PVKH18EN6, containing a coding region for a fluorescent protein at the beginning of the polylinker, or at the end of polylinker, pET28b and pGEX-4T1-GS were cut with restriction endonucleases, respectively *BamH*I-*Sac*I, *Xba*I-*Sal*I, *Nco*I-*Sal*I, *BamH*I-*Sac*I.

The vectors were prepared by using restriction enzymes from Fermentas. Digestion reactions were performed at 37 ºC for 1.5 hours. After that, the DNA was purified by using GFX PCR DNA and gel band purification kit. Then the vectors were loaded on agarose gel and purified like in section 2.2.5.

2.2.7 Ligation reaction

Vector and DNA insert were quantified on agarose gels using GeneRuler 1 kb DNA Ladder as a reference. The ligation was prepared in 20 µl total volume reaction containing ligation buffer 1x purchased from Invitrogen (www.invitrogen.com), 1µl of clean open vector (10 ng), 1 unit of T4 DNA ligase and ligated with a five fold molar excess of insert. The mixture was incubated at 16 °C overnight.

2.2.8 Preparation of competent *E. coli* MC1061

E. coli MC1061 cells were streaked on LB plates with antibiotic (streptomycin 50

µg/ml) than incubated overnight at 37 °C. A single colony was inoculated in 3 ml

YT medium and incubated at 37 °C with shaking at 200 rpm until the O.D.$_{550}$ was

0.300. The culture was then poured into 200 ml of pre-warmed (37 °C) YT

medium and incubated at 37 °C with shaking at 200 rpm. When the O.D.$_{550}$ was

0.480 the culture was transferred into four sterile 50 ml Falcon tubes (BD Falcon)

and left on ice for 5 min. The cells were then centrifuged at 5,000 rpm in a

Beckman's table top centrifuge, equipped with JA 30.10 rotor at 4 °C for 20 min.

At the end of the centrifugation the supernatant was eliminated. While cells were

resuspended in a total of 80 ml of ice-cold TFB I buffer and placed on ice for 5

min. The suspension was centrifuged as before and the pellet was resuspended

in 8 ml of TFB II buffer and left on ice for 15 min. Aliquots of 100 µl were pipetted

into pre-chilled Eppendorf tubes and frozen in liquid N_2. These aliquots were

stored at -80 °C.

2.2.9 Preparation of competent *E. coli* BL21 and *E. coli* BL21 (DE3)

A single colony of BL21 *E. coli* cells was inoculated into 5 ml of LB medium and

grown overnight with 200 rpm shaking at 37 °C. The culture (3 ml) was poured

into a 250 ml flask, grown at 37 °C, shaken at 200 rpm, until O.D.$_{590}$ was 0.5.

The bacterial cells were transferred into 50 ml Falcon tubes and chilled on ice for

15 min. The cells were then centrifuged for 20 min at 5,000 rpm, 4°C. The

supernatant was removed and the pellet resuspended in 50 ml of a $CaCl_2$

solution (20 mM) and centrifuged for 10 min at 5,000 rpm. After removing the

supernatant, the pellet was resuspended in 20 ml CaCl$_2$ solution 20 mM and was

left on ice for 30 min. Subsequently, cells were centrifuged for 10 min at 5000

rpm, the supernatant was removed and the pellet was resuspended in 1 ml of

CaCl$_2$ solution. Cells were aliquoted into prechilled, sterile 1.5 ml tubes (100 μl

aliquots) and stored at -80 °C.

2.2.10 Competent *E. coli* transformation

The frozen competent cells (*E. coli* MC1061, *E. coli* BL21 or BL21 (DE3)) were

kept from -80 °C and thawed on ice. The plasmid solution (3 μl) or a ligation

mixture (7 μl) was added to the competent cells, mixed, and incubated on ice for

20 min. The cell suspension was then heat-shocked at 42 °C for 30 seconds and

rapidly transferred to ice for 5 min. LB medium (800 μl) was added to each tube

and incubated at 37 °C for 1 hour with shaking at 170 rpm. Subsequently, cells

were transferred onto an LB plate with the appropriate antibiotic selection and

grown overnight at 37 °C.

2.2.11 Preparation of competent *A. tumefaciens*

A single colony of *A. tumefaciens* (GV3101) was inoculated in 5 ml of LB medium

supplemented with antibiotic (gentamycin 15 μg/ml) and incubated overnight with

shaking at 250 rpm. Two ml of culture were inoculated into 50 ml of LB in a

sterile 250 ml flask and grown at 28 °C until the O.D.$_{600}$ reached approximately

0.5-1.0, then transferred in ice for 10 min. Cells were collected by centrifugation

for 10 min at 5,000 rpm at 4 °C. The supernatant was removed and gently

resuspended in 1 ml of sterile cold 20 mM CaCl$_2$. Aliquots (40 µl) of the cell

suspension were frozen in liquid nitrogen for further storage at –80 °C.

2.2.12 Plasmid DNA extraction (Minipreps)

A single colony was inoculated into 3 ml of liquid LB supplemented with the

specific antibiotic for plasmid selection and grown overnight at 37 °C with shaking

at 180 rpm. Successively, the cell suspensions were transferred into eppendorf

tubes and centrifuged at 14,000 rpm. The supernatant was removed and the

pellet resuspended in 250 µl of P1 solution supplemented with 0.25 µl of RNase

A (Fermentas) (stock: 10 mg/ml in ddH$_2$O), and incubated at room temperature

for 15 min. P2 (250 µl) solution was added and the mixture was incubated at

room temperature for 10 min. Then 350 µl of P3 solution was added and

incubated at 4 °C for 10 min, followed by centrifugation at 14,000 rpm for 10 min.

The supernatant (750 µl) was transferred into an eppendorf tube with 750 µl of

isopropanol followed by centrifugation at 14,000 rpm for 30 min. The pellet was

left to dry at 37 °C for 10 min. Then the pellet was resuspended in 50 µl of

distilled water and stored at - 20 °C.

2.2.13 Maxiprep for preparation of high quality DNA

A pre-culture was grown from a single colony in 3 ml of LB medium (plus

appropriate antibiotic for selection) for 8 hours at 37°C, shaking at 300 rpm. The

preculture was then used to inoculate 100 ml of LB at 37 °C and incubated for 16

hours at 37 °C with shaking. After incubation the culture was centrifuged at

5,000 rpm for 10 min. The supernatant was removed and the pellet harvested

with QIAGEN plasmid maxi kit (http://www1.qiagen.com).

2.2.14 Competent *A. tumefaciens* transformation

Plasmid DNA (7 µl) was mixed with an aliquot of competent *A. tumefaciens* cells

GV3101 and left on ice for 5 min, followed by snap freezing in liquid nitrogen for

5 min. Then cells were transferred to the 37 °C water bath and incubated for 5

min. LB medium (800 µl) was added to the cells. Cells were incubated for 4 hours

at 28 °C with shaking at 120-130 rpm. Then the cell suspension was spread onto

selective LB plate and incubated at 28 °C for two days to obtain visible colonies.

2.2.15 Transient *N. tabacum* plants transformation

Four weeks old *N. tabacum* plants were used for *A. tumefaciens* (strain GV3101)

mediated transient expression as described previously (Batoko et al., 2000). For

the agro-infiltration procedure, cultures of *A. tumefaciens* were grown at 28ºC in

LB supplemented with kanamycin (100 μg/ml) and gentamycin (25 μg/ml) with

shaking at 200 rpm for about 20 hours. Bacterial cells were collected by

centrifugation at 8,000 g for 5 min at room temperature and resuspended in IF

(infiltration) buffer. The bacterial optical density (O.D.$_{600}$) used for plant

transformation was 0.1 for AGD5, AGD5-R59 and SYP61, 0.05 for ARF1 and its

mutants, and 0.2 for ERD2 constructs. The suspensions of transformed

Agrobacterium cells were injected through the entire leaf into the abaxial air

spaces of tobacco leaves by using a sterile 1ml hypodermic syringe (Kapila et al.,

1997).

2.2.16 Stable *A. thaliana* plants transformation

A. thaliana plants were grown in pots with the soil covered with window screen.

After one month, the first bolts were clipped to promote proliferation of many

secondary bolts. Optimal plants ready for Agrobacterium transformation need to

have many immature flower clusters and not fertilized siliques. A large liquid

culture of *A. tumefaciens* carrying gene of interest on a binary vector were grown

at 28 ºC in LB supplemented with kanamycin (100 μg/ml) and gentamycin (25

μg/ml) with shaking at 200 rpm for to O.D.$_{600}$ = 0.8. Bacterial cells were collected

by centrifugation at 8,000 g for 5 min at room temperature. The pelletted cells

were resuspended in dipping buffer. For each two or three small pots to be

dipped is necessary 200-500 ml. Before dipping, tween-20 was added to a

concentration of 0.05 % and mixed well. Above-ground parts of the plant were

dipped in Agrobacterium solution for 30 seconds, with gentle agitation.

Finally, the plants were laid on their side in a plastic bag for 16 to 24 hours to

maintain high humidity. When the seeds become mature they were harvested.

Transformants were selected on agar plates using hygromycin (25 μg/ml).

2.2.17 *A. thaliana* pollen germination

Flowers collected from *A. thaliana* plants were used for the examination of pollen

tube phenotypes. Pollen was germinated on an agar medium containing 16.6 %

sucrose, 3.65 % sorbitol, 0.01 % boric acid, 1 mM MgSO4, 10 mM CaCl2, 1 mM

KCl, 5mM MES, and 1 % agar, pH 5.8. Pollen grains from transgenic and

Columbia wild-type plants were transferred to agar medium by dipping the

flowers on agar. Pollen was germinated at room temperature for 5 hours, and

examined using a confocal microscope.

2.2.18 Proteins interaction using heterologous *E.coli* cells extract

(heterologous *E.coli* cells system)

The coding region for ARF1 and its mutant forms were subcloned into the

expression vector pET-28b (+) which, at the end of the polylinker, contains a

coding region for 6 histidines; therefore these 6 histidines will be added to the C-

terminal of the coding region for the protein inserted in the vector. On the other

hand, the coding region for the AGD5 was subcloned into the expression vector

pGEX-4T1-GS which, at beginning of the polylinker, containing a coding region

for Glutathione S-Transferase (GST). The expression vector so prepared were

used to transform *E. coli* strain BL21 and BL21 (DE3), respectively. A single

colony was initially inoculated into 5 ml of LB, containing kanamycin (100 µg/ml)

for pET-28b (+) or ampicillin (100 µg/ml) for pGEX-4T1-GS, and then incubated

for 15 hours at 37 ºC with shaking at 200 rpm. Successively, 3 ml of overnight

culture was transfered into a 100 ml LB medium with antibiotic by using a 250 ml

flask to obtain a bigger culture. Bacteria were grown with shaking at 230 rpm at

30 ºC until O.D.$_{600}$ reached approximately 1.0. At this point, the expression of

recombinant protein was induced by 1mM IPTG (isopropyl-beta-D-

thiogalactopyranoside) for 5 hours at 30 ºC with shaking at 230 rpm. Bacterial

cells were then pelleted at 5,000 rpm for 10 min at 4 ºC. Cells were stored at -20

ºC until resuspension in GST-extraction buffer (1 ml/10 ml *E. coli* culture). The

cell suspension was subjected to sonication at 15 watt for 10 seconds for 3 times

and centrifuged at 12,000 g for 30 min. *E. coli* extracts were prepared under

native conditions in order to discharge insoluble proteins in the pellet and they

were cleared of inclusion bodies by centrifugation (12,000 g x 30 min). The pellet

was then eliminated and the soluble supernatants were used for protein

quantification by using a Coomassie (Bradford) protein assay kit based on the

Bradford dye-binding procedure (Bradford, 1976). For protein-protein interaction

assays, GST-tagged proteins extracts from *E. coli* were loaded onto glutathione

resin columns (2ml) (BD Biosciences) for binding of GST-tagged proteins. After

three steps of washing to remove the aspecific bound proteins, the columns were

loaded with His-tagged protein extracts from *E. coli* and incubated 1 hour on ice

without disturbing the resin. Subsequently, the unbound protein was removed by

washing, and elution of tagged proteins was performed by adding three 1ml

aliquots of elution buffer to the column. The eluate was collected in 1ml fractions

(according to the BDbiosciences instructions).

2.2.19 Coomassie (Bradford) protein assay

The Coomassie (Bradford) protein assay kit was purchased from Pierce

(www.piercenet.com). It is a rapid and ready-to-use modification of the well-

known Bradford method for total protein quantification.

The Bradford assay is used for determining protein concentrations and is based

on the fact that the maximum absorbance for an acidic solution of Coomassie

brilliant blue G-250 shifts from 465 nm to 595 nm when binding to protein occurs,

with a concomitant colour change from brown to blue. A small amount of protein

sample (5 µl) was mixed with 1,5 ml assay reagent, incubated for 10 min at room

temperature and the absorbance was measured at 595 nm. Protein

concentrations were estimated accordingly to the absorbance obtained for a

series of standard albumin protein dilutions.

2.2.20 Leaf protein extraction

N. tabacum plant leaves were inoculated with *A. tumefaciens* by carrying the

expression vector pVKH18EN6 that contained a coding region for ARF1-YFP.

Leaves were harvested from plants after 48 hours. One gram of leaves was snap

frozen in liquid nitrogen, ground to a fine powder with a mortar and pestle; the

powder was then transferred to a 15 ml falcon tube containing NE buffer (2,5

ml/g of leaves), with protease inhibitor cocktail (33 µl/g of leaves) (Sigma P9599).

The extract was centrifuged at 5,000 g for 10 min, the supernatant filtered

through a membrane Nitex filters 160 µm mesh and the pellet was discarded.

Successively the filtered material was centrifuged at 14,000 g for 15 min at 4 ºC

and the supernatant pooled to ensure a homogenous mixture. This protein

extract was then used for protein interactions as described in 2.2.18.

2.2.21 Proteins interaction using plant and *E.coli* cells extract (planta-*E. coli* system)

E. coli BL21 (400 ml) culture expressing GST-AGD5 were extracted with 15 ml of GST extraction buffer, then centrifuged at 12,000 g for 30 min at 4 ºC. Subsequently, the supernatant was loaded onto columns containing 1 ml of glutathione-agarose beads suspension (www.bdbiosciences.com) (72 % in NS buffer). After several washes to remove unbound proteins, 150 μl of bead slurry was transferred into eppendorf tube (150 μl for each interaction). Then incubated with 1 ml of the supernatant, which was obtained from leaf extract expressing ARF1wt-YFP or its mutant forms. The mix was kept at 4 °C for 3 hours with gentle rotation. The beads were centrifuged at 4 °C, 500 g for 1 min and then washed five times with NS buffer. Bound proteins were eluted from the beads with an appropriate volume of 5 x SDS-PAGE sample buffer (in a proportion sample: buffer = 1:0.4, respectively) and run on a 10 % SDS-PAGE gel (refer to section 2.2.22).

2.2.22 SDS-PAGE

Proteins were separated by SDS-gel electrophoresis as described by Laemmli (Laemmli, 1970). SDS gels were prepared as described in Table A7. The SDS-PAGE gel unit, Mini-PROTEAN 3 electrophoresis cell (Biorad, www.biorad.com), was assembled accordingly to the manufacturer's instructions. Protein samples were prepared to be loaded on gel for electrophoresis by the addition of 5 x sample buffer, followed by heating at 95 °C for 5 min to denature completely the

protein. Samples were slowly loaded onto the gel by using a Hamilton syringe.

The prestained protein molecular weight standard was purchased from

Fermentas (#SM0441) (www.fermentas.com). Samples were run at 100 V, for 1-

2 hours.

2.2.23 Western blotting

Proteins separated by SDS gel-electrophoresis were transferred to a

nitrocellulose membrane (lifesciences BIOTRACE NT 3M) (www.vwr.com) by

using a Bio-Rad mini protean3 trans blot module in 1x blotting buffer; samples

were transferred at 100 V for 60 min. Successively, the membrane was washed

with distilled water and incubated for 30 seconds with Ponceau S to visualize the

transferred proteins. After destaining in PBS-Tween 0.1 % for 15 min, the

membrane was washed again using PBS for 5 min and then incubated with

blocking solution for 4 hours or overnight. After this incubation, the filter was

washed twice for 5 min with PBS. Then an appropriate primary antibody from

rabbit was added at a suitable dilution (1:2000 for anti-GFP; 1:200 for anti-His6;

1:500 for anti-GST) in working solution and incubated for a minimum of 4 hours.

The primary antibodies used in this work were anti-GFP (Abcam,

www.abcam.com); anti-His6 (Santa Cruz Biotechnology, www.scbt.com); anti-

GST (Abcam).

The working solution was then discarded and the filter was washed 3 times for 10

min with PBS-Tween. After washing, the secondary antibody (goat anti-rabbit

IgG linked to horseradish peroxidase) (Santa Cruz Biotechnology,

www.scbt.com) was added at a dilution of 1:5000 in working solution and

incubated for at least 2 hours. The filter was washed 3 times for 10 min with

PBS-Tween and then other two times with PBS for 5 min. Then the filter was

immerged in ECL solutions and the luminescent signals were detect by GelDoc It

system (www.uvp.com). The ECL solutions were prepared as described in Table

A2.

2.2.24 *N. tabacum* protoplasts preparation

The abaxial surface of a *N. tabacum* leaf was punched using a device consisting

of 30 stainless steel needles set into a circular block. The midrib was removed

and the two halves of the leaf were placed with the abaxial side into a Petri dish

containing 7 ml of leaf digestion mix and incubated in the dark overnight. After

the overnight incubation the plates were gently shaken to allow protoplasts

release from the cuticle. The resulting heterogeneous mixture was then filtered

through a 100 µm nylon mesh filter and washed with washing buffer. The

protoplast solution obtained was centrifuged in 50 ml falcon tubes in a swing-out

rotor (Beckman Allegra centrifuge) at 100 g for 15 minutes. Pasteur pipette

connected to a peristaltic pump was used to remove the underlying medium and

the pellet of dead cells which were present under the floating band of living

protoplasts. The living protoplasts were resuspended in 25 ml of protoplasts

washing buffer and centrifuged at 100 g for 10 minutes. The dead cells and

underlying medium were removed as before and the entire procedure was

repeated twice more. Finally, the protoplasts were resuspended in an appropriate

final volume with MMM solution.

2.2.25 *N. tabacum* protoplasts transient transformation

Protoplasts suspension (300 µl) was gently pipetted into a 15 ml falcon tube

using a P-1000 tip with the cut end. A 30 µg aliquot of plasmid DNA was used

for the protoplasts transformation. Polyethylene glycol (PEG, Fluka) method was

used for direct gene transfer (Di Sansebastiano et al., 1998). Once the addition

of 300 µl of PEG, protoplasts were resuspended in 2 ml of TEX buffer. After 2

hours from the addition of the PEG, the protoplasts were rinsed to remove the

PEG. Then protoplasts were resuspended in 2 ml of TEX buffer and incubated at

26 °C in the dark, for 24 hours.

2.2.26 Harvesting of protoplasts and culture medium

After PEG transformation, the protoplast suspension inside the 15 ml falcon tube

was centrifuged in a swing-out rotor at 100 g for 5 minutes. The floating cell

layer was crossed using a refined Pasteur pipette to keep a sample of the culture

medium that was then collected into an Eppendorf tube on ice. The remaining

cell suspension was diluted 10-fold with 250 mM NaCl, and centrifuged as

before. The supernatant was removed with a Pasteur pipette connected to a

peristaltic pump and the resulting pellet was placed on ice. The proteins from the

cellular fraction were extracted by resuspending the pellet in 500 µl of 0.1 M Na-

acetate pH 5, followed by sonication for 5 seconds and centrifugation at 14,000

rpm for 10 min. at 4°C. The culture medium was centrifuged at 14,000 rpm for 5

min. at 4 °C, after the aliquots were taken for enzyme assay.

2.2.27 SecRGUS (Secreted Rat β-glucuronidase) assay

The extract and the medium saved after harvesting the cells were both directly

used to measure secRGUS (Leucci et al., 2007) and α-mannosidase (the

constitutive enzyme used as internal control) enzymatic activity. The reaction

substrates were 4-methyl-umbelliferyl-β-D-glucuronide (Sigma) and 4-methyl-

umbelliferyl-D-mannoside (Sigma) to measure secRGUS and α-mannosidase

activity, respectively. The samples were excited at 370 nm and the fluorescence

emitted measured at 480 nm using a multi-well microplate reader (TECAN Infinite

200) (http://www.tecan.com).

The criteria for evaluating the efficiency of secretion is provided by the ratio

between extra- and intracellular enzymatic activity this parameter represents the

"secretion index" (SI) (Denecke et al., 1990). Alpha-mannosidase, which is an

intracellular enzyme has been used as marker for contamination, caused by cell

breakage.

2.2.28 Alpha-amylase assay

The cells were resuspended in α-amylase extraction buffer (Crofts et al., 1999)

via sonication for 5 seconds. The extracts were centrifuged and the clean soluble

supernatant was recovered. The culture medium was also spun to remove

residual cell debris. The α-amylase assays and calculation of the secretion index

were performed as previously described (Crofts et al., 1999; Phillipson et al., 2001). The secretion index represents the ratio between the extracellular and intracellular activity (Crofts et al., 1999).

2.2.29 Confocal microscopy

Fluorescent proteins are able to absorb light at specific wavelengths and to emit light at longer wavelength. For example, the green fluorescent protein adsorbs light blue and emits green fluorescence (Morise et al., 1974). In figure 2.1 are represented the main components of Leica SP5 confocal microscope. In contrast to the confocal microscopes proposed by other manufactures (Zeiss, Olympus, Nikon), the microscope SP5 Leica is deprived of dichroic filters. The excitation light emitted from the laser, passes through a crystal called acousto optical beam splitter (AOBS). The reflected light is focused on the sample by the objective lens. The light emitted from the sample is collected from the objective and it is directed in focus on the pinhole. This means that the focal plane on the sample and the pinhole are confocal, i.e. they are situated on conjugated planes. So the only light that can cross the pinhole and be collected from photomultiplier comes from the confocal plane.

Confocal imaging was performed by using an upright Leica SP5, and a 63 x oil immersion objective or 20 x dry objective. For imaging expression of GFP constructs, YFP constructs or both were used imaging settings as described: excitation lines of an argon ion laser of 458 nm for GFP and 514 nm for YFP were used alternately with line switching on the sequential scan facility of the

microscope. GFP fluorescence was detected by using an AOBS with 500- to

520-nm spectral range, and YFP fluorescence was detected with a 560- to 600-

nm spectral range. In this manner, it was possible to avoid every kind of

communication and bleeding of fluorescence (Hutter, 2004). The cyan

fluorescent protein was excited by using a 405 nm violet diode laser and

detected by using a 460-530 nm spectral range. In all the figures, image

acquisition was carried out with same imaging settings of the microscope (laser

intensity, pinhole aperture, detector gains, zoom and line averaging). Cells'

images with similar levels of saturation of the imaging pixels, as determined by

the palette function of the microscope software, were acquired. This method

allows us to compare the fluorescent proteins expression levels among cells

(daSilva et al., 2004). Adobe photoshop imaging suite was used for further image

handling.

① Visible range lasers (up to 5)	⑨ Multi Function Port (MFP)	⑱ X1-emission port
② IR laser	⑩ Tandem Scanner	⑲ Spectrophotometer prism
③ UV laser	⑪ Calibration target	⑳ PMT channel 1
④ Visible range AOTF	⑫ Field rotation optics	㉑ PMT channel 2
⑤ IR EOM	⑬ Objective lens	㉒ PMT channel 3
⑥ UV AOTF	⑭ Transmitted light dedector	㉓ PMT channel 4 (optional FLIM)
⑦ UV optics imaging	⑮ Reflected light NDD	㉔ PMT channel 5 (optional FLIM)
⑧ AOBS	⑯ Confocal detection pinhole	
Acousto Optical Beam Splitter	⑰ Filter- and polarizer wheel	

From Leica (www.Leica.com)

Figure 2.1: Schematic representation of a confocal microscope.

3. RESULTS

3.1 AGD5 Localizes at the Trans-Golgi Network

3.1.1 Bioinformatic analysis of AGD proteins

The *A. thaliana* genome encodes for 15 proteins of the ARFGAP family and, among them, three groups are relatively similar to the yeast ARFGAPs acting at the TGN, Age2p, Gcs1p and Glo3p (Donaldson, 2000; Jensen et al., 2000; Jurgens and Geldner, 2002).

A bioinformatics search of *A. thaliana* genomic database (http://mips.gsf.de) was performed by using the yeast Age2p (accession number P40529) as a query sequence. In particular, At5g54310 is judged to be the plant homologue of yeast Age2p (Jurgens and Geldner, 2002), and human SMAP2 (stromal membrane-associated protein 2), which is a GAP for ARF6. Using this data, a phylogenetic tree was constructed (Figure 3.1). AGD5 was also used as subject on the Eukaryotic Linear Motif (ELM) (http://elm.eu.org/) resource for predicting functional sites in protein sequences. This analysis revealed that at the amino acid level in the position 293-297 emerges a FxDxF motif which in animal cells is responsible for the binding of accessory endocytic proteins to the appendage of the alpha-subunit of adaptor protein complex AP-2 (Figure 3.2). These data support the idea that AGD5 may be involved in the post-Golgi trafficking.

In non-plant systems, the mechanism by which GAP proteins stimulate GTP hydrolysis on GTPases was demonstrated to involve an arginine residue that is located inside the GAP domain. Therefore, multiple sequence alignment by ClustalW (http://www.ebi.ac.uk/clustalw/) of the ARFGAP proteins from human,

yeast and Arabidopsis revealed that the arginine residue in the ARFGAP domain

of AGD5 is conserved (Figure 3.3).
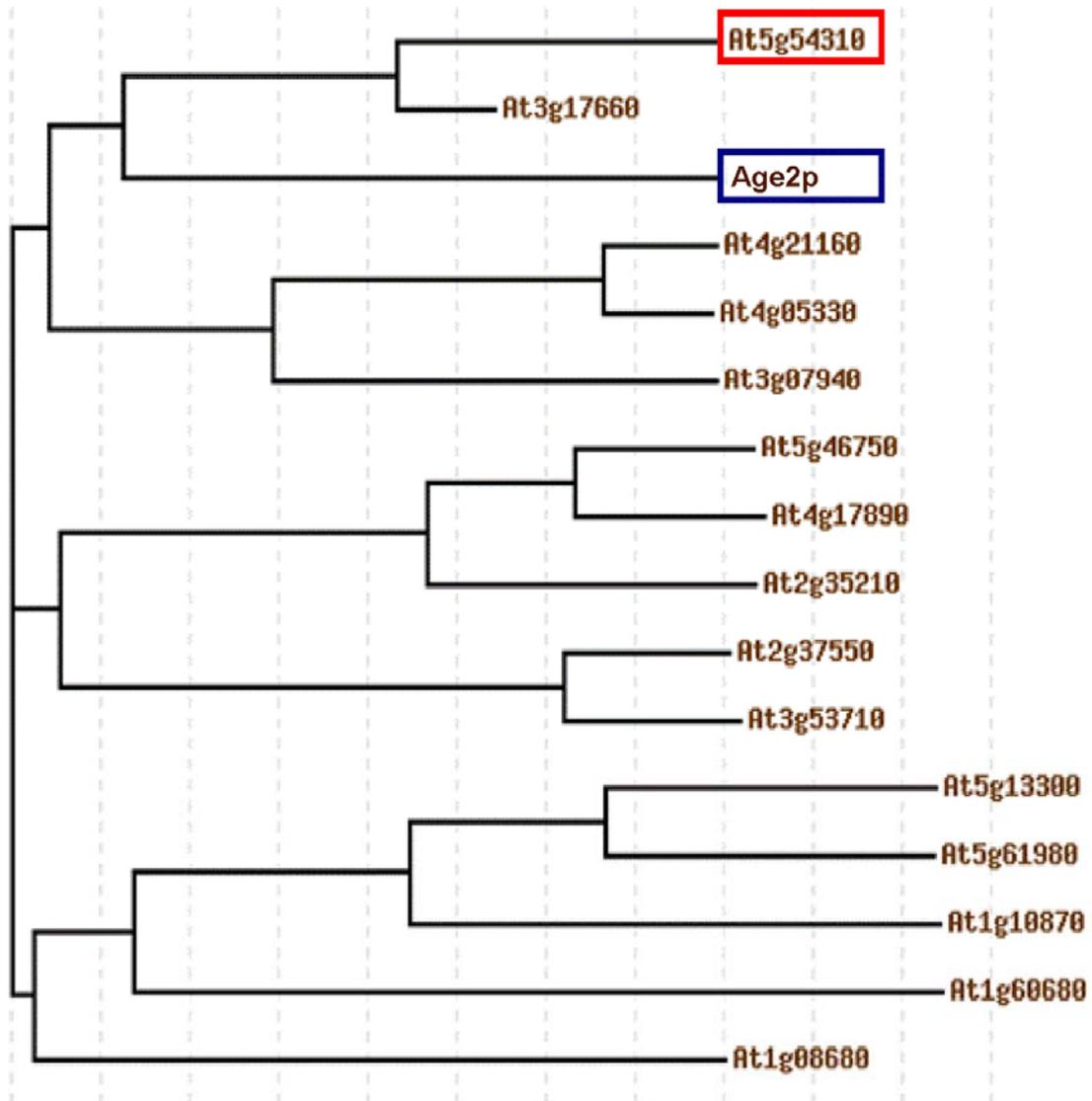
Figure 3.1: Phylogenetic tree of AGD1-AGD15 from Arabidopsis and Age2p from yeast.

Loci numbers of *AtAGD1* to *AtAGD15* are as follows: At5g61980 (*AtAGD1*), At1g60680

(*AtAGD2*), At4g13300 (*AtAGD3*), At1g10870 (*AtAGD4*), At5g54310 (*AtAGD5*), At3g53710

(*AtAGD6*), At2g37550 (*AtAGD7*), At4g17890 (*AtAGD8*), At5g46750 (*AtAGD9*), At2g35210

(*AtAGD10*), At3g07490 (*AtAGD11*), At4g21160 (*AtAGD12*), At4g05330 (*AtAGD13*), At1g08680

(*AtAGD14*), and At3g17660 (*AtAGD15*).
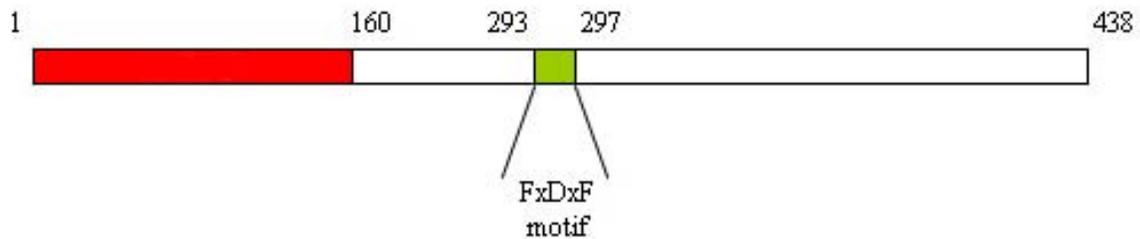
Figure 3.2: Functional domain and motif of the AGD5 protein. These regions include a GAP

activity domain (aa1-160), a FxDxF motif important for the binding of accessory endocytic

proteins to the alpha-subunit of adaptor protein complex AP-2 (aa293-297).

Figure 3.3: Multiple sequence alignment by ClustalW of ARFGAPs. *A. thaliana* AGD5

(At5g54310), *S. cerevisiae* Age2p (YIL044C) and human SMAP2 (Q8WU79). The conserved

arginine amino acid is highlighted by a black rectangle.

3.1.2 Subcellular distribution of AGD5 in *N. tabacum* plant cells

One of the aims of this study is to define the cellular role of AGD5 and its

localization in plant cells. To determine the subcellular localization of AGD5, the

DNA was amplified, then cloned into a binary vector pVKH18EN6 to create a

fusion between the 3' end of the DNA sequence coding for YFP (yellow

fluorescent protein) and. The plasmid was then used to transform *A.*

tumefaciens. Then, *N. tabacum* leaves were infiltrated with *A. tumefaciens* strain,

and examined 48 or 72 hours later by confocal microscopy. The protein

expression at low levels obtained using a low concentration (O.D.$_{600}$ = 0.05) of *A.*

tumefaciens, shown by fluorescence in the cell, was localized at punctate

structures (Figure 3.4, arrowhead) and in the cytosol (Figure 3.4, arrow). The

punctate structure looks like that of plant Golgi complex. To investigate if the

dots belonged to the Golgi apparatus, co-transformation experiments were

performed by using ERD2-CFP, a Golgi apparatus marker (Boevink et al., 1998).

Laser scanning confocal microscopy revealed that YFP- AGD5 does not co-

localize with ERD2-CFP, but labels punctate structures that were not labelled by

the Golgi apparatus marker. Furthermore, the structures were often close to the

Golgi apparatus and sporadically moved jointly inside the cytoplasm, but their

closeness was only temporary (Figure 3.4).

To determine the identity of these non-Golgi structures, YFP-AGD5 was

coexpressed with plant post-Golgi markers. One of the post-Golgi markers used

for co-expression experiments was the TGN marker, SYP61. A colocalization of

AGD5 and SYP61 was found (Figure 3.5). Therefore, it is possible to deduce that

the punctate structures highlighted from AGD5 are TGN. Furthermore, since

YFP-AGD5 strictly localize at the TGN, it can be considered as a new TGN

marker.
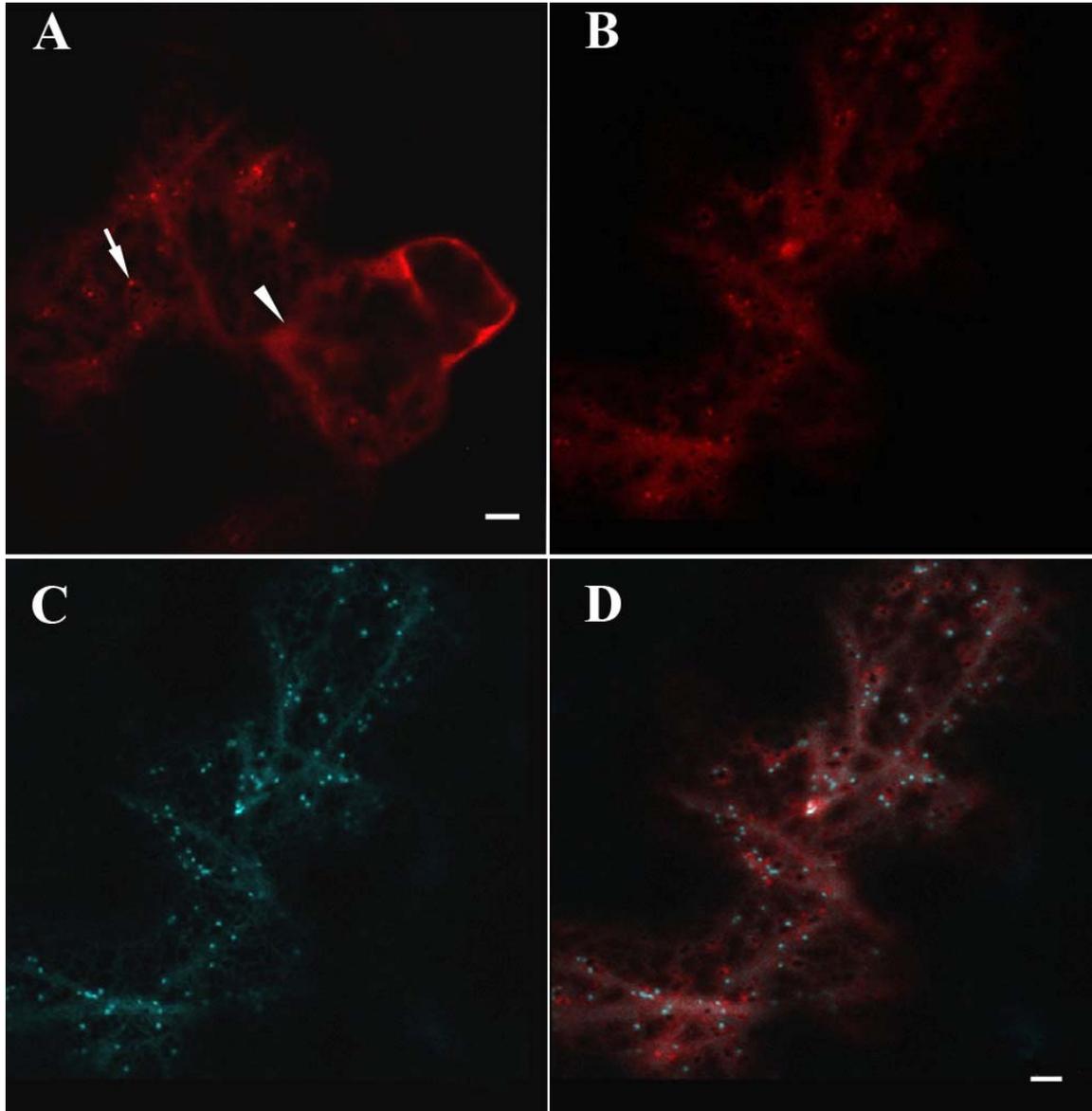
Figure 3.4: Subcellular distribution of AGD5 in *N. tabacum* plant cells A-D. Confocal images

of tobacco leaf epidermal cell 2 days after *A.tumefaciens* infiltration. YFP-AGD5 either alone (**A**)

or with a Golgi marker, ERD2-CFP (**B-D**) shows that the fluorescence was distributed as punctate

structures (arrow) and in the cytosol (arrowhead). **C.** ERD2-CFP **D.** Merged image of **B** and **C**.

Scale bars = 5 μm.
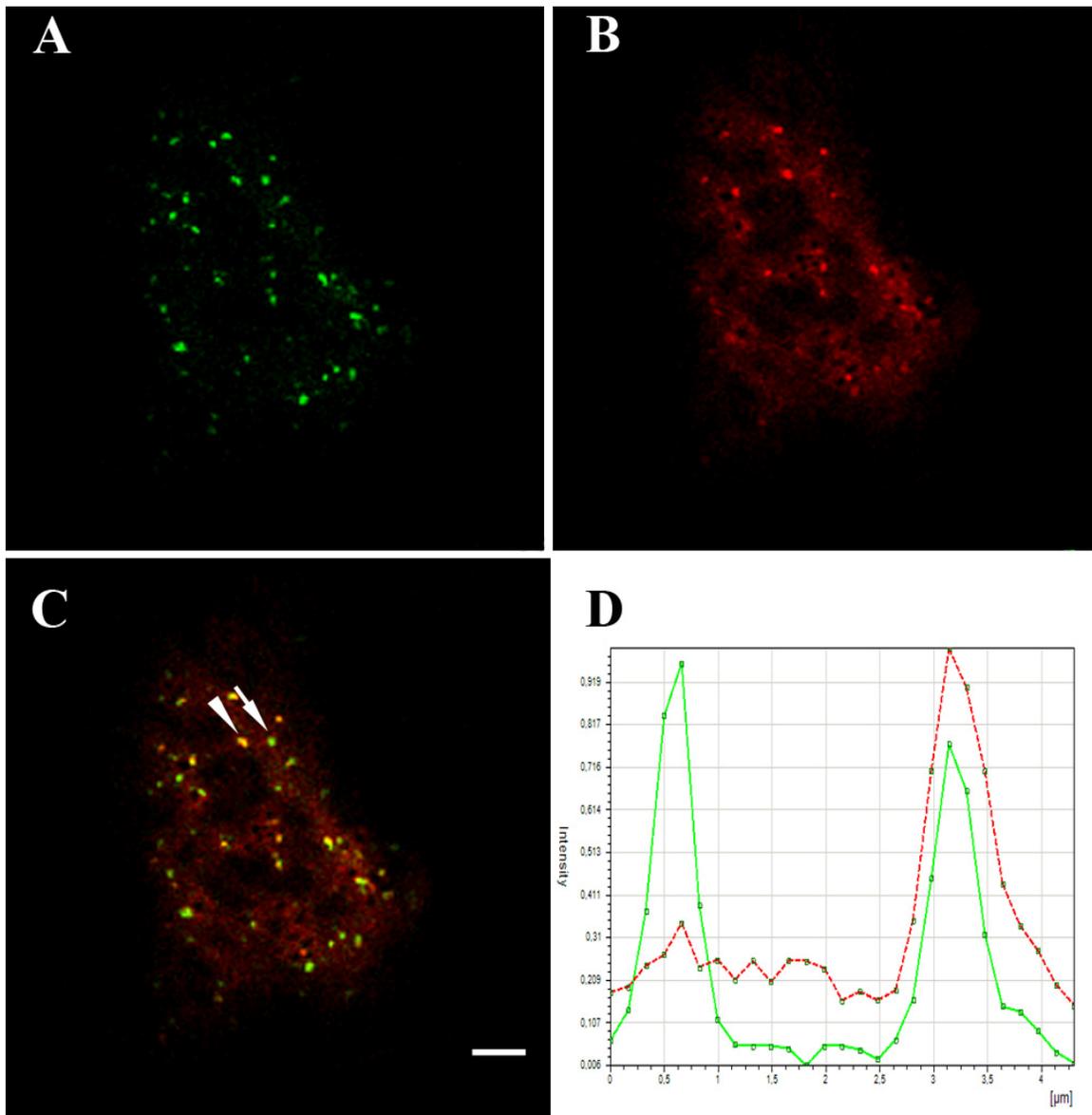
Figure 3.5: Subcellular distribution of AGD5 and with SYP61 in *N. tabacum* plant cells. A-C.

Confocal images of tobacco leaf epidermal cell 2 days after *A.tumefaciens* infiltration.YFP-AGD5

with a TGN marker, GFP-SYP61 (**A-C**) shows that the fluorescence was distributed as punctate

structures, which colocalize with the TGN, but it possible to observe additional SYP61 dots

(arrow).**B**. GFP-SYP61D. Merged image of **A** and **B**. Scale bars = 5 µm.

3.2 AGD5 localizes with the ARF1 on the Trans-Golgi Network

3.2.1 AGD5 is distributed in the same cellular compartments as ARF1GTPase

In yeast cells, the potential involvement of ARF1 in the post-Golgi transport, AP-1 and AP-3 pathways has been showed (Cowles et al., 1997; Stepp et al., 1997; Yahara et al., 2001).

Studies on plant cells, have shown that ARF1 localizes to the Golgi complex and also resides to organelles not labelled by the Golgi apparatus markers, but stained using the endocytic marker FM4-64 (Bolte et al., 2004; Xu and Scheres, 2005; Stefano et al., 2006).

Since the subcellular distribution of AGD5 looks like ARF1 non-Golgi structures, tobacco leaf epidermal cells were co-transformed with the YFP-AGD5 and ARF1-GFP fusion, then observed by confocal microscopy 48 hours after *A. tumefaciens* infiltration. Colocalization studies showed that ARF1-GFP partially overlaps with YFP-AGD5, which was previously found on the TGN (Figure 3.6).
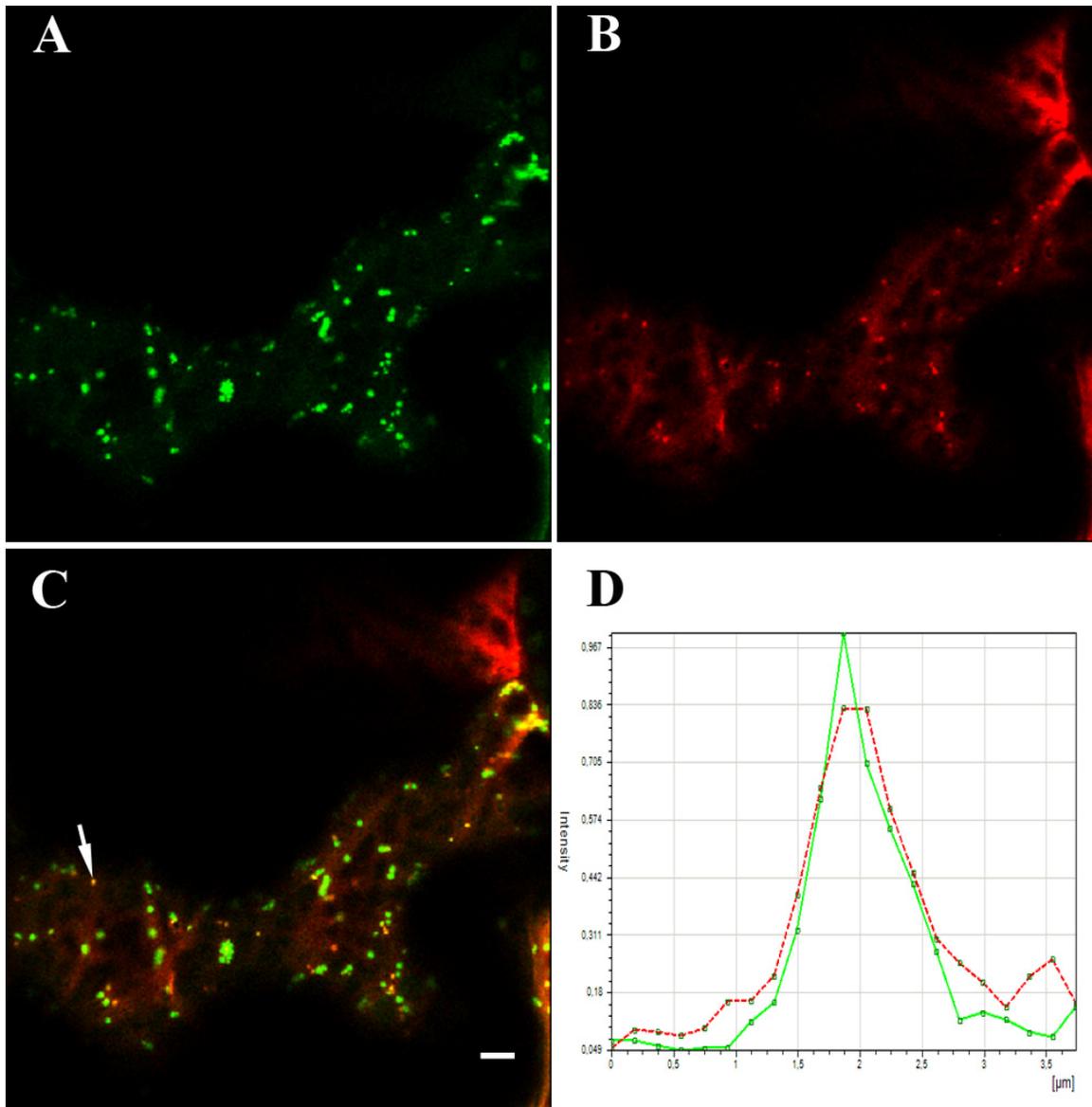
Figure 3.6: Subcellular distribution of AGD5 and ARF1 in *N. tabacum* plant cells. A-C.

Confocal images of tobacco leaf epidermal cell 2 days after *A.tumefaciens* infiltration. YFP-AGD5

fluorescence (**A**) partially overlaps with ARF1-GFP (**B**) **C**. Merged image of **A** and **B**. Scale bars

= 5 µm.

3.2.2 Interaction between ARF1 protein produced in planta and AGD5 obtained from *E. coli* cells (planta-*E. coli* system)

The partial fluorescence overlap for AGD5 and ARF1 led me to question whether AGD5 could bind ARF1GTP bound form, considering that GAP proteins assist GTPase molecules in stimulating GTP hydrolysis. To investigate the interaction between AGD5 and ARF1GTP, the DNA AGD5 sequence was amplified and sub-cloned into pGEX-4T1-GS vector downstream of the Glutathione S-Transferase (GST) coding sequence (GST- AGD5). The interaction of a recombinant GST- AGD5 with protein extract from tobacco leaves, expressing ARF1-YFP protein, was performed by glutathione-agarose resin. Then GST-AGD5 protein was conjugated with glutathione-agarose beads and tested to determine if AGD5 would bind a mutant form of ARF1 (*ARF1GTP-YFP*) a protein expressed in tobacco leaves (Figure 3.7). The interaction between these proteins was analyzed by western blot probed with an anti-GFP antibody. The western blot showed that *ARF1GTP-YFP* fusion proteins, from leaf extracts can interact with recombinant GST-AGD5 (Figure 3.7, lanes 4).

These data suggest that AGD5 is involved in the GTP hydrolysis of plant ARF1 to the TGN compartment. However, this experiment did not reveal if the interaction of ARF1 with AGD5 is direct or mediated by other proteins.
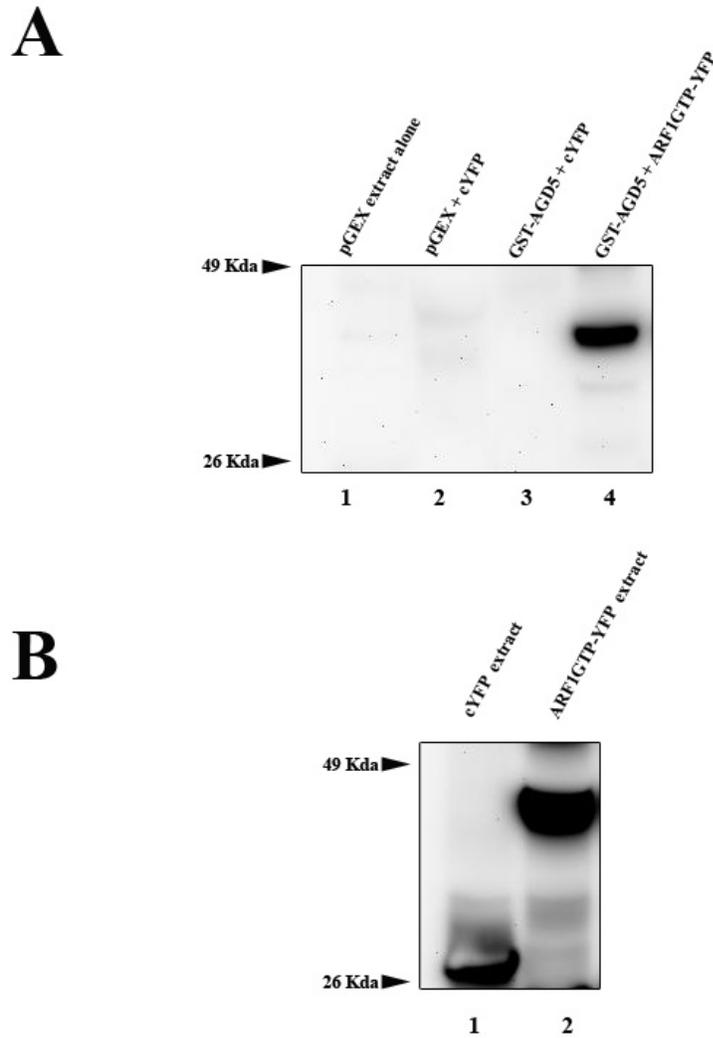
Figure 3.7: Interaction between GST-AGD5 and *ARF1GTP* protein produced in *N. tabacum* plant. A. Western blot probed with an anti-GFP antibody. *ARF1GTP-YFP* (lane 4) was retained by GST-AGD5. Negative controls: extracts of pGEX and pGEX loaded with cytosolic YFP to test the specificity of the resin (lane 1-2); Negative controls: GST-AGD5 did not retain cytosolic YFP (lane 3). **B**. Western blot analysis with anti-GFP antibody of the extracts of leaves expressing the YFP fusions of cYFP (lane 1) and *ARF1GTP-YFP* (lane 2).

3.2.3 Interaction between AGD5 and ARF1 proteins produced in

heterologous *E.coli* cells

The data obtained with the planta-*E. coli* system (described in Section 3.7)

showed that the small GTPase ARF1 from leaf extracts was able to bind the

AGD5 protein; however these results do not discriminate between a direct or

indirect binding of the GTP hydrolysis activity. In fact, AGD5 should necessitate a

cofactor or adaptor protein to bind the GTPase ARF1. It not excluded that an

intermediary protein functions like an activator between the GTPase and AGD5

protein. Therefore, to determine if the interaction between ARF1 and AGD5

required the presence of adaptors, either cytosolic or TGN associated proteins,

the interaction between ARF1 and AGD5 was tested in an acellular system. In

addition, an heterologous *E.coli* cell system interaction was used to measure the

specificity of the interaction between ARF1 proteins and AGD5. An equal amount

of purified ARF1 protein and its mutants was used for the binding assay. In each

glutathione column an equal amount of bacterial lysate of *E. coli* expressing

GST-AGD5 was loaded; this method allowed to observe a possible difference in

the interaction between GDP or GTP bound form of ARF1 and the AGD5.

Subsequently, the unbound proteins were removed from the glutathione columns

with different steps of washing. Then, bacterial lysates of strains expressing

ARF1wt-His6, *ARF1GDP-His6* or *ARF1GTP-His6* were applied onto the columns

containing the GST-AGD5 linked to the resin. The bound proteins were eluted

and loaded on an SDS-gel, and transferred to nitrocellulose membranes. The

western blot was analyzed with anti-His6 antibody (Figure 3.8, lanes 1-4). To

show that GST-AGD5 was equally loaded on each column, a western blot was

performed and analyzed with anti-GST antibody (Figure 3.8, lanes 5-8). Finally,

to prove that similar quantities of ARF1wt-His6, *ARF1GDP-His6* and *ARF1GTP-*

His6 were loaded on the GST-AGD5 columns, a western blot on a fraction of the

total protein extracts from *E. coli*, expressing the His6-tagged ARF1 proteins,

was performed. After detection with anti-His6 antibody, it was possible to see

comparable amounts of the ARF1 proteins from *E. coli* extracts (Figure 3.8). This

control was necessary to be sure that the same amount of protein was loaded,

excluding the possibility that the result could be due to a different quantity of

proteins applied to the columns. Taken together, these data have been the first to

show that the association of ARF1 with AGD5 occurs with all the three ARF1

forms. This suggests that the interaction of AGD5 happens in a way that is

independent of the ARF1 active or inactive form (Figure 3.8). Moreover, this

experiment confirmed the results from the interaction between ARF1 and AGD5

obtained with glutathione-agarose beads, by using *N.tabacum* leaf cells extracts,

suggesting that the interaction between active ARF1 and AGD5 does not require

other adaptor proteins but is direct.
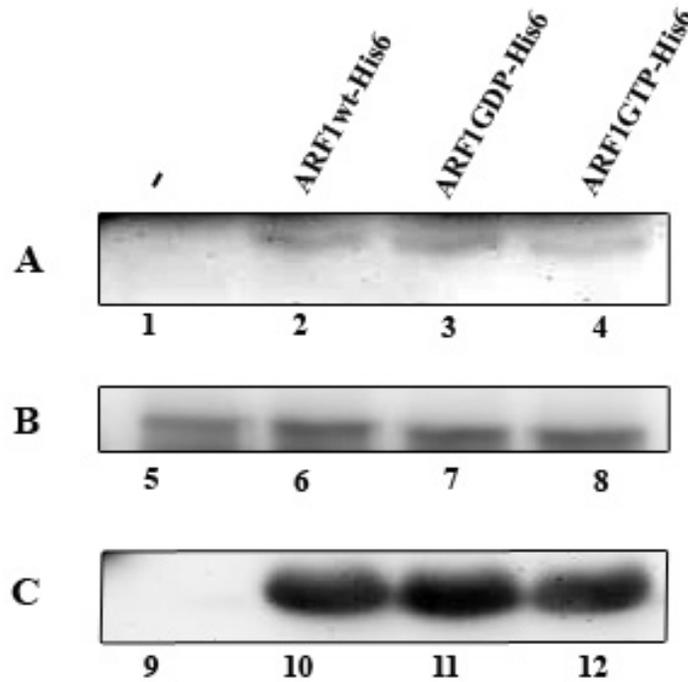
Figure 3.8: Interaction between AGD5 and ARF1 proteins produced in heterologous *E.coli*

cells. A. Lanes 1-4: Western blot probed with anti-His6 antibody. Extracts of *E. coli* at identical

total protein concentration, expressing His6-tagged *ARF1GDP* (lane 2) and *ARF1GTP* mutants

(lane 3), were loaded onto GST-AGD5 beads. Eluates of these columns were subject to

immunoblot analysis. Negative control: extracts from *E. coli* expressing His6-tag alone (lane 1).

B. Lanes 5-8: Western blot probed with anti-GST antibody showing that the amount of GST-

AGD5 bound to agarose beads was similar for all samples. **C. Lanes 9-12**: western blot with a

His6-antibody on a fraction of *E. coli* extracts loaded onto the GST columns showing that

comparable amounts of ARF1wt (lane 10), *ARF1GDP* (lane11) and *ARF1GTP* (lane 12) mutants

were used for the experiment. Negative control: extracts from *E. coli* expressing His6-tag alone

(lane 9).

3.3 Catalytic activity of AGD5 towards ARF1

3.3.1 Site-directed mutagenesis of the AGD5

To study in detail the catalytic activity of AGD5 towards ARF1, the amino acid

residue of the AGD5 involved in the GTP hydrolysis of the small GTPase ARF1,

which is a conserved residue and mediate this process in yeast and in

mammalian cells , was mutated (Szafer et al., 2000). The mutant of the AGD5

was obtained by substituting the highly conserved arginine at position 59 with

glutamine (*AGD5[R59Q]*) (Figure 3.3). Overlapping PCR as described in section

2.2.2 produced the mutant (*AGD5[R59Q]*). Then, *AGD5[R59Q]* was subcloned in

the pVKH18EN6 vector downstream the YFP coding sequence (*YFP-*

AGD5[R59Q]).

3.3.2 Subcellular distribution of AGD5 mutant

To examine the subcellular distribution of AGD5 mutant *in vivo*, i.e. in tobacco

leaf epidermal cells, the sequences of AGD5 mutant with a fluorescent protein

fused at the N-terminus was used for confocal microscopy analysis. Then *YFP-*

AGD5[R59Q] expressed in tobacco leaves by using Agro-infiltration (Figure 3.9).

Laser scanning confocal microscopy revealed that this mutant was still capable

to bind to the TGN apparatus, labelled with SYP61. This result shows that

arginine in position 59 does not abolish the protein's TGN association. This also

suggests, that this amino acid was not directly involved in the binding to the TGN

compartment (Figure 3.9). The subcellular localization in tobacco cells, combined

with the heterologous *E.coli* cells system results of AGD5 with ARF1wt, GDP and

GTP supports the idea that AGD5 directly binds ARF1 for recruitment to the

TGN, independently from the arginine 59.
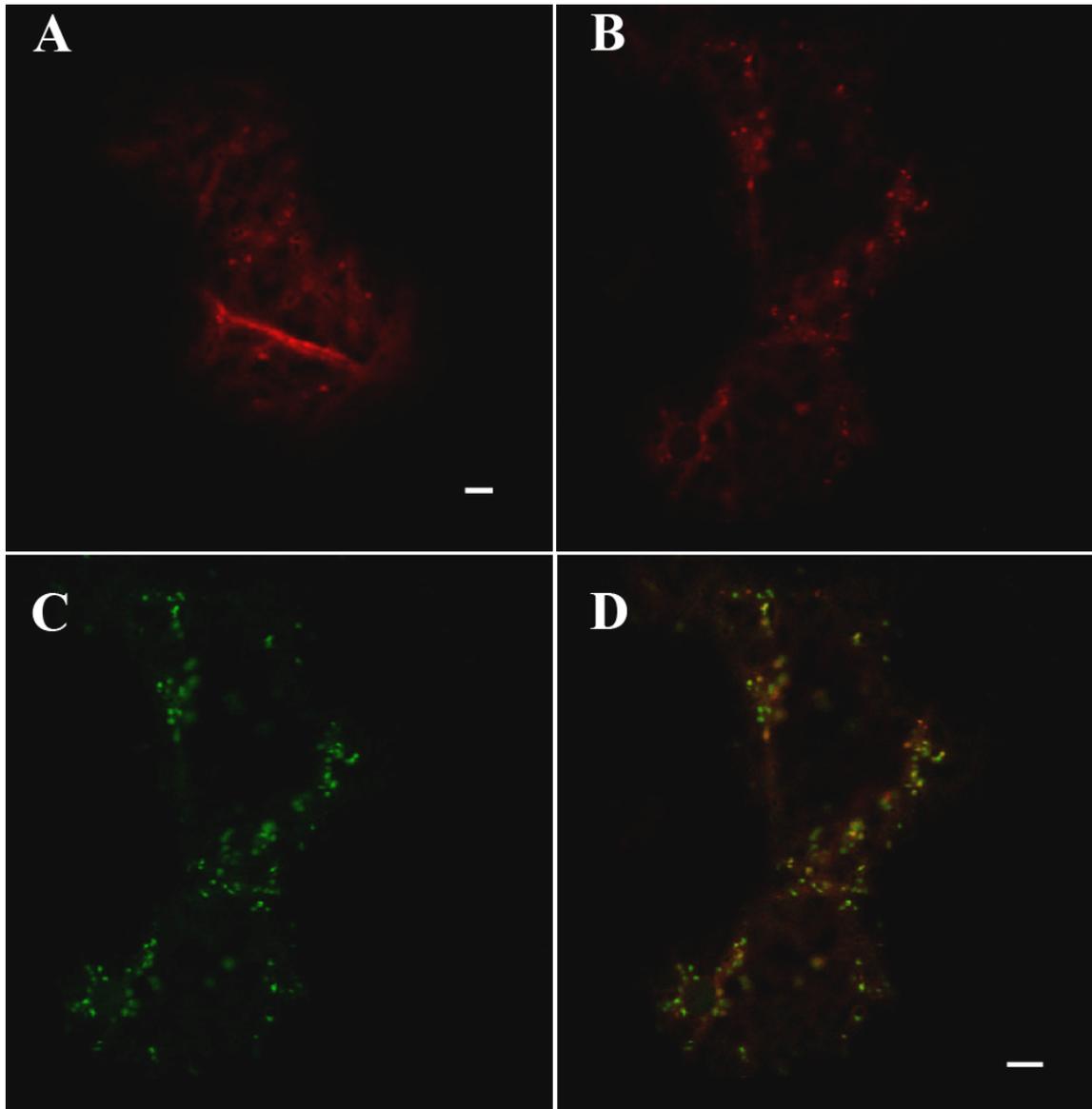
Figure 3.9: Subcellular distribution of AGD5 mutant. Confocal images of tobacco leaf

epidermal cells 2 days after *A.tumefaciens* infiltration. YFP-AGD5 either alone (**A**) or with a TGN

marker, (GFP-SYP61) (**D**) shows that the fluorescence was distributed as punctate structures and

in the cytosol. **C.** GFP-SYP61 **D.** Merged image of **B** and **C**. Scale bars = 5 μm.

3.3.3 Subcellular distribution ARF1 and AGD5 mutant proteins in *N. tabacum* plant cells

To investigate whether the highly conserved residue in position 59 of AGD5, could have a reduced activity for the GTP hydrolysis of ARF1 onto the TGN membrane, a coexpression experiment was performed. ARF1wt-GFP was coexpressed with *YFP-AGD5[R59Q]* in tobacco leaf epidermal cells for confocal microscopy investigation. The effect of this mutant form on the subcellular localization of ARF1wt-GFP was examined (Figure 3.10). Laser scanning confocal microscopy revealed that the fluorescence relative to the protein ARF1wt was mainly localized in the cytosol. Whereas, ARF1wt was mostly associated with the Golgi apparatus and non-Golgi structures when coexpressed with AGD5 wild type form, which has not mutated arginine residue (Figure 3.10). All these results confirm the predicted structural data that arginine 59 is involved in the catalytic activity responsible for switching ARF1 to the GDP bound form.
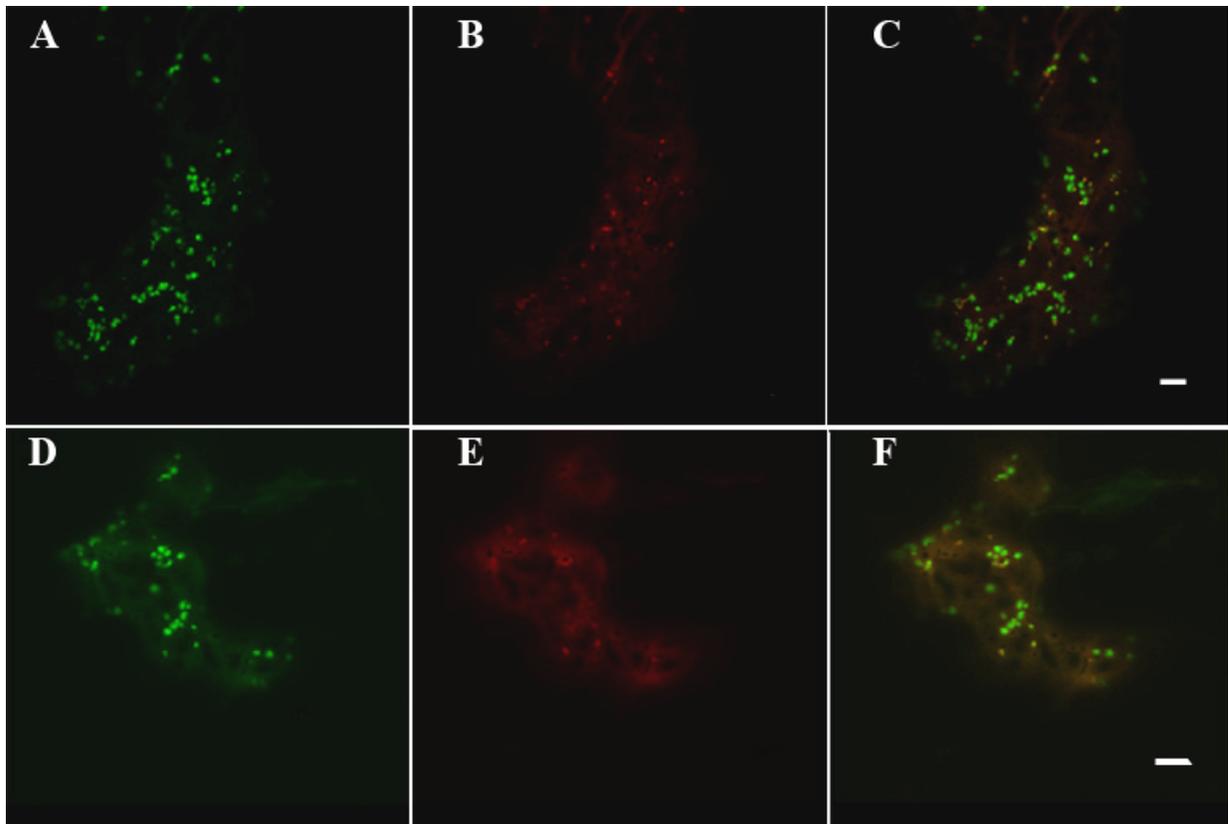
Figure 3.10: Subcellular distribution of ARF1 in presence of AGD5 and its mutant. Confocal

images of tobacco leaf epidermal cells 2 days after *A.tumefaciens* infiltration. Wild-type AGD5

(**B**), overlap to TGN bodies jointly with ARF1-GFP (**A**). *AGD5[R59Q]* (**E**) redistributes ARF1 in the

cytosol (**D**). Note that the mutation at position 59 nearly abolished the protein's Golgi association.

C, **F** are merged images respectively of **A** and **B**, **D** and **E**. Scale bars = 5 µm.

3.4 YFP-AGD5, in transgenic *A. thaliana* plants

3.4.1 YFP-AGD5 is specifically localized to root cells

In plant cells, relatively little is known about the establishment of polarity and its

effect on morphogenesis. Post-Golgi network and endocytic cycling of plasma

membrane proteins were considered for its potential role in cell polarity and

development (Geldner et al., 2003; Meckel et al., 2004, 2005; Xu and Scheres,

2005).

To determine the cellular expression pattern of AGD5 in plants, the P35S: YFP-

AGD5 construct was introduced into *A. thaliana* via Agrobacterium-mediated

transformation. After antibiotic selection, the overexpression line was subject to

RNA extraction. The mRNA level of AGD5 overexpression differs significantly

compared to the wild type (Figure 3.11). Confocal microscopy on transgenic lines

showed that the fluorescence is mainly distributed along the root. The subcellular

distribution of YFP-AGD5 was detected as punctate structures along the root but

mainly in the apical part (Figure 3.12). Furthermore, analysis of root hair in

transgenic lines overexpressing AGD5 displays the bulged root hair phenotype.

Additionally, in the apical part when AGD5 is highly overexpressed root tip

showed an abnormal phenotype (Figure 3.13).
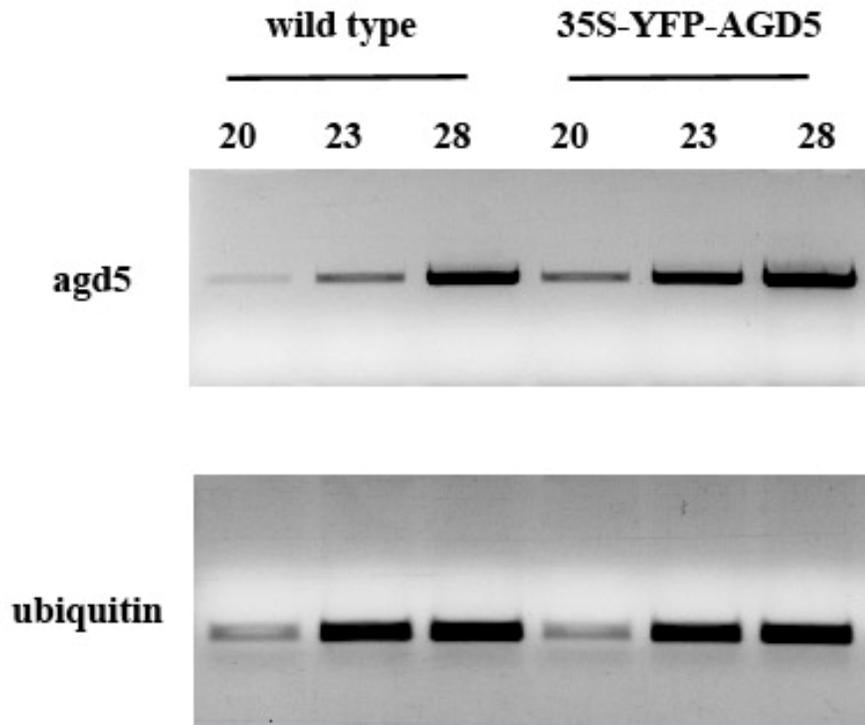
Figure 3.11: RT-PCR analysis of agd5 gene. Two week-old plants PCR products were

visualized by staining with ethidium bromide after electrophoresis.
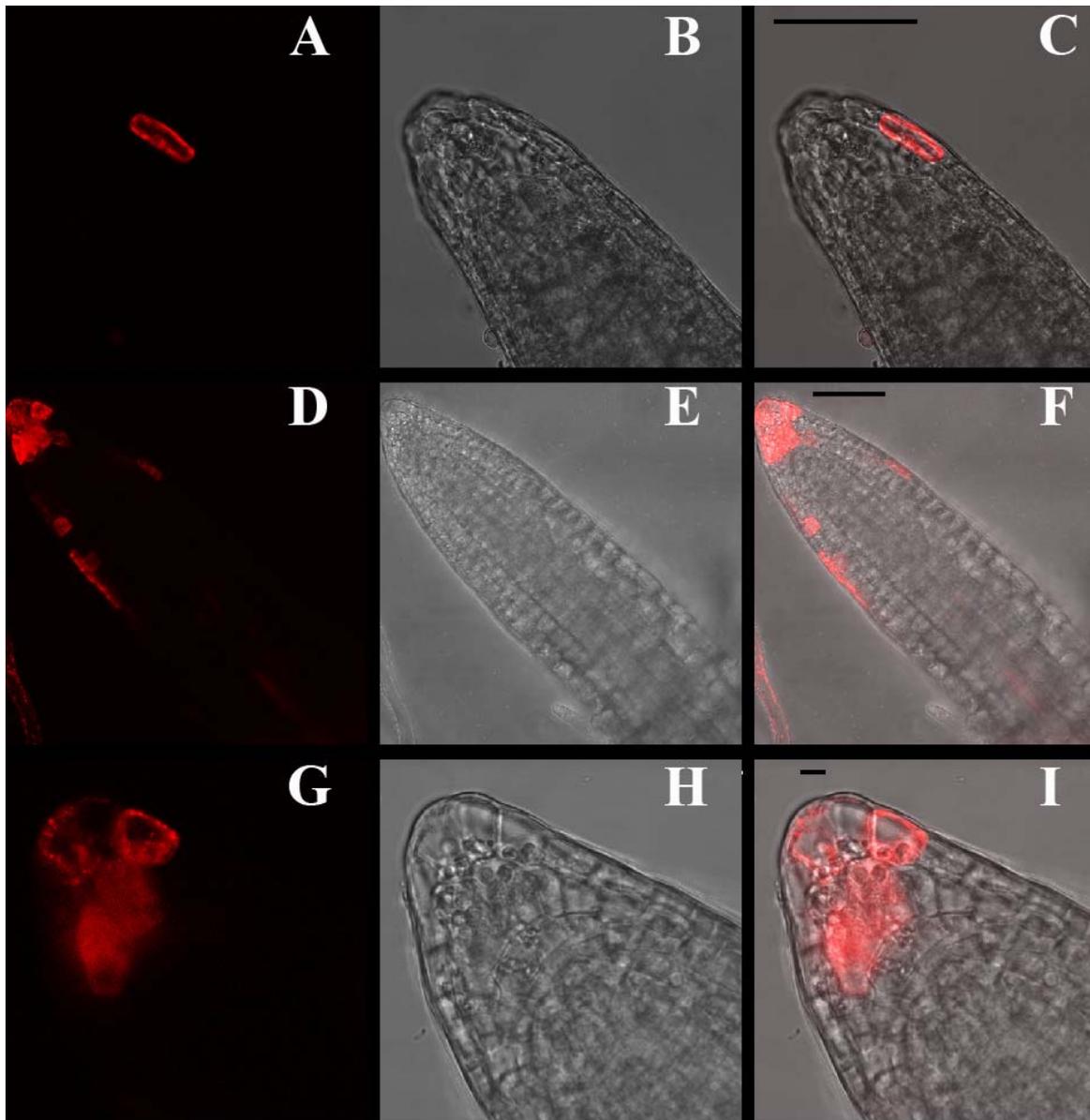
Figure 3.12: Subcellular distribution of AGD5 in *A. thaliana* root cells A-I. Confocal images

of stable Arabidopsis root cells. YFP-AGD5 was distributed in the root apex. Scale bars = 50 µm.
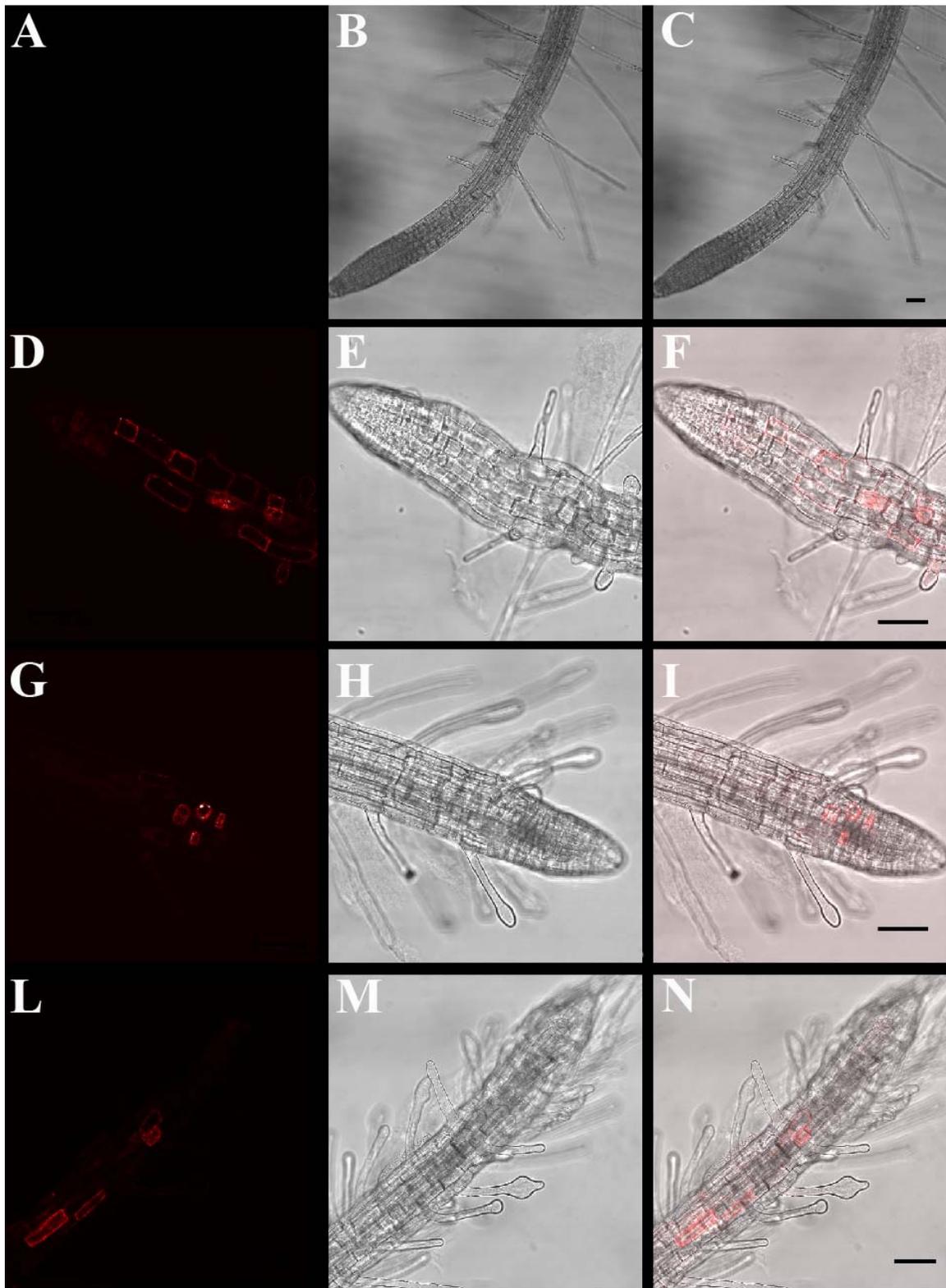
Figure 3.13: Subcellular distribution of AGD5 in Arabidopsis root cells. D-N. Arabidopsis

wild type **A-C.** Confocal images of stable Arabidopsis root cells. YFP-AGD5 was distributed in

the root apex and hair root show various phenotypes compared to the wild type. Scale bars = 50 µm

3.4.2 Overexpression YFP-AGD5 in *A. thaliana* pollen

To examine the viability of pollen grains in the AGD5 overexpressed lines; pollen grains were collected from transgenic plants and observed after 5 hours of germination in a growth medium. Laser confocal microscopy revealed that the pollen viability of transgenic plants was high compared to the wild type plants. In addition, the germinated pollens displayed different phenotypes.

Most of the pollen grains of transgenic plants showed expanded tubes with swollen tips, twisted tubes, and bifurcate tips (Figure 3.14).
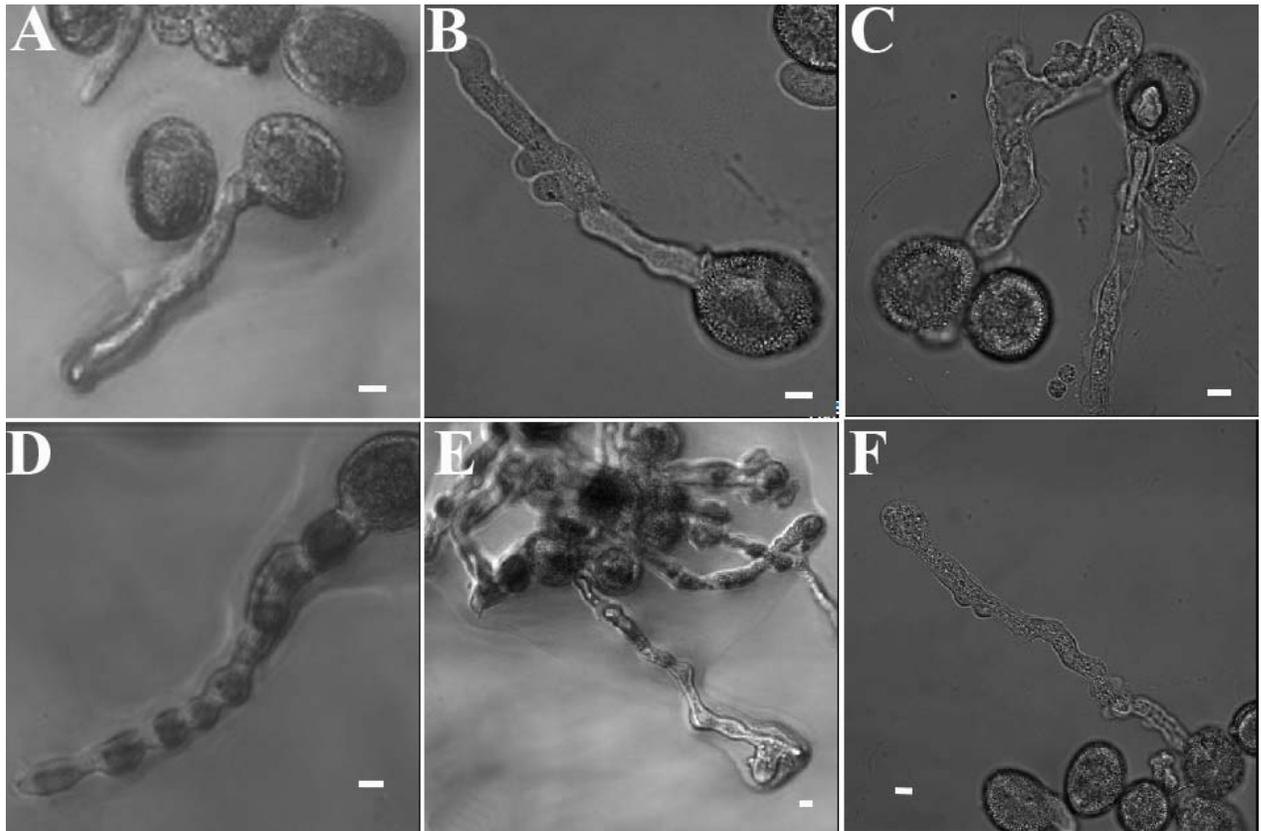
Figure 3.14: *A. thaliana* pollen development A-F images of Arabidopsis pollen after 5 hours of germination. Wild type (**A**) and transgenic line overexpressing YFP-AGD5 (**B-F**) shows various phenotypes. Scale bars = 5 μm.

3.5 ARF1 and AGD5 affects protein secretion in *N. tabacum* transformed protoplasts

3.5.1 ARF1 mutants affect protein secretion in *N. tabacum* protoplasts

To test the effects on the secretory pathway exercised by ARF1-GFP in comparison to the untagged counterpart, it was determined whether this fusion protein, and its GDP- and GTP-restricted mutants exhibited similar effects on protein secretion as the equivalent untagged ARF1 wild-type and its mutant forms (Phillipson et al., 2001). To test the effect of the GFP-protein fusions on secretion, *N. tabacum* leaf protoplasts were cotransfected with the secretory marker α-amylase (Phillipson et al., 2001) and a dilution series of ARF1-GFP, *ARF1GDP-GFP*, and *ARF1GTP-GFP*. It was expected that ARF1 dosage alone should not affect secretion; in contrast, the two mutant proteins (GDP and GTP bound forms) should have a negative effect on the α-amylase secretion (Phillipson et al., 2001; Takeuchi et al., 2002; Pimpl et al., 2003). Accordingly, ARF1-GFP does not affect α-amylase secretion form (Figures 3.15). These data indicate that ARF1 dosage alone does not affect the secretory pathway, as reported in previous studies, and that ARF1-GFP has the same effect as the untagged counterpart. In contrast, the tagged *ARF1GDP* and *ARF1GTP* proteins

have a negative effect on the α-amylase secretion, which is stronger using the

GDP blocked (Figures 3.15).
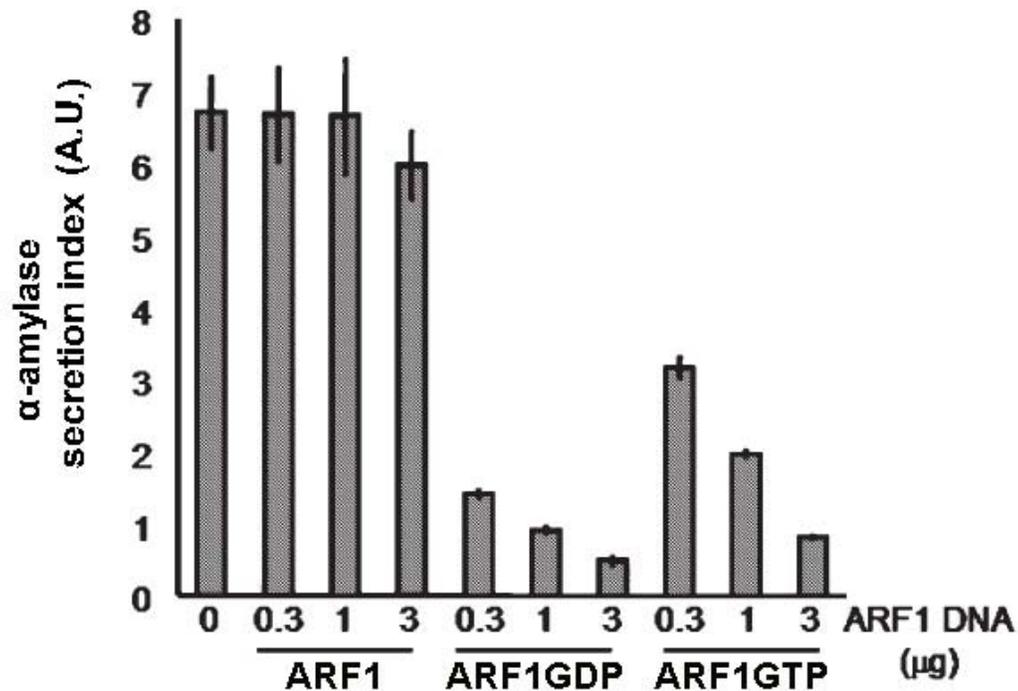
Figure 3.15: Secretion α-amylase assay using *N. tabacum* leaf protoplasts. The graph

shows the secretion index of α-amylase [ratio of extracellular and intracellular activities which is

expressed in arbitrary units, Phillipson et al. (2001)] in protoplasts expressing untagged ARF1,

ARF1GDP, and *ARF1GTP*. Concentrations of DNA for each sample are indicated along the x-

axis. Error bars = standard error of the mean for three independent repetitions. (Figure from

(Stefano et al., 2006).

3.5.2 AGD5 mutant affects protein secretion in *N. tabacum* protoplasts

The data from confocal microscopy and biochemical experiments presented before indicate that AGD5 is involved in the binding and GTP hydrolysis of ARF1 onto TGN. To further demonstrate that *AGD5[R59Q]* (a GAP negative mutant) has a negative effect compared to AGD5 wild type form, on protein export from the TGN, tobacco leaf protoplasts was cotransfected with the secretory marker SecRGUS, which is a modified variant of rat preputial β-glucuronidase well secreted (Denecke et al., 1990; Leucci et al., 2007).

Tobacco protoplasts were transiently transformed with the following plasmids: SecRGUS alone (used as control), SecRGUS and *YFP-AGD5[R59Q]*, SecRGUS and YFP-AGD5, SecRGUS and ARF1GDPGFP (used as control). The SecRGUS secretion index was evaluated 24 hours after transient transformation. The secretion index (ratio of extracellular and intracellular activities) in protoplasts expressing SecRGUS alone or in combination with ARF1GDP-YFP, *YFP-AGD5[R59Q],* YFP-AGD5 was compared. Enzymatic activity in the medium as well as in the intracellular extracts was measured using as substrate the 4-methylumbelliferyl β-D-glucuronide. Furthermore, the extracellular fraction was evaluated for intracellular enzymes contamination and was estimated measuring α-mannosidase activity by using 4-methylumbelliferyl α-D-mannopyranoside as substrate.

In protoplasts, coexpressing YFP-AGD5 and SecRGUS the presence of the GAP protein does not affects the percentage of secretion. When tobacco cells are

coexpressed with *ARF1GDP*, as already showed with α-amylase test, the

percentage of secretion is reduced. On protoplasts, transiently coexpressing

SecRGUS and *YFP-AGD5[R59Q]*, it was observed a negative effect on the

secretion of SecRGUS, which can be considered lower compared to *ARF1GDP*

(Figure 3.16). These data resemble to the effect obtained using *ARF1GTP* on α-

amylase test (see Figure 3.15 above). These data mirror confocal microscopy

results showing that AGD5 affected the distribution and functioning of ARF1 at

the TGN, perhaps blocking the protein in the GTP bound form.
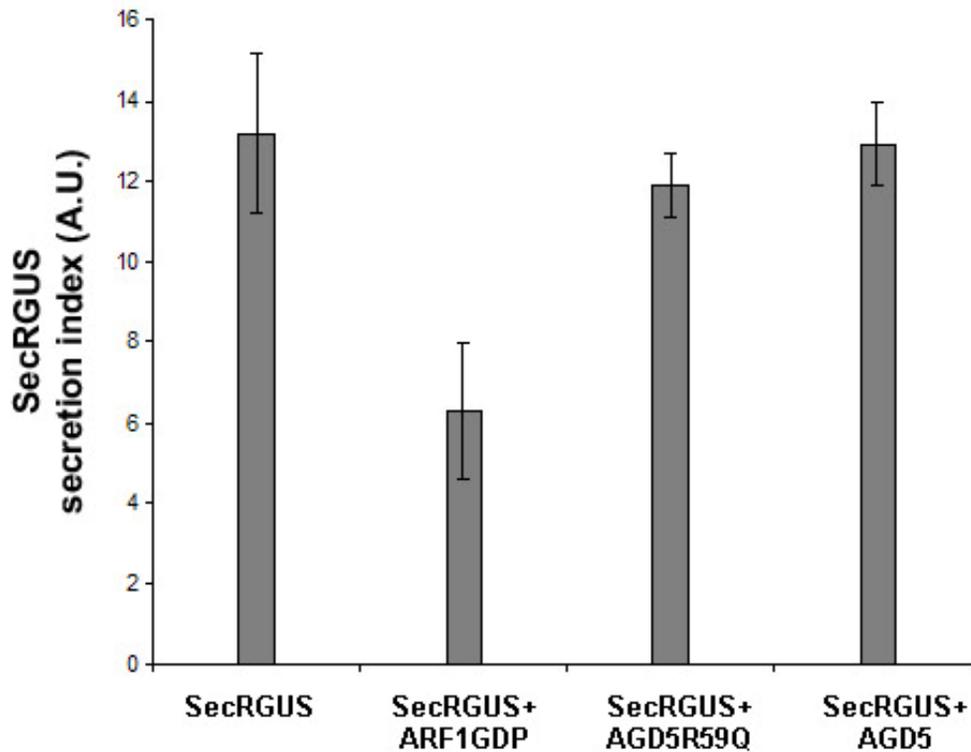
Figure 3.16: Secretion assay using *N. tabacum* leaf protoplasts. The graph shows the

secretion index of SecRGUS [ratio of extracellular and intracellular activities which is expressed

in arbitrary units] in protoplasts expressing SecRGUS alone or in combination with *ARF1GDP-*

YFP, *YFP-AGD5[R59Q]* and YFP-AGD5. Error bars = standard error of the mean for three

independent repetitions.

4.0 DISCUSSION

The function of some members of the GTPase activating proteins like ARFGAPs, which are involved in membrane trafficking, have been well studied in mammalian and yeast cells (Goldberg, 1999; Yanagisawa et al., 2002; Bigay et al., 2003; Liu et al., 2005; Natsume et al., 2006). Nevertheless, the role of the ARFGAP proteins is less understood in plant cells. Recently, the members of this family have been classified and grouped into four distinct classes based on phylogenetic analyses (Vernoud et al., 2003). In this work, the subcellular localization and a biological role of AGD5 have been described; Bioinformatics analysis showed that this protein is the plant homologue of yeast Age2p (Jurgens and Geldner, 2002), and human SMAP2 (stromal membrane-associated protein 2), which work on post-Golgi trafficking. Detailed analysis of AGD5 at the amino acid level has also revealed an FxDxF motif which in animal cells is in charge for the binding of accessory endocytic proteins to the appendage of the alpha-subunit of adaptor protein complex AP-2. These support the idea that AGD5 may be involved in the post-Golgi trafficking.

Furthermore, in this study, a plant ARF1GTPase, which mainly localizes in Golgi apparatus and non-Golgi structures was investigated as possible effector of AGD5. In this thesis, a live cell-imaging approach, together with biochemical assays, were used to analyze the cellular functions and molecular mechanism of action of AGD5, and its effector ARF1, highlighting the highly conserved residues involved in the GTP hydrolysis of ARF1 at the TGN membrane. The data provided by this work showed that AGD5 and the GTPase ARF1, interacts at the

TGN and the AGD5 appeared to have a role in the cycle of activation-inactivation of the plant ARF1 to the TGN membrane. An amino acid residue that is present in the GAP region confers the catalysis activity of AGD5 for the ARF1. These data suggested that proteins and mechanisms regulating the vesicular trafficking pathway appear to be conserved across the eukaryotes.

4.1 Intracellular localization of AGD5

In this work, localization analysis shows that AGD5 is distributed to punctate structures. The nature of the YFP-AGD5 labelled structures was evinced by analogy with the known distribution of TGN markers, SYP61 (Uemura et al., 2004). Furthermore, in this study was used a small GTPase ARF1, which is known to localize to the Golgi apparatus but also to non-Golgi structures (Xu and Scheres, 2005; Stefano et al., 2006). ARF1 binds the Golgi membrane in the active form (GTP locked) and it is released from the Golgi apparatus in the inactive form (GDP locked) (Vasudevan et al., 1998; Presley et al., 2002). ARF activity in the cell is regulated by a GEF that is sufficient to catalyze the exchange of GDP to GTP on Golgi apparatus membrane. The ARF activity is also regulated by a GAP (GTPase Activating Protein) that stimulates the hydrolysis of bound GTP releasing ARF1 to the cytosol (Teal et al., 1994; Vasudevan et al., 1998). As shown in colocalization experiments, only part of the ARF1-GFP punctate structures localizes at the TGN, overlapping with the GAP, AGD5. This distribution is not surprising since ARF1 may execute multiple functions besides retrograde Golgi/ER protein transport, including roles in post-

Golgi traffic and endocytic pathway (Aniento et al., 1996; Gu et al., 1997; Yahara et al., 2001; Pimpl et al., 2003). These findings support the hypothesis that AGD5 play a pivotal role as GAP protein for ARF1 at the Trans-Golgi Network.

4.2 AGD5 is involved in the GTP hydrolysis of the ARF1 at the TGN

The data here presented, obtained with heterologous *E.coli* cells system and planta-*E.coli* cells system experiments, suggest that AGD5 represents a specific GAP protein for ARF1 on TGN compartment. In fact, planta-*E.coli* cells system studies, using protein extracts from leaves overexpressing ARF1, have shown that this GTPase is able to bind the GST-AGD5 immobilized onto glutathione beads. Subsequently, experiments using heterologous *E.coli* cells system have demonstrated that the interaction between AGD5 and ARF1 is direct. These two proteins were also investigated in detail to find the residue involved in the GTP hydrolysis activity executed by AGD5 on ARF1. In mammalian cells, the mechanism by which GAP proteins stimulate GTP hydrolysis on GTPases was demonstrated to involve an arginine residue that is located inside the GAP domain. Experimental evidence in non-plant systems has shown that in GAP1, SMAP1 and SMAP2 the arginine residue in position 50th, 61th, 56th, respectively, is involved in the functionality of the GAP activity. This amino acid appears to fit into the GTP-binding pocket of the GTPase catalyzing the GTP hydrolysis (Szafer et al., 2000). In fact, studies using GAP1 have revealed that replacing Arg-50 with alanine, lysine or glutamine, completely abolished GAP activity on GTPase ARF1 (Szafer et al., 2000).

The specificity of catalysis was investigated by using point mutation in a specific

conserved residue that, with ClustalW alignment, appears to be conserved from

mammalian and yeast homologues. When this mutant tagged with YFP (*YFP-*

AGD5[R59Q]) was coexpressed in the presence of ARF1-GFP, it determines a

redistribution of most of ARF1-GFP into the cytosol, suggesting that AGD5

mutant may compete for the GTP hydrolysis activity of ARF1 at the TGN with the

endogenous GAP protein. These results indicate the existence of a correlation

between the interaction AGD5/ARF1GTP and its TGN targeting.

These data do not exclude that other small GTPase proteins, beside ARF1, may

be regulated at the TGN by the action of AGD5. In the *A. thaliana* genome, 15

proteins of the ARFGAP family have been identified (Vernoud et al., 2003),

unfortunately knowledge about their cellular roles remains completely vague.

Therefore, this study represents a starting point to elucidate ARFGAP functions

and mechanisms in plant cells.

4.3 The effect of AGD5 overexpression on root and pollen development

As depicted recently, ARF machinery serves as system for polar auxin transport

in planta (Geldner et al., 2003). Cell polarity process is known to be affected by

auxin, but not all the molecular mechanisms involved in the control of polarity and

morphogenesis have been determined in detail. Recently, post-Golgi network

and endocytic cycling of plasma membrane proteins were considered for its

potential role in cell polarity and development (Geldner et al., 2003; Meckel et al.,

2004, 2005; Xu and Scheres, 2005). The use of the Arabidopsis root has become a popular material to dissect different features of cell polarity.

Processes like root-hair initiation and tip growth is thought to involve the coordinated and highly regulated trafficking of Golgi vesicles containing hydrolytic enzymes and cell wall components (Schiefelbein et al., 1993; Masucci and Schiefelbein, 1994; Schiefelbein et al., 1997; Ovecka et al., 2005).

In this study, AGD5, an ARFGAP, was used to dissect its roles in Arabidopsis. Here, it has been shown that manipulation of Arabidopsis AGD5 function influences processes such as tip and hair root growth as well as pollen development. Previous results on ARF1 have been shown to localize to Golgi apparatus and endocytic organelles in mammalian and plant cells (Vasudevan et al., 1998; Xu and Scheres, 2005). ARF dependent vesicle trafficking has been demonstrated to play an important role in cell polarity and in root hair tip growth (Grebe et al., 2002). In this work, ARF1 was detected on TGN suggesting that it plays a pivotal role together with AGD5 in the Trans-Golgi Network.

Here, transgenic lines that overexpress AGD5 appear to interfere with cell polarity and development. The establishment of apical-basal trichoblast polarity appears to be influenced by auxin transport machinery and actin cytoskeleton (Masucci and Schiefelbein, 1994; Xu and Scheres, 2005). It has been shown that ARF1 manipulation can affect apical-basal polarity and interferes with PIN2-EGFP recycling, indicating that auxin influx and efflux carriers as well as an intact actin-mediated vesicle trafficking require a well functional ARF1 machinery (Geldner et al., 2003; Grebe et al., 2003; Geldner et al., 2004). This suggests

that AGD5 influencing ARF1 also influences vesicular cycling of auxin efflux carriers in an indirect way. Further dissection of specific ARF1-interacting proteins, such as ARFGEFs and ARFGAPs, can provide specificity to ARF1 action to understand in a better way its role in multiple distinct polarization events. Therefore, this work represents a starting point to analyze the ARFGAP influence on ARF1 functionality during auxin receptors recycling.

4.4 AGD5 and ARF1 mutants influences reporter protein secretion

To study the mechanism by which ARF1, under the involvement of AGD5 controls exit of reporter proteins from the secretory pathway, two secretory proteins, α-amylase and SecRGUS were used. The α-amylase is a naturally secreted protein that follows the anterograde pathway, the COPII route (Phillipson et al., 2001). Secretion of α-amylase is inhibited by the GTP-locked mutant ARF1, which specifically inhibit COPI transport (Pimpl et al., 2003; Stefano et al., 2006). Like α-amylase, SecRGUS is a protein efficiently secreted that represent a new secretory reporter protein (Leucci et al., 2007). The results in this work show that AGD5 wild type form as well as ARF1 wild type did not affect α-amylase or SecRGUS secretion. On the contrary, *ARF1GDP* locked form *ARF1GTP* locked form and the *AGD5[R59Q]* mutant exhibited a negative effect on the secretion of α-amylase or SecRGUS. In addition, it is evident that *AGD5[R59Q]* has similar effects to ARF1GTP on the secretion index, this suggests that AGD5 mutant bind ARF1 and block the protein in the GTP bound form, because *AGD5[R59Q]* is unable to catalyze the GTP hydrolysis.

In addition to transport steps of the default secretory pathway to the cell surface has been suggested that ARF1 controls the transport route to the vacuole that is mediated by BP80 (Binding Protein of 80 Kda). In fact, the GTP-locked mutant of ARF1 has shown to influence the route between the TGN and the vacuole more than COPI or COPII pathways (Pimpl et al., 2003). Based on Pimpl et al. (2003) data and these findings, it is tempting to speculate that ARF1 may influence the secretory route at the level of the TGN and later. ARF1 should play a role in the formation of clathrin-coated vesicles via the recruitment of the adaptor complex (AP-1) to the trans-Golgi (Robinson and Kreis, 1992; Stamnes and Rothman, 1993) or independently from AP-1 via the GGA protein family (Golgi-associated, gamma-adaptin homologous, ARF1p interacting proteins) (Puertollano et al., 2001).

These data mirror the confocal microscopy results showing that AGD5 affects the distribution of ARF1 at the TGN, suggesting that the mutant form may block protein export.

4.4 Concluding remarks

In plant cells, AGD5 represents the first member of ARFGAP family with an established subcellular localization on the TGN and a potential role in the GTP hydrolysis of ARF1GTPase. Results in this study represent a starting point for future research about ARFGAP family and its role in protein transport along the plant endocytic pathway. In eukaryotic cells, the entire specific cellular function of ARFGAPs and their interacting molecule ARFs, is still not completely

understood. In mammalian cells, recent evidence shows that ARFGAP may also

be a component of a vesicle coat complex that promotes cargo sorting and

selection. In addition, it can drive vesicle formation (Inoue and Randazzo, 2007).

Therefore, the identification and functions of possible homologue interacting

proteins of ARFGAPs in plants could elucidate its detailed role in the secretory

and endocytic pathway.

5. APPENDIX
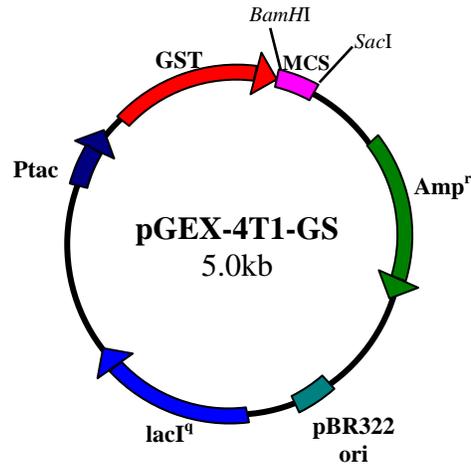
Figure A1. Schematic structure of pGEX-4T1-GS (derivative from pGEX-4T1) which carries the Glutathione S-Transferase gene (GST), the Ampicillin resistance (Amp^r), lacI gene encoding the lac repressor, the multiple cloning site (MCS), pBR322 origin for low copy replication and maintenance of the plasmid in *E. coli*, the tac promoter/operator (Ptac), which is IPTG inducible.
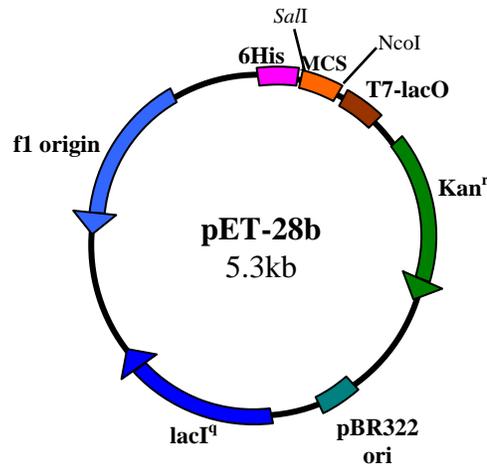
Figure A2. Schematic structure of pET-28b which carries an Histidine tag sequence (6His), the kanamycin resistance (Kan^r), lacI gene encoding the lac repressor, the multiple cloning site (MCS), the T7-lacO promoter, pBR322 origin for low copy replication and maintenance of the plasmid in *E. coli*, the f1 origin of replication for the production of single stranded plasmid DNA
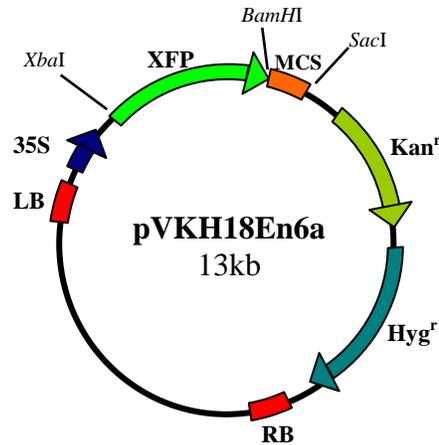
Figure A3. Schematic structure of pVKH18En6a which carries the kanamycin resistance (Kan^r in bacteria), hygromycin resistance (Hyg^r in plants), the multiple cloning site (MCS), gene encoding for fluorescent protein (XFP) (X = green, cyan or yellow) at the N-terminal of MCS, the 35S promoter, the left border (LB) and right border (RB) flanking the T-DNA.
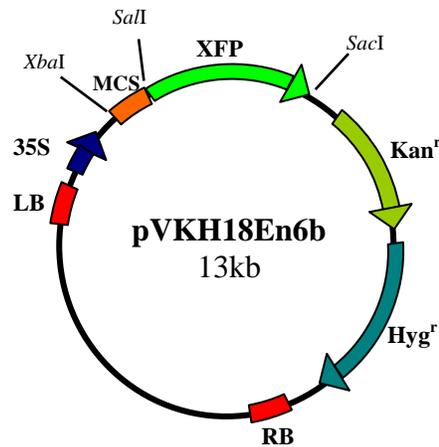
Figure A4. Schematic structure of pVKH18En6b which carries the kanamycin resistance (Kan^r in bacteria), hygromycin resistance (Hyg^r in plants), the multiple cloning site (MCS), gene encoding for green fluorescent protein (XFP) (X = green, cyan or yellow) at the C-terminal of MCS, the 35S promoter, the left border (LB) and right border (RB) flanking the T-DNA.

Table A1. Plasmids, *Agrobacterium tumefaciens* and *E. coli* strains used in this
work.

Plasmids	resistance
pET 28b[a]	Kanamycin
pGEX[b]-4T1-GS	Ampicillin
pVKH18EN6a[c]	Kanamycin, Hygromycin
pVKH18EN6b[c]	Kanamycin , Hygromycin

Agrobacterium tumefaciens strain	
GV3101[d]	Gentamycin

Escherichia coli strains	
MC1061[e]	Streptomycin
BL21[f]	*E. coli* B F$^-$ *dcm ompT hsdS*(r$_B^-$ m$_B^-$) *gal*

(a) Novagen (www.novagen.com), (b) (Kaelin et al., 1992), (c) (Batoko et al.,
2000), (d) Brandizzi lab's stock, (e) Invitrogen (www.invitrogen.com), (f)
Stratagene (www.stratagene.com).

Table A2. Solutions. All the solutions were prepared as in (a) QIAGEN-

QIAexpressionist; (b) Sambrook et al., 1989; (c) Thorpe and Kricka, 1986; (d) BD

biosciences, glutathione resins user manual; (e) Lu and Hong, 2003.

Solutions	Fomulations
Sample buffer 5X [a]	0.225 M Tris-HCl, pH 6.8; 50 % glycerol; 5 % SDS; 0.05 % bromophenol blue; 0.25 M DTT.
TFBI [b]	30 mM $KC_2H_3O_2$, 100 mM RbCl, 10 mM $CaCl_2$-$2H_2O$, 50 mM MnCl2-4H2O, 15 % glycerol, pH 5.8 with 0.2 M CH3COOH.
TFBII [b]	10 mM MOPS, 10 mM RbCl, 75 mM $CaCl_2$-$2H_2O$, 15 % glycerol, pH 6.6 with 1M KOH.
50X TAE [b]	242 g/l Tris base, 57.1ml/L glacial acetic acid, 37.2 Na_2EDTA2H_2O.
Loading buffer 10X [b]	35 % glycerol, 2.5 g/l Bromophenol blue in 10 X TAE.
P1 [a]	1 mM EDTA, 50 mM TRIS, pH 8.0.
P2 [a]	0.2 N NaOH, 1 % SDS.

Solutions	Fomulations
P3 [a]	11.5 % acetic acid, 3 M potassium acetate, pH 5.5.
10X SDS-PAGE running buffer [b]	30 g/l Tris base, 144 g/l glycine, 10 g/l SDS.
Blotting buffer [b]	3.03 g/l Tris base, 144 g/l glycine, 20 % v/v methanol.
Ponceau S solution [b]	0.1 % w/v Ponceau S, 5 % v/v acetic acid.
Blocking solution [b]	5 % (w/v) nonfat dry milk, 0.05 % tween 20, 0.02 % sodium azide in PBS.
Working solution [b]	1 % (w/v) nonfat dry milk, 0.05 % tween 20, 0.02 % sodium azide in PBS.
10X PBS [b]	87 g/l NaCl, 22.5 g/l $Na_2HPO4-2H_2O$, 2 g/l KH_2PO_4, pH 7.4.
ECL1 [c]	1 M Tris-HCl pH 8.5, 90 mM p-coumaric acid, 250 mM Luminol.
ECL2 [c]	1 M Tris-HCl pH 8.5, 3 % H_2O_2.
GST Extraction/lysis buffer (loading) [d]	140 mM NaCl; 10 mM Na_2HPO_4; 1.8 mM KH_2PO_4 (pH 7.5).

Solutions	Fomulations
Elution buffer[d]	20 mM Glutathione in 50 mM Tris-HCl (pH 8.0).
NE buffer[e]	20 mM HEPES, pH 7.5, 100 mM NaCl, 10 mM EDTA, 5 mM $MgCl_2$.
NS buffer[e]	20 mM HEPES, pH 7.5, 100 mM NaCl, 5 mM $MgCl_2$.
α-amylase extraction buffer	50 mM malic acid, 50 mM NaCl, 2 μM $CaCl_2$, 0.02% w/v sodium azide, 0.02% w/v BSA pH 6.8
Washing solution [b]	136.9 g/l sucrose (0.4M), 2.4 g/l Hepes, 6 g/l KCl, 600 mg/l CaCl2×2H2O, pH7.2 (with KOH)
TEX Buffer	3.1 g/l Gamborg`s B5 Salts (Sigma), 500 mg/l MES, 750 mg/l CaCl2×2H2O, 250 mg/l NH4NO3, 136.9 g/l sucrose (0.4M), pH5.7 (with 1M KOH)
10X leaf digestion mix	2% w/v macerozyme R-10, 4%w/v cellulase R-10 in TEX buffer
PEG solution	40% PEG4000, 0.4M mannitol, 0.1M Ca(NO3)2×4H2O, pH8 with 0.5M KOH

Solutions	Fomulations
MMM solution	0.5M Mannitol, 15mM MgCl2, 0.1% MES
IPTG	Stock solution in water 1 M, kept at -20ºC.
IF	20 mM $Na_3(PO_4)$, 500 mM MES, 200 mM acetosyringone, 5 mg/ml glucose.

Table A3. Primers used in PCR reactions. All the primers were purchased from

Invitrogen, desalted and with a scale of 50 nanomoles.

Primer	Sequence	Restriction site	Protein generated
GS23F	GGATCCGGTGCCATGAACGAGAAAGCCAACGTCTCT	*BamHI*	AGD5
GS24F	GAGCTCTCAATGTTTTGTGAACATTCCATCCATC	*Sac*I	AGD5
GS83F	TGTTCTGGGATTCACCAGAGTCTCGGGGTACAC	n.a.	AGD5[R59Q]
GS84F	GTGTACCCCGAGACTCTGGTGAATCCCAGAACA	n.a.	AGD5[R59Q]
GS95F	CAGGACGTCTAGATGGGGTTGTCATTCGGAAAGTTGTTCAGC	*xbaI*	ARF1
GS96F	CATGACCGTCGACTTTGCCTTGCTTGCGATGTTGTTGGAG	*Sal*I	ARF1
GS97F	GCTGCTGGTAAGAACACTATCCTCTAC	n.a.	ARF1GDP
GS98F	GTAGAGGATAGTGTTCTTACCAGCAGC	n.a.	ARF1GDP
GS99F	GATGTTGGGGGTCTAGACAAGATCCGT	n.a.	ARF1GTP
GS100F	ACGGATCTTGTCTAGACCCCC AACATC	n.a.	ARF1GTP
GS167F	GGTGCTACCATGGGGTTGTCATTCGGAAAGTT GTTC	*Nco*I	ARF1
GS116F	AGCTCCGTCGACTGCCTTGCTTGCGATGTTGTTGGAG	*Sal*I	ARF1

(n.a.= non applicable because these are internal primers used for overlapping

PCRs).

Table A4. Media. All the media described were prepared as in Sambrook et al. (1989).

Medium	Formulation
LB liquid	10 g/l bacto peptone-tryptone, 5 g/l yeast extract, 10 g/l NaCl.
LB solid	10 g/l bacto peptone-tryptone, 5 g/l yeast extract, 10 g/l NaCl, 10 g/l agar.
YT	16 g/l bacto-tryptone, 10 g/l yeast extract, 5 g/l NaCl, pH 7.0.

Table A5. Composition of PCR reactions

Reagent	Quantity, for 200µl of reaction mixture
Template DNA	1 µl
Pfu buffer (10x)+ MgSO$_4$(25 mM)	20 µl
Pfu DNA Polimerase (Fermentas)	1 µl
Sense primer (50 pmol/ µl)	0.6 µl
Antisense primer (50 pmol/ µl)	0.6 µl
dNTP (100 mM)	4 µl
Sterile distilled H$_2$O	172. 8 µl

(Aliquoted in two tubes and overlaid with mineral oil).

Table A6. Mutations produced using the overlapping PCR.

Mutations	Primers used	cDNA used	Protein generated	Vector used
R59Q	GS83F GS84F	AGD5	AGD5[R59Q]	PVKH18En6 pGEX-4T1
T31N	GS97F GS98F	ARF1	ARF1GDP	PVKH18En6 pET28b
Q71L	GS99F GS100F	ARF1	ARF1GTP	PVKH18En6 pET28b

Table A7. Solutions for preparing separating and stacking gels.

Separating gel 10%	Final volume 10ml
dH$_2$O	4.0ml
30% acrylamide/bisacrylamide mix	3.3ml
1.5M Tris (pH 8.8)	2.5ml
10% SDS	0.1ml
10% ammonium persulfate	0.1ml
TEMED	0.004ml

Stacking gel 5%	Final volume 4ml
dH$_2$O	2.7ml
30% acrylamide/bisacrylamide mix	0.67ml
1.5M Tris (pH 6.8)	0.5ml
10% SDS	0.04ml
10% ammonium persulfate	0.04ml
TEMED	0.004ml

6. REFERENCES

Altan-Bonnet, N., Phair, R.D., Polishchuk, R.S., Weigert, R., and Lippincott-Schwartz, J. (2003). A role for Arf1 in mitotic Golgi disassembly, chromosome segregation, and cytokinesis. Proc Natl Acad Sci U S A **100,** 13314-13319.

Aniento, F., Emans, N., Griffiths, G., and Gruenberg, J. (1993). Cytoplasmic dynein-dependent vesicular transport from early to late endosomes. J Cell Biol **123,** 1373-1387.

Aniento, F., Gu, F., Parton, R.G., and Gruenberg, J. (1996). An endosomal beta COP is involved in the pH-dependent formation of transport vesicles destined for late endosomes. J Cell Biol **133,** 29-41.

Aoe, T., Cukierman, E., Lee, A., Cassel, D., Peters, P.J., and Hsu, V.W. (1997). The KDEL receptor, ERD2, regulates intracellular traffic by recruiting a GTPase-activating protein for ARF1. EMBO J **16,** 7305-7316.

Aridor, M., and Balch, W.E. (1999). Integration of endoplasmic reticulum signaling in health and disease. Nat Med **5,** 745-751.

Aridor, M., Fish, K.N., Bannykh, S., Weissman, J., Roberts, T.H., Lippincott-Schwartz, J., and Balch, W.E. (2001). The Sar1 GTPase coordinates biosynthetic cargo selection with endoplasmic reticulum export site assembly. J Cell Biol **152,** 213-229.

Balguerie, A., Sivadon, P., Bonneu, M., and Aigle, M. (1999). Rvs167p, the budding yeast homolog of amphiphysin, colocalizes with actin patches. J Cell Sci **112 (Pt 15),** 2529-2537.

Baluska, F., Samaj, J., Hlavacka, A., Kendrick-Jones, J., and Volkmann, D. (2004). Actin-dependent fluid-phase endocytosis in inner cortex cells of maize root apices. J Exp Bot **55,** 463-473.

Batoko, H., Zheng, H.Q., Hawes, C., and Moore, I. (2000). A rab1 GTPase is required for transport between the endoplasmic reticulum and golgi apparatus and for normal golgi movement in plants. Plant Cell **12,** 2201-2218.

Bigay, J., Gounon, P., Robineau, S., and Antonny, B. (2003). Lipid packing sensed by ArfGAP1 couples COPI coat disassembly to membrane bilayer curvature. Nature **426,** 563-566.

Bischoff, F., Molendijk, A., Rajendrakumar, C.S., and Palme, K. (1999). GTP-binding proteins in plants. Cell Mol Life Sci **55,** 233-256.

Boehm, M., Aguilar, R.C., and Bonifacino, J.S. (2001). Functional and physical interactions of the adaptor protein complex AP-4 with ADP-ribosylation factors (ARFs). EMBO J **20,** 6265-6276.

Boevink, P., Martin, B., Oparka, K., Santa Cruz, S., and Hawes, C. (1999). Transport of virally expressed green fluorescent protein through the secretory pathway in tobacco leaves is inhibited by cold shock and brefeldin A. Planta **208,** 392-400.

Boevink, P., Oparka, K., Santa Cruz, S., Martin, B., Betteridge, A., and Hawes, C. (1998). Stacks on tracks: the plant Golgi apparatus traffics on an actin/ER network. Plant J **15,** 441-447.

Bolte, S., Brown, S., and Satiat-Jeunemaitre, B. (2004). The N-myristoylated Rab-GTPase m-Rabmc is involved in post-Golgi trafficking events to the lytic vacuole in plant cells. J Cell Sci **117,** 943-954.

Boman, A.L. (2001). GGA proteins: new players in the sorting game. J Cell Sci **114,** 3413-3418.

Boman, A.L., Zhang, C., Zhu, X., and Kahn, R.A. (2000). A family of ADP-ribosylation factor effectors that can alter membrane transport through the trans-Golgi. Mol Biol Cell **11,** 1241-1255.

Bonifacino, J.S., and Weissman, A.M. (1998). Ubiquitin and the control of protein fate in the secretory and endocytic pathways. Annu Rev Cell Dev Biol **14,** 19-57.

Borner, G.H., Lilley, K.S., Stevens, T.J., and Dupree, P. (2003). Identification of glycosylphosphatidylinositol-anchored proteins in Arabidopsis. A proteomic and genomic analysis. Plant Physiol **132,** 568-577.

Bradford, M.M. (1976). A rapid and sensitive method for the quantitation of microgram quantities of protein utilizing the principle of protein-dye binding. Analytical biochemistry **72,** 248-254.

Brandhorst, D., and Jahn, R. (2006). Endosome Fusion (Landes Bioscience and Springer Science+Business Media, LLC).

Brandizzi, F., Snapp, E.L., Roberts, A.G., Lippincott-Schwartz, J., and Hawes, C. (2002a). Membrane protein transport between the endoplasmic reticulum and the Golgi in tobacco leaves is energy dependent but cytoskeleton independent: evidence from selective photobleaching. Plant Cell **14,** 1293-1309.

Brandizzi, F., Frangne, N., Marc-Martin, S., Hawes, C., Neuhaus, J.M., and Paris, N. (2002b). The destination for single-pass membrane proteins is

influenced markedly by the length of the hydrophobic domain. Plant Cell **14,** 1077-1092.

Brown, M.T., Andrade, J., Radhakrishna, H., Donaldson, J.G., Cooper, J.A., and Randazzo, P.A. (1998). ASAP1, a phospholipid-dependent arf GTPase-activating protein that associates with and is phosphorylated by Src. Mol Cell Biol **18,** 7038-7051.

Burd, C.G., Strochlic, T.I., and Gangi Setty, S.R. (2004). Arf-like GTPases: not so Arf-like after all. Trends Cell Biol **14,** 687-694.

Carter, L.L., Redelmeier, T.E., Woollenweber, L.A., and Schmid, S.L. (1993). Multiple GTP-binding proteins participate in clathrin-coated vesicle-mediated endocytosis. J Cell Biol **120,** 37-45.

Cluett, E.B., and Brown, W.J. (1992). Adhesion of Golgi cisternae by proteinaceous interactions: intercisternal bridges as putative adhesive structures. J Cell Sci **103 (Pt 3),** 773-784.

Cole, N.B., and Lippincott-Schwartz, J. (1995). Organization of organelles and membrane traffic by microtubules. Curr Opin Cell Biol **7,** 55-64.

Cowles, C.R., Odorizzi, G., Payne, G.S., and Emr, S.D. (1997). The AP-3 adaptor complex is essential for cargo-selective transport to the yeast vacuole. Cell **91,** 109-118.

Crofts, A.J., Leborgne-Castel, N., Hillmer, S., Robinson, D.G., Phillipson, B., Carlsson, L.E., Ashford, D.A., and Denecke, J. (1999). Saturation of the endoplasmic reticulum retention machinery reveals anterograde bulk flow. Plant Cell **11,** 2233-2248.

Cukierman, E., Huber, I., Rotman, M., and Cassel, D. (1995). The ARF1 GTPase-activating protein: zinc finger motif and Golgi complex localization. Science **270,** 1999-2002.

Damke, H., Baba, T., Warnock, D.E., and Schmid, S.L. (1994). Induction of mutant dynamin specifically blocks endocytic coated vesicle formation. J Cell Biol **127,** 915-934.

daSilva, L.L., Snapp, E.L., Denecke, J., Lippincott-Schwartz, J., Hawes, C., and Brandizzi, F. (2004). Endoplasmic reticulum export sites and Golgi bodies behave as single mobile secretory units in plant cells. Plant Cell **16,** 1753-1771.

Denecke, J., Botterman, J., and Deblaere, R. (1990). Protein secretion in plant cells can occur via a default pathway. Plant Cell **2,** 51-59.

Dettmer, J., Hong-Hermesdorf, A., Stierhof, Y.D., and Schumacher, K. (2006). Vacuolar H+-ATPase activity is required for endocytic and secretory trafficking in Arabidopsis. Plant Cell **18,** 715-730.

Di Sansebastiano, G.P., Paris, N., Marc-Martin, S., and Neuhaus, J.M. (1998). Specific accumulation of GFP in a non-acidic vacuolar compartment via a C-terminal propeptide-mediated sorting pathway. Plant J **15,** 449-457.

Donaldson, J.G. (2000). Filling in the GAPs in the ADP-ribosylation factor story. Proc Natl Acad Sci U S A **97,** 3792-3794.

Donaldson, J.G., and Jackson, C.L. (2000). Regulators and effectors of the ARF GTPases. Curr Opin Cell Biol **12,** 475-482.

Dunn, K.W., and Maxfield, F.R. (1992). Delivery of ligands from sorting endosomes to late endosomes occurs by maturation of sorting endosomes. J Cell Biol **117,** 301-310.

Dupree, P., and Sherrier, D.J. (1998). The plant Golgi apparatus. Biochim Biophys Acta **1404,** 259-270.

Etxeberria, E., Baroja-Fernandez, E., Munoz, F.J., and Pozueta-Romero, J. (2005). Sucrose-inducible endocytosis as a mechanism for nutrient uptake in heterotrophic plant cells. Plant Cell Physiol **46,** 474-481.

Franke, W.W., Kartenbeck, J., Krien, S., VanderWoude, W.J., Scheer, U., and Morre, D.J. (1972). Inter- and intracisternal elements of the Golgi apparatus. A system of membrane-to-membrane cross-links. Z Zellforsch Mikrosk Anat **132,** 365-380.

Gebbie, L.K., Burn, J.E., Hocart, C.H., and Williamson, R.E. (2005). Genes encoding ADP-ribosylation factors in Arabidopsis thaliana L. Heyn.; genome analysis and antisense suppression. J Exp Bot **56,** 1079-1091.

Geldner, N., Richter, S., Vieten, A., Marquardt, S., Torres-Ruiz, R.A., Mayer, U., and Jurgens, G. (2004). Partial loss-of-function alleles reveal a role for GNOM in auxin transport-related, post-embryonic development of Arabidopsis. Development **131,** 389-400.

Geldner, N., Anders, N., Wolters, H., Keicher, J., Kornberger, W., Muller, P., Delbarre, A., Ueda, T., Nakano, A., and Jurgens, G. (2003). The Arabidopsis GNOM ARF-GEF mediates endosomal recycling, auxin transport, and auxin-dependent plant growth. Cell **112,** 219-230.

Goldberg, J. (1999). Structural and functional analysis of the ARF1-ARFGAP complex reveals a role for coatomer in GTP hydrolysis. Cell **96,** 893-902.

Grebe, M., Xu, J., Mobius, W., Ueda, T., Nakano, A., Geuze, H.J., Rook, M.B., and Scheres, B. (2003). Arabidopsis sterol endocytosis involves actin-mediated trafficking via ARA6-positive early endosomes. Curr Biol **13,** 1378-1387.

Grebe, M., Friml, J., Swarup, R., Ljung, K., Sandberg, G., Terlou, M., Palme, K., Bennett, M.J., and Scheres, B. (2002). Cell polarity signaling in Arabidopsis involves a BFA-sensitive auxin influx pathway. Curr Biol **12,** 329-334.

Gruenberg, J., Griffiths, G., and Howell, K.E. (1989). Characterization of the early endosome and putative endocytic carrier vesicles in vivo and with an assay of vesicle fusion in vitro. J Cell Biol **108,** 1301-1316.

Gu, F., Aniento, F., Parton, R.G., and Gruenberg, J. (1997). Functional dissection of COP-I subunits in the biogenesis of multivesicular endosomes. J Cell Biol **139,** 1183-1195.

Hadlington, J.L., and Denecke, J. (2000). Sorting of soluble proteins in the secretory pathway of plants. Curr Opin Plant Biol **3,** 461-468.

Hammond, A.T., and Glick, B.S. (2000). Dynamics of transitional endoplasmic reticulum sites in vertebrate cells. Mol Biol Cell **11,** 3013-3030.

Hammond, C., and Helenius, A. (1995). Quality control in the secretory pathway. Curr Opin Cell Biol **7,** 523-529.

Hanton, S.L., Bortolotti, L.E., Renna, L., Stefano, G., and Brandizzi, F. (2005). Crossing the divide--transport between the endoplasmic reticulum and Golgi apparatus in plants. Traffic **6,** 267-277.

Hawes, C., and Satiat-Jeunemaitre, B. (2005). The plant Golgi apparatus--going with the flow. Biochim Biophys Acta **1744,** 466-480.

Higuchi, R., Krummel, B., and Saiki, R.K. (1988). A general method of in vitro preparation and specific mutagenesis of DNA fragments: study of protein and DNA interactions. Nucleic Acids Res **16,** 7351-7367.

Hillmer, S., Movafeghi, A., Robinson, D.G., and Hinz, G. (2001). Vacuolar storage proteins are sorted in the cis-cisternae of the pea cotyledon Golgi apparatus. J Cell Biol **152,** 41-50.

Hinz, G., Hillmer, S., Baumer, M., and Hohl, I.I. (1999). Vacuolar storage proteins and the putative vacuolar sorting receptor BP-80 exit the golgi apparatus of developing pea cotyledons in different transport vesicles. Plant Cell **11,** 1509-1524.

Ho, S.N., Hunt, H.D., Horton, R.M., Pullen, J.K., and Pease, L.R. (1989). Site-directed mutagenesis by overlap extension using the polymerase chain reaction. Gene **77,** 51-59.

Hutter, H. (2004). Five-colour in vivo imaging of neurons in Caenorhabditis elegans. J Microsc **215,** 213-218.

Inoue, H., and Randazzo, P.A. (2007). Arf GAPs and their interacting proteins. Traffic **8,** 1465-1475.

Itin, C., Rancano, C., Nakajima, Y., and Pfeffer, S.R. (1997). A novel assay reveals a role for soluble N-ethylmaleimide-sensitive fusion attachment protein in mannose 6-phosphate receptor transport from endosomes to the trans Golgi network. J Biol Chem **272,** 27737-27744.

Jackson, C.L., and Casanova, J.E. (2000). Turning on ARF: the Sec7 family of guanine-nucleotide-exchange factors. Trends Cell Biol **10,** 60-67.

Jackson, M.R., Nilsson, T., and Peterson, P.A. (1993). Retrieval of transmembrane proteins to the endoplasmic reticulum. J Cell Biol **121,** 317-333.

Jensen, R.B., Lykke-Andersen, K., Frandsen, G.I., Nielsen, H.B., Haseloff, J., Jespersen, H.M., Mundy, J., and Skriver, K. (2000). Promiscuous and specific phospholipid binding by domains in ZAC, a membrane-associated Arabidopsis protein with an ARF GAP zinc finger and a C2 domain. Plant Mol Biol **44,** 799-814.

Jin, J.B., Kim, Y.A., Kim, S.J., Lee, S.H., Kim, D.H., Cheong, G.W., and Hwang, I. (2001). A new dynamin-like protein, ADL6, is involved in trafficking from the trans-Golgi network to the central vacuole in Arabidopsis. Plant Cell **13,** 1511-1526.

Jurgens, G., and Geldner, N. (2002). Protein secretion in plants: from the trans-Golgi network to the outer space. Traffic **3,** 605-613.

Kaelin, W.G., Jr., Krek, W., Sellers, W.R., DeCaprio, J.A., Ajchenbaum, F., Fuchs, C.S., Chittenden, T., Li, Y., Farnham, P.J., Blanar, M.A., and et al. (1992). Expression cloning of a cDNA encoding a retinoblastoma-binding protein with E2F-like properties. Cell **70,** 351-364.

Kapila, J., De Rycke, R., Van Montagu, M., and Angenon, G. (1997). An Agrobacterium-mediated transient gene expression system for intact leaves. Plant Science **122,** 101-108.

Kirchhausen, T. (2000). Three ways to make a vesicle. Nat Rev Mol Cell Biol **1,** 187-198.

Kirsch, T., Paris, N., Butler, J.M., Beevers, L., and Rogers, J.C. (1994). Purification and initial characterization of a potential plant vacuolar targeting receptor. Proc Natl Acad Sci U S A **91,** 3403-3407.

Kornfeld, S. (1990). Lysosomal enzyme targeting. Biochem Soc Trans **18,** 367-374.

Ladinsky, M.S., Mastronarde, D.N., McIntosh, J.R., Howell, K.E., and Staehelin, L.A. (1999). Golgi structure in three dimensions: functional insights from the normal rat kidney cell. J Cell Biol **144,** 1135-1149.

Laemmli, U.K. (1970). Cleavage of structural proteins during the assembly of the head of bacteriophage T4. Nature **227,** 680-685.

Lalanne, E., Honys, D., Johnson, A., Borner, G.H., Lilley, K.S., Dupree, P., Grossniklaus, U., and Twell, D. (2004). SETH1 and SETH2, two components of the glycosylphosphatidylinositol anchor biosynthetic pathway, are required for pollen germination and tube growth in Arabidopsis. Plant Cell **16,** 229-240.

Lam, S.K., Siu, C.L., Hillmer, S., Jang, S., An, G., Robinson, D.G., and Jiang, L. (2007). Rice SCAMP1 defines clathrin-coated, trans-golgi-located tubular-vesicular structures as an early endosome in tobacco BY-2 cells. Plant Cell **19,** 296-319.

Lefebvre, B., Batoko, H., Duby, G., and Boutry, M. (2004). Targeting of a Nicotiana plumbaginifolia H+ -ATPase to the plasma membrane is not by default and requires cytosolic structural determinants. Plant Cell **16,** 1772-1789.

Leucci, M.R., Di Sansebastiano, G.P., Gigante, M., Dalessandro, G., and Piro, G. (2007). Secretion marker proteins and cell-wall polysaccharides move through different secretory pathways. Planta **225,** 1001-1017.

Liu, W., Duden, R., Phair, R.D., and Lippincott-Schwartz, J. (2005). ArfGAP1 dynamics and its role in COPI coat assembly on Golgi membranes of living cells. J Cell Biol **168,** 1053-1063.

Masucci, J.D., and Schiefelbein, J.W. (1994). The rhd6 Mutation of Arabidopsis thaliana Alters Root-Hair Initiation through an Auxin- and Ethylene-Associated Process. Plant Physiol **106,** 1335-1346.

Matheson, L.A., Hanton, S.L., Rossi, M., Latijnhouwers, M., Stefano, G., Renna, L., and Brandizzi, F. (2007). Multiple roles of ADP-ribosylation factor 1 in plant cells include spatially regulated recruitment of coatomer and elements of the Golgi matrix. Plant Physiol **143,** 1615-1627.

Maxfield, F.R., and McGraw, T.E. (2004). Endocytic recycling. Nat Rev Mol Cell Biol **5,** 121-132.

Meckel, T., Hurst, A.C., Thiel, G., and Homann, U. (2004). Endocytosis against high turgor: intact guard cells of Vicia faba constitutively endocytose fluorescently labelled plasma membrane and GFP-tagged K-channel KAT1. Plant J **39,** 182-193.

Meckel, T., Hurst, A.C., Thiel, G., and Homann, U. (2005). Guard cells undergo constitutive and pressure-driven membrane turnover. Protoplasma **226,** 23-29.

Mellman, I. (1996). Endocytosis and molecular sorting. Annu Rev Cell Dev Biol **12,** 575-625.

Memon, A.R. (2004). The role of ADP-ribosylation factor and SAR1 in vesicular trafficking in plants. Biochim Biophys Acta **1664,** 9-30.

Meyer, C., Zizioli, D., Lausmann, S., Eskelinen, E.L., Hamann, J., Saftig, P., von Figura, K., and Schu, P. (2000). mu1A-adaptin-deficient mice: lethality, loss of AP-1 binding and rerouting of mannose 6-phosphate receptors. EMBO J **19,** 2193-2203.

Mollenhauer, H.H., and Morré, D.J. (1994). Structure of Golgi apparatus. Protoplasma **180,** 14-28.

Mongrand, S., Morel, J., Laroche, J., Claverol, S., Carde, J.P., Hartmann, M.A., Bonneu, M., Simon-Plas, F., Lessire, R., and Bessoule, J.J. (2004). Lipid rafts in higher plant cells: purification and characterization of Triton X-100-insoluble microdomains from tobacco plasma membrane. J Biol Chem **279,** 36277-36286.

Morise, H., Shimomura, O., Johnson, F.H., and Winant, J. (1974). Intermolecular energy transfer in the bioluminescent system of Aequorea. Biochemistry **13,** 2656-2662.

Mukherjee, S., Ghosh, R.N., and Maxfield, F.R. (1997). Endocytosis. Physiol Rev **77,** 759-803.

Mullins, C., and Bonifacino, J.S. (2001). Structural requirements for function of yeast GGAs in vacuolar protein sorting, alpha-factor maturation, and interactions with clathrin. Mol Cell Biol **21,** 7981-7994.

Munn, A.L. (2000). The yeast endocytic membrane transport system. Microsc Res Tech **51,** 547-562.

Murphy, A.S., Bandyopadhyay, A., Holstein, S.E., and Peer, W.A. (2005). Endocytotic cycling of PM proteins. Annu Rev Plant Biol **56,** 221-251.

Natsume, W., Tanabe, K., Kon, S., Yoshida, N., Watanabe, T., Torii, T., and Satake, M. (2006). SMAP2, a Novel ARF GTPase-activating Protein, Interacts with Clathrin and Clathrin Assembly Protein, and Functions on the AP-1-positive Early Endosome/Trans-Golgi Network. Mol Biol Cell.

Nebenführ, A., Gallagher, L.A., Dunahay, T.G., Frohlick, J.A., Mazurkiewicz, A.M., Mechl, J.B., and Staehelin, L.A. (1999). Stop-and-go movement of plant Golgi stacks are mediated by the actomyosin system. Plant Physiology **121,** 1127-1141.

Ovecka, M., Lang, I., Baluska, F., Ismail, A., Illes, P., and Lichtscheidl, I.K. (2005). Endocytosis and vesicle trafficking during tip growth of root hairs. Protoplasma **226,** 39-54.

Paris, N., and Neuhaus, J.M. (2002). BP-80 as a vacuolar sorting receptor. Plant Mol Biol **50,** 903-914.

Paris, N., Stanley, C.M., Jones, R.L., and Rogers, J.C. (1996). Plant cells contain two functionally distinct vacuolar compartments. Cell **85,** 563-572.

Pepperkok, R., Scheel, J., Horstmann, H., Hauri, H.P., Griffiths, G., and Kreis, T.E. (1993). Beta-COP is essential for biosynthetic membrane transport from the endoplasmic reticulum to the Golgi complex in vivo. Cell **74,** 71-82.

Phillipson, B.A., Pimpl, P., daSilva, L.L., Crofts, A.J., Taylor, J.P., Movafeghi, A., Robinson, D.G., and Denecke, J. (2001). Secretory bulk flow of soluble proteins is efficient and COPII dependent. Plant Cell **13,** 2005-2020.

Picton, J.M., and Steer, M.W. (1983). The effect of cycloheximide on dictyosome activity in Tradescantia pollen tubes determined using cytochalasin D. Eur J Cell Biol **29,** 133-138.

Pimpl, P., Hanton, S.L., Taylor, J.P., Pinto-daSilva, L.L., and Denecke, J. (2003). The GTPase ARF1p controls the sequence-specific vacuolar sorting route to the lytic vacuole. Plant Cell **15,** 1242-1256.

Pimpl, P., Movafeghi, A., Coughlan, S., Denecke, J., Hillmer, S., and Robinson, D.G. (2000). In situ localization and in vitro induction of plant COPI-coated vesicles. Plant Cell **12,** 2219-2236.

Polishchuk, R.S., and Mironov, A.A. (2004). Structural aspects of Golgi function. Cell Mol Life Sci **61,** 146-158.

Poon, P.P., Wang, X., Rotman, M., Huber, I., Cukierman, E., Cassel, D., Singer, R.A., and Johnston, G.C. (1996). Saccharomyces cerevisiae

Gcs1 is an ADP-ribosylation factor GTPase-activating protein. Proc Natl Acad Sci U S A **93,** 10074-10077.

Premont, R.T., Claing, A., Vitale, N., Freeman, J.L., Pitcher, J.A., Patton, W.A., Moss, J., Vaughan, M., and Lefkowitz, R.J. (1998). beta2-Adrenergic receptor regulation by GIT1, a G protein-coupled receptor kinase-associated ADP ribosylation factor GTPase-activating protein. Proc Natl Acad Sci U S A **95,** 14082-14087.

Presley, J.F., Ward, T.H., Pfeifer, A.C., Siggia, E.D., Phair, R.D., and Lippincott-Schwartz, J. (2002). Dissection of COPI and Arf1 dynamics in vivo and role in Golgi membrane transport. Nature **417,** 187-193.

Puertollano, R., Randazzo, P.A., Presley, J.F., Hartnell, L.M., and Bonifacino, J.S. (2001). The GGAs promote ARF-dependent recruitment of clathrin to the TGN. Cell **105,** 93-102.

Randazzo, P.A., and Hirsch, D.S. (2004). Arf GAPs: multifunctional proteins that regulate membrane traffic and actin remodelling. Cell Signal **16,** 401-413.

Randazzo, P.A., Andrade, J., Miura, K., Brown, M.T., Long, Y.Q., Stauffer, S., Roller, P., and Cooper, J.A. (2000). The Arf GTPase-activating protein ASAP1 regulates the actin cytoskeleton. Proc Natl Acad Sci U S A **97,** 4011-4016.

Rehman, R.U., Stigliano, E., Lycett, G.W., Sticher, L., Sbano, F., Faraco, M., Dalessandro, G., and Di Sansebastiano, G.P. (2008). Tomato Rab11a characterization evidenced a difference between SYP121-dependent and SYP122-dependent exocytosis. Plant Cell Physiol **49,** 751-766.

Ritzenthaler, C., Nebenfuhr, A., Movafeghi, A., Stussi-Garaud, C., Behnia, L., Pimpl, P., Staehelin, L.A., and Robinson, D.G. (2002). Reevaluation of the effects of brefeldin A on plant cells using tobacco Bright Yellow 2 cells expressing Golgi-targeted green fluorescent protein and COPI antisera. Plant Cell **14,** 237-261.

Robinson, M.S., and Kreis, T.E. (1992). Recruitment of coat proteins onto Golgi membranes in intact and permeabilized cells: effects of brefeldin A and G protein activators. Cell **69,** 129-138.

Roth, M.G. (1999). Snapshots of ARF1: implications for mechanisms of activation and inactivation. Cell **97,** 149-152.

Rothman, J.H., and Stevens, T.H. (1986). Protein sorting in yeast: mutants defective in vacuole biogenesis mislocalize vacuolar proteins into the late secretory pathway. Cell **47,** 1041-1051.

Saint-Jore-Dupas, C., Gomord, V., and Paris, N. (2004). Protein localization in the plant Golgi apparatus and the trans-Golgi network. Cell Mol Life Sci **61,** 159-171.

Saint-Jore, C.M., Evins, J., Batoko, H., Brandizzi, F., Moore, I., and Hawes, C. (2002). Redistribution of membrane proteins between the Golgi apparatus and endoplasmic reticulum in plants is reversible and not dependent on cytoskeletal networks. Plant J **29,** 661-678.

Schiefelbein, J., Galway, M., Masucci, J., and Ford, S. (1993). Pollen tube and root-hair tip growth is disrupted in a mutant of Arabidopsis thaliana. Plant Physiol **103,** 979-985.

Schiefelbein, J.W., Masucci, J.D., and Wang, H. (1997). Building a root: the control of patterning and morphogenesis during root development. Plant Cell **9,** 1089-1098.

Schwaninger, R., Plutner, H., Bokoch, G.M., and Balch, W.E. (1992). Multiple GTP-binding proteins regulate vesicular transport from the ER to Golgi membranes. J Cell Biol **119,** 1077-1096.

Shao, X., Li, C., Fernandez, I., Zhang, X., Sudhof, T.C., and Rizo, J. (1997). Synaptotagmin-syntaxin interaction: the C2 domain as a Ca2+-dependent electrostatic switch. Neuron **18,** 133-142.

Son, O., Yang, H.-S., Lee, H.-J., Lee, M.-Y., Shin, K.-H., Jeon, S.-L., Lee, M.-S., Choi, S.-Y., Chun, J.-Y., Kim, H., An, C.-S., Hong, S.-K., Kim, N.-S., Koh, S.-K., Cho, M.J., Kim, S., Verma, D.P.S., and Cheon, C.-I. (2003). Expression of srab7 and SCaM genes required for endocytosis of Rhizobium in root nodules. Plant Science **165,** 1239-1244.

Staehelin, A. (1991). What Is a Plant Cell? A Response. Plant Cell **3,** 553.

Staehelin, L.A. (1997). The plant ER: a dynamic organelle composed of a large number of discrete functional domains. Plant J **11,** 1151-1165.

Staehelin, L.A., and Moore, I. (1995). The Plant Golgi Apparatus: Structure, Functional Organization and Trafficking Mechanisms. Annual Review of Plant Physiology and Plant Molecular Biology **46,** 261-288.

Stamnes, M.A., and Rothman, J.E. (1993). The binding of AP-1 clathrin adaptor particles to Golgi membranes requires ADP-ribosylation factor, a small GTP-binding protein. Cell **73,** 999-1005.

Stefano, G., Renna, L., Chatre, L., Hanton, S.L., Moreau, P., Hawes, C., and Brandizzi, F. (2006). In tobacco leaf epidermal cells, the integrity of protein export from the endoplasmic reticulum and of ER export sites depends on active COPI machinery. Plant J **46,** 95-110.

Steinman, R.M., Mellman, I.S., Muller, W.A., and Cohn, Z.A. (1983). Endocytosis and the recycling of plasma membrane. J Cell Biol **96,** 1-27.

Stepp, J.D., Huang, K., and Lemmon, S.K. (1997). The yeast adaptor protein complex, AP-3, is essential for the efficient delivery of alkaline phosphatase by the alternate pathway to the vacuole. J Cell Biol **139,** 1761-1774.

Szafer, E., Pick, E., Rotman, M., Zuck, S., Huber, I., and Cassel, D. (2000). Role of coatomer and phospholipids in GTPase-activating protein-dependent hydrolysis of GTP by ADP-ribosylation factor-1. J Biol Chem **275,** 23615-23619.

Takeuchi, M., Ueda, T., Yahara, N., and Nakano, A. (2002). Arf1 GTPase plays roles in the protein traffic between the endoplasmic reticulum and the Golgi apparatus in tobacco and Arabidopsis cultured cells. Plant J **31,** 499-515.

Teal, S.B., Hsu, V.W., Peters, P.J., Klausner, R.D., and Donaldson, J.G. (1994). An activating mutation in ARF1 stabilizes coatomer binding to Golgi membranes. J Biol Chem **269,** 3135-3138.

Teuchert, M., Schafer, W., Berghofer, S., Hoflack, B., Klenk, H.D., and Garten, W. (1999). Sorting of furin at the trans-Golgi network. Interaction of the cytoplasmic tail sorting signals with AP-1 Golgi-specific assembly proteins. J Biol Chem **274,** 8199-8207.

Uemura, T., Ueda, T., Ohniwa, R.L., Nakano, A., Takeyasu, K., and Sato, M.H. (2004). Systematic analysis of SNARE molecules in Arabidopsis: dissection of the post-Golgi network in plant cells. Cell Struct Funct **29,** 49-65.

Vasudevan, C., Han, W., Tan, Y., Nie, Y., Li, D., Shome, K., Watkins, S.C., Levitan, E.S., and Romero, G. (1998). The distribution and translocation of the G protein ADP-ribosylation factor 1 in live cells is determined by its GTPase activity. J Cell Sci **111 (Pt 9),** 1277-1285.

Vernoud, V., Horton, A.C., Yang, Z., and Nielsen, E. (2003). Analysis of the small GTPase gene superfamily of Arabidopsis. Plant Physiol **131,** 1191-1208.

Vitale, A., and Denecke, J. (1999). The endoplasmic reticulum-gateway of the secretory pathway. Plant Cell **11,** 615-628.

Vitale, A., and Galili, G. (2001). The endomembrane system and the problem of protein sorting. Plant Physiol **125,** 115-118.

Waguri, S., Dewitte, F., Le Borgne, R., Rouille, Y., Uchiyama, Y., Dubremetz, J.F., and Hoflack, B. (2003). Visualization of TGN to endosome trafficking through fluorescently labeled MPR and AP-1 in living cells. Mol Biol Cell **14,** 142-155.

Wigge, P., and McMahon, H.T. (1998). The amphiphysin family of proteins and their role in endocytosis at the synapse. Trends Neurosci **21,** 339-344.

Willemsen, V., Friml, J., Grebe, M., van den Toorn, A., Palme, K., and Scheres, B. (2003). Cell polarity and PIN protein positioning in Arabidopsis require STEROL METHYLTRANSFERASE1 function. Plant Cell **15,** 612-625.

Wu, M., Lu, L., Hong, W., and Song, H. (2004). Structural basis for recruitment of GRIP domain golgin-245 by small GTPase Arl1. Nat Struct Mol Biol **11,** 86-94.

Xu, J., and Scheres, B. (2005). Dissection of Arabidopsis ADP-RIBOSYLATION FACTOR 1 function in epidermal cell polarity. Plant Cell **17,** 525-536.

Yahara, N., Ueda, T., Sato, K., and Nakano, A. (2001). Multiple roles of Arf1 GTPase in the yeast exocytic and endocytic pathways. Mol Biol Cell **12,** 221-238.

Yanagisawa, L.L., Marchena, J., Xie, Z., Li, X., Poon, P.P., Singer, R.A., Johnston, G.C., Randazzo, P.A., and Bankaitis, V.A. (2002). Activity of specific lipid-regulated ADP ribosylation factor-GTPase-activating proteins is required for Sec14p-dependent Golgi secretory function in yeast. Mol Biol Cell **13,** 2193-2206.

Yang, J.S., Lee, S.Y., Gao, M., Bourgoin, S., Randazzo, P.A., Premont, R.T., and Hsu, V.W. (2002). ARFGAP1 promotes the formation of COPI vesicles, suggesting function as a component of the coat. J Cell Biol **159,** 69-78.

Zerial, M., and McBride, H. (2001). Rab proteins as membrane organizers. Nat Rev Mol Cell Biol **2,** 107-117.

Zhou, M., and Schekman, R. (1999). The engagement of Sec61p in the ER dislocation process. Mol Cell **4,** 925-934.

Journal articles

Stefano G., et al., (to be submitted). AGD5, an ARFGAP, interacts at the trans-Golgi with ARF1 GTPase protein.

Agati G., **Stefano G**., Biricolti S., Tattini M. Localization/functional relationship of flavonoids in high light-stressed leaves as assessed by multispectral fluorescence microimaging. Plant and Cell Physiology, submitted (2009).

Masi E., Ciszak M., **Stefano G.,** Renna L., Azzarello E., Pandolfi C., Mugnai S., Baluška F., Arecchi F.T., Mancuso S.. Spatio-temporal dynamics of the electrical network activity in the root apex. PNAS, in press (2009).

Matheson L.A., Hanton S.L., Rossi M., Latijnhouwers M., **Stefano G.,** Renna L., Brandizzi F. Multiple roles of arf1 in plant cells include spatially-regulated recruitment of coatomer and elements of the golgi matrix. Plant Physiol. (2007) 143(4):1615-27.

Stefano G., Renna L., Chatre L., Hanton S.L., Moreau P., Hawes C. and Brandizzi F. In tobacco leaf epidermal cells the integrity of protein export from the endoplasmic reticulum and of ER export sites depends on active COPI machinery. Plant Journal (2006) 46(1):95-110.

Stefano G., Renna L., Chatre L., Hanton S.L., Haas T.A., Brandizzi F. Arl1 plays a role in the binding of a grip domain of a periferal matrix protein to the golgi apparatus in plant cell. Plant Mol Biol (2006) 61(3):431-49.

Hanton S.L., Renna L., Bortolotti L.E., Chatre L., **Stefano G.,** Brandizzi F. Diacidic motifs influence the export of transmembrane proteins from the endoplasmic reticulum in plant cells. Plant Cell. (2005) 17(11):3081-93.

Renna L., Hanton S.L., **Stefano G.,** Bortolotti L., Misra V., Brandizzi F. Identification and characterization of AtCASP, a plant transmembrane Golgi matrix protein. Plant Mol Biol (2005) 58: 109-122

Hanton S.L., Bortolotti L., Renna L., **Stefano G**., Brandizzi F. Crossing the divide--transport between the endoplasmic reticulum and Golgi apparatus in plants. Traffic (2005) 6: 267-277.

Abstracts

2004: Brandizzi F., Hawes C., Hanton S.L., Renna L., **Stefano G.**: Use of fluorescent proteins to dissect the dynamics of the plant secretory pathway. European Microscopy Congress 2004, Antwerpen, BELGIUM. August 2004

2006: Matheson L., **Stefano G.**, Brandizzi F. Dissection of the molecular mechanisms for matrix protein targeting to the plant Golgi apparatus. 23rd Annual Meeting of the International Society for Analytical Cytology", May 20-24, 2006. Quebec City, Quebec, CANADA

2006: Matheson L., **Stefano G.**, Brandizzi F. Matrix protein targeting to the plant Golgi apparatus. Plant Biology 2006: Friday, August 5 - Wednesday August 9, 2006 - Boston, Massachusetts, USA

2007: Masi E., Ciszak M., Montina A., Malachovska V., Mugnai S., Azzarello E., Pandolfi C., Renna L., **Stefano G.**, Voigt B., Hlavacka A., Arecchi F.T., Mancuso S.: Spatio-temporal dynamics of the electrical network activity in the root apex. A multi-electrode array (MEA) study. 3rd International Symposium on Plant Neurobiology 14-18 May 2007, Štrbské pleso, SLOVAKIA

2008: Masi E., Ciszak M., Pandolfi C., Azzarello E., Mugnai S., Renna L., **Stefano G.**, Voigt B., Mancuso S.: Characteristics of the artificial electrical activity generated in plant roots under artificial changes in gravity. 4rd International Symposium on Plant Neurobiology 6-9 June 2008, Fukuoka, JAPAN.

International acknowledgments

Citation from **Faculty of 1000 Biology** for the publication: Matheson LA, Hanton SL, Rossi M, Latijnhouwers M, Stefano G, **Renna L**, Brandizzi F. Multiple roles of ADP-ribosylation factor 1 in plant cells include spatially regulated recruitment of coatomer and elements of the Golgi matrix. Plant Physiol. 2007 Apr;143(4):1615-27. Epub 2007 Feb 16. http://www.f1000biology.com/article/id/1085875
"This paper identifies a new effector (GDAP1) for ADP-ribosylation factor..."
Evaluated by Faculty of 1000 Biology member **David Oppenheimer** (University of Florida, United States of America
.

Relevant course completed during MSc program

    BIOL 825.3 Current Topics in Plant Molecular Biology

    BIOL 832.3 Control of Plant Growth and Development

    BIOL 898.3 Plant Cell Structure

Language

Mother language: Italian, French, English.

References

Prof. **Stefano Mancuso**
Dipartimento di ortoflorofrutticoltura
Universita`degli studi di Firenze
Viale delle idee 30
50019 Sesto fiorentino (FI)
Tel 055-457 4063
Email: stefano.mancuso@unifi.it

Dr. **Federica Brandizzi**
Associate Professor
MSU-DOE Plant Research Laboratory,
S-238 Plant Biology
Michigan State University, East Lansing, MI 48824
Tel.: Office 517-353-7872, Lab 517-353-3383
Fax: 517-353 9168
Email: brandizz@msu.edu

Dr. **G-P Di Sansebastiano**
Laboratory of Botany - Di.S.Te.B.A.; University of Lecce, Campus ECOTEKNE
Prov. Lecce-Monteroni 73100 Lecce - Italy
Office: +39 0832 298713
E-Mail: gp.disansebastiano@unile.it

AKNOWLEDGEMENTS

DECLARATION

I declare that the work submitted here is result of my own investigation, except

where otherwise stated. This work has not been submitted to any other

University or Institute towards the partial fulfillment of any degree.

Bonn,

Giovanni Stefano